TECHNISCHE UNIVERSITÄT MÜNCHEN

Lehrstuhl für Biotechnologie

The role of E-cadherin in EGFR signal transduction and EGFR-inhibitory treatment in gastric cancer

Stefan Heindl

Vollständiger Abdruck der von der Fakultät für Chemie der Technischen Universität München zur Erlangung des akademischen Grades eines

Doktors der Naturwissenschaften (Dr. rer. nat.)

genehmigten Dissertation.

Vorsitzender: Univ.-Prof. Dr. A. Itzen

Prüfer der Dissertation: 1. Univ.-Prof. Dr. J. Buchner

2. apl. Prof. Dr. B. Luber

Die Dissertation wurde am 03.12.2012 bei der Technischen Universität München eingereicht und durch die Fakultät für Chemie am 09.04. 2013 angenommen.

TABLE OF CONTENTS

TABLE OF FIGURES

1 INTRODUCTION

1.1 Gastric Cancer

1.1.1 Epidemiology

Despite a steady decrease in the incidence with about one million new cases diagnosed annually, gastric cancer (GC) contributes 7.8% to the overall cancer incidences and represents the fourth most common cancer worldwide (Fig. 1.1; [1]). Behind lung cancer (18.2%), GC is the second leading cause of cancer-related death (9.7%), and the fourteenth most common cause of death overall worldwide [2].
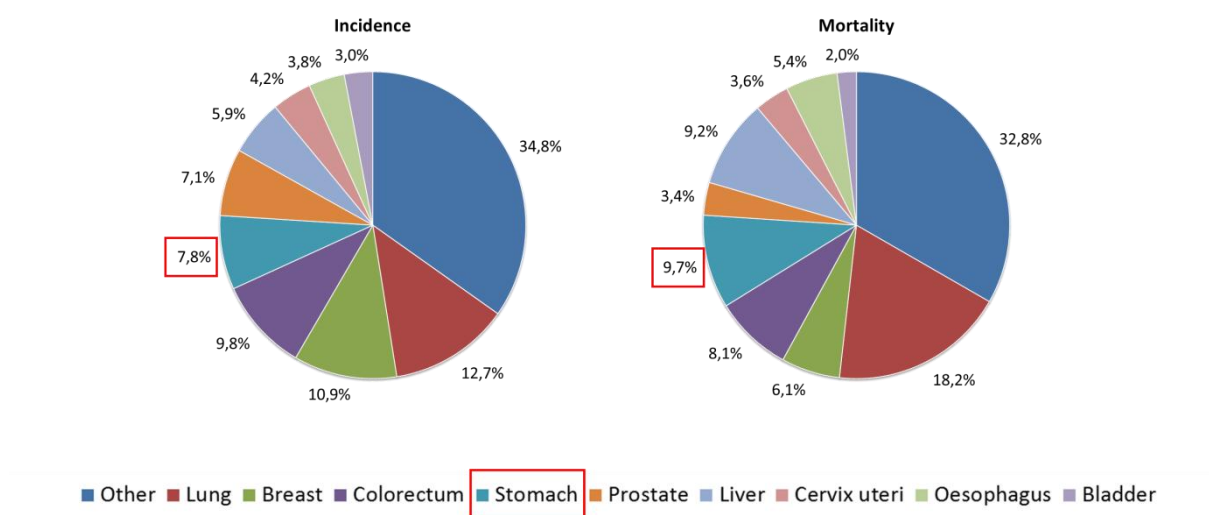
Figure 1.1 Cancer incidence and mortality: The pie charts represent the estimated percentages of worldwide cancer cases and cancer deaths of both sexes and all ages. Gastric cancer (turquois) is the fourth most common cancer and the second leading cause of cancer-related death. (Source: GLOBOCAN 2008)

Due to the asymptomatic early stages of the disease and the associated late diagnosis, the average age of presentation is between 60 and 70 years [1, 3]. The incidence rates are about twice as high in men than in women. The 5-year survival rate among GC patients for all stages of the disease is ~ 25% [4, 5]. There is a considerable variation in the geographical distribution of GC worldwide. More than 70% of the cases occur in developing countries [1]. The highest incidence rates are found in Japan, China, Central and Eastern Europe as well as in the Andean region in South America. In contrast, incidence rates are low in North and East Africa, Northern Europe and North America [6]. Based on the

geographic location, race and socio-economic status, the incidence by tumor sub-site varies considerably. For developing countries and lower socio-economic groups, distal GC (lower part of the stomach) is predominating, whereas proximal tumors (upper part of the stomach) are more common in developed countries and in higher socio-economic classes [3].

1.1.2 Pathology and classification

The stomach can be divided in 5 sections, the cardia, fundus, body, antrum and pylorus. It is wrapped by 5 layers, which are from the lumen outwards, the mucosa, submucosa, muscularis, subserosa, and serosa (Fig. 1.2).

Approximately 90% of all malign tumors of the stomach are adenocarcinoma. Interestingly, in the last decades the anatomical distribution has shifted to the proximal stomach, displaying a progressive increase in adenocarcinoma of the cardia and fundus (Fig. 1.2).
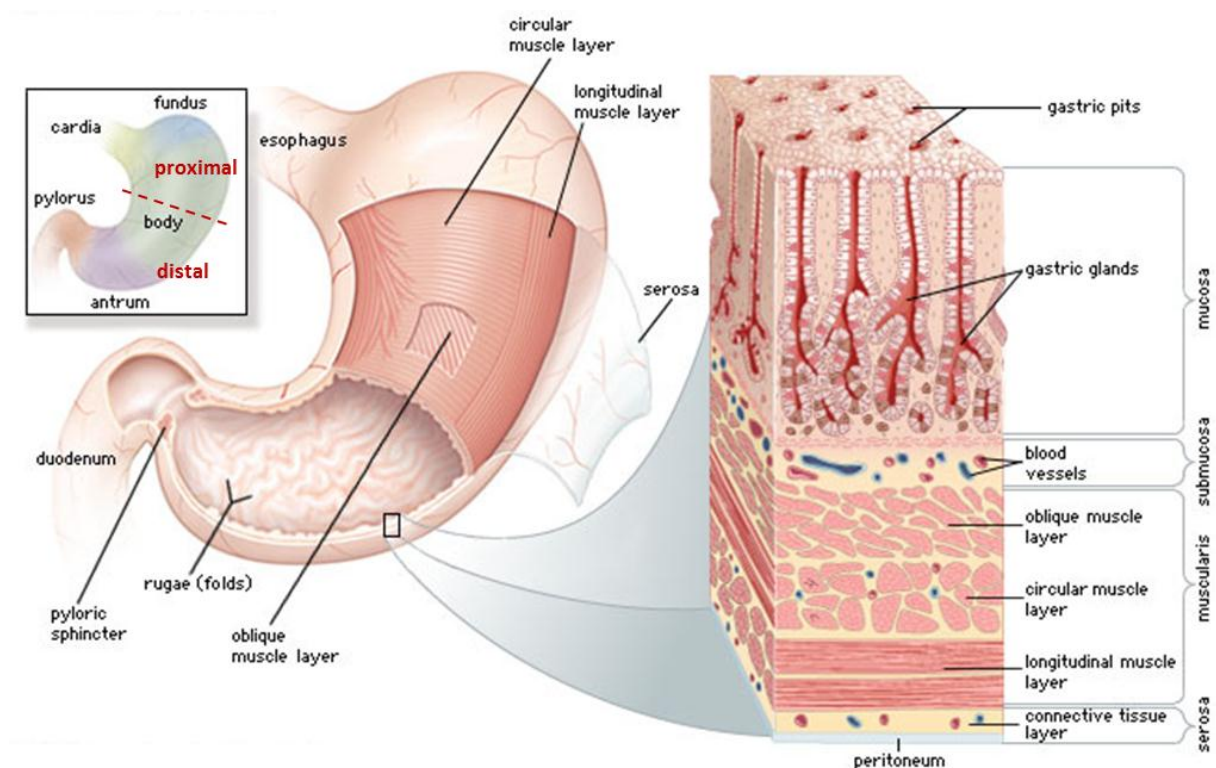
Figure 1.2 Anatomy of the stomach: The stomach is made up of five layers. The mucosa is the innermost layer and is responsible for the production of the stomach acid and digestive juices. The following submucosa is surrounded by the muscularis, a layer of muscle that moves and mixes the stomach contents. The next two layers, the subserosa and the serosa (the outermost layer) act as wrapping for the stomach. (Source: Encyclopaedia Britannica Inc. 2009; www.metrohealth.org)

For the classification of gastric adenocarcinoma, the Laurén classification is predominantly used worldwide. Based on the microscopic morphology of the tumor, it distinguishes two main histologic subtypes, the intestinal type and the diffuse type [7, 8]. The intestinal type is characterized by cohesive neoplastic cells, forming gland like tubular structures. This subtype occurs more often in the distal stomach and is often preceded by an intestinal metaplasia [9, 10].

In the poorly differentiated diffuse type cell cohesion is absent and individual cells infiltrate the stomach wall. It is associated with a worse prognosis [8]. Signet ring cell carcinoma occur, if the tumor cells secrete mucus that accumulates within the cell and pushes the nucleus to the periphery [11]. The intestinal type accounts for approximately 50% of cases, the diffuse type for 35% and the remaining 15% represent "unclassifiable" or mixed types [8, 12-14].

In order to achieve a global standard ensuring accurate prognosis and adequate treatment, the so-called TNM classification system is used for the staging of malignant tumors. It has been developed and maintained by the International Union against Cancer (UICC), and is also used by the American Joint Committee on Cancer (AJCC). The TNM classification determines the penetration depth of the primary tumor (T) and the spread to lymph nodes (N) or distant metastasis (M). The staging of GC according to the TNM classification is illustrated in Fig. 1.3.
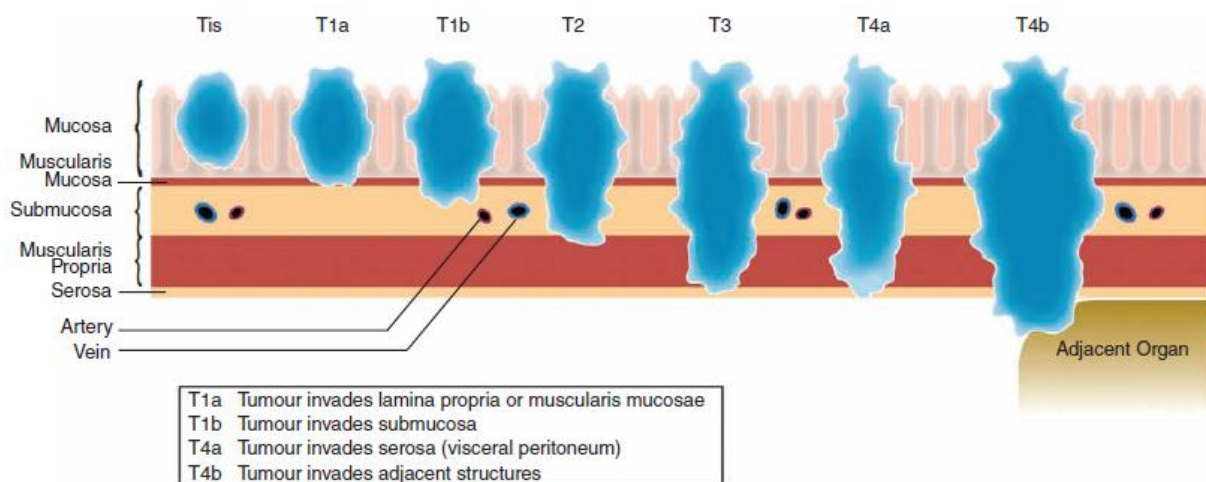
Figure 1.3 Gastric cancer staging system: Primary Tumor (T): The TNM classification system stages the tumors according to their penetration depth. TX Primary tumor cannot be assessed; T0 No evidence of primary tumor; Tis Carcinoma in situ; T1 Tumor invades lamina propria or submucosa; T1a Tumor invades lamina propria; T1b Tumor invades submucosa; T2 Tumor invades muscularis propria; T3 Tumor invades subserosa; T4a Tumor perforates serosa; T4b Tumor invades adjacent structure; **Regional Lymph Nodes (N):** NX Regional lymph nodes cannot be assessed; N0 No regional lymph nodes metastasis; N1 Metastasis in 1 to 2 regional lymph nodes; N2 Metastasis in 3 to 6 regional lymph nodes; N3a Metastasis in 7 to 15 regional lymph nodes; N3b Metastasis in more than 16 regional lymph nodes; **Distant Metastasis (M):** MX Distant metastasis cannot be assessed; M0 No distant metastasis; M1 Distant metastasis. (Source: UICC/AJCC 2009; DAKO)

1.1.3 Etiology

1.1.3.1 Risk factors

Chronic infection with the gram-negative, micro-aerophilic and spiral-shaped bacterium *Helicobacter pylori* (*H. pylori*) represents the leading infectious cause of cancer and the most important cause of GC worldwide [10, 15-18]. *H. pylori* associated inflammation plays a key role in the carcinogenic process by increasing the production of free radicals, apoptotic and necrotic epithelial cell death as well as cell proliferation [19-22]. Interestingly, in some populations, only a small percentage of infected individuals develop neoplasias [23]. Diverse factors, such as personal hygiene and dietary habits, the host genetic background or genetic diversity of *H. pylori* strains are considered to influence the different outcomes of the infection [24-27].

Other risk factors include smoking, diet and obesity [3, 28]. Since 2004 tobacco smoking is accepted as a cause of GC and between 11% and 18% of cases are attributable to smoking [28]. Dietary habits, for instance high consumption of salt-preserved and smoked foods as well as heavy alcohol intake are associated with GC [29, 30]. In contrast, many epidemiological studies display that consumption of vitamin C-containing fruits and vegetables has preventive effects [29, 31, 32]. Since the early 20th century, a steady decline of incidence rates could be observed, which is probably due to the popularization of refrigerators and the diminishing prevalence of *H. pylori* [21, 31].

1.1.3.2 Genetic predisposition

Only 10 % of GC cases have an inherited familial background [33, 34]. Genetic predisposition for GC is indicated by germline mutations of the *CDH1* gene. Its protein product is the cell adhesion molecule E-cadherin, which is essential in development, cell differentiation and maintenance of epithelial architecture. E-cadherin loss is associated with a diffuse phenotype, and the disease is therefore referred to as Hereditary Diffuse Gastric Cancer (HDGC). Approximately 1-3 % of GC cases with inherited familial background are attributable to HDGC [15, 35-37]. Over 20 different germline mutations in the *CDH1* gene have been documented, and they account for 30-40% of HDGC cases. The risk of developing GC for these patients is 67% in men and 83% in women. The latter further exhibit an increased risk for lobular breast carcinoma [38]. The average age of onset is 38 years, which is much younger than that of sporadic GC [36].

There are several other inherited cancer predisposition syndromes preceding the development of GC. Patients of the hereditary non-polyposis colorectal cancer (HNPCC) syndrome share an increased risk for developing GC due to inherited mutations that impair the DNA mismatch repair. Mutations of *MSH2* and *MLH1* represent the two most frequent alterations and account for approximately 60% and

30% of cases, respectively [39, 40]. These alterations lead to microsatellite instability (MSI), which is a hallmark of HNPCC. In HNPCC intestinal-type adenocarcinoma is the most commonly reported pathology.

Further inherited precancerous syndromes predisposing patients for the development of GC are familial adenomatous polyposis (FAP), Li-Fraumeni syndrome (LFS) and Peutz-Jeghers syndrome (PJS) [41]. FAP and LFS are clearly associated with germline mutations of the tumor suppressors *APC* and *p53*, respectively. In the case of PJS, a mutation of the tumor-suppressive serine-threonine kinase STK11 is supposed to be the molecular cause of the disease.

1.1.3.3 Molecular alterations

Approximately 90% of GC cases occur sporadically and are characterized by the sequential acquisition of multiple genetic or epigenetic alterations in numerous oncogenes or tumor suppressor genes (Fig. 1.4). Mutations, overexpression or amplification of specific genes have been identified that play important roles in diverse cellular functions such as cell adhesion, signal transduction, differentiation, development, gene transcription and DNA repair.

In diffuse type GC somatic mutations of the E-cadherin gene *CDH1* are observed in 40-50% of cases, whereas they play no role in the intestinal type [42]. Furthermore, amplification of the oncogene *K-sam* (*KATO-III cell derived stomach cancer amplified gen*) seems to be specific for the diffuse subtype [43]. Amplification of the oncogene *c-erbB2* encoding the receptor tyrosine kinase (RTK) HER2/neu (*human epidermal growth factor receptor 2*) occurs predominantly in intestinal-type GC and is associated with invasion and lymph node metastasis [44, 45]. Oncogenic activation of β-catenin also seems to be restricted to the intestinal type [46]. The proto-oncogene c-*MET* belongs to the group of oncogenes that is amplified in both histological subtypes of GC. It encodes the hepatocyte growth factor receptor and similar to c-erbB2 is associated with invasion and lymph node metastasis [47, 48]. Genetic alteration of the *Kirsten rat sarcoma viral oncogene homolog* (*K-RAS*) is a very rare event in GC and is predominately found in the intestinal subtype. MSI represents an early event in gastric carcinogenesis and is found in approximately 20% of GC cases, mainly of the intestinal type. In addition, to *MLH1 and MSH2,* inactivation also of the mismatch repair genes *hMSH6* or *PMS2* is causative for MSI [38, 49-51]. Furthermore, the loss of heterozygosity (LOH) occurs frequently in GC and leads to the loss of multiple tumor suppressor genes [34, 52]. One of the best studied examples is p53, the so-called „guardian of the genome". It acts as regulator of the cell cycle and conserves stability by preventing genome mutation. It can be inactivated either by mutation or LOH. [53, 54].
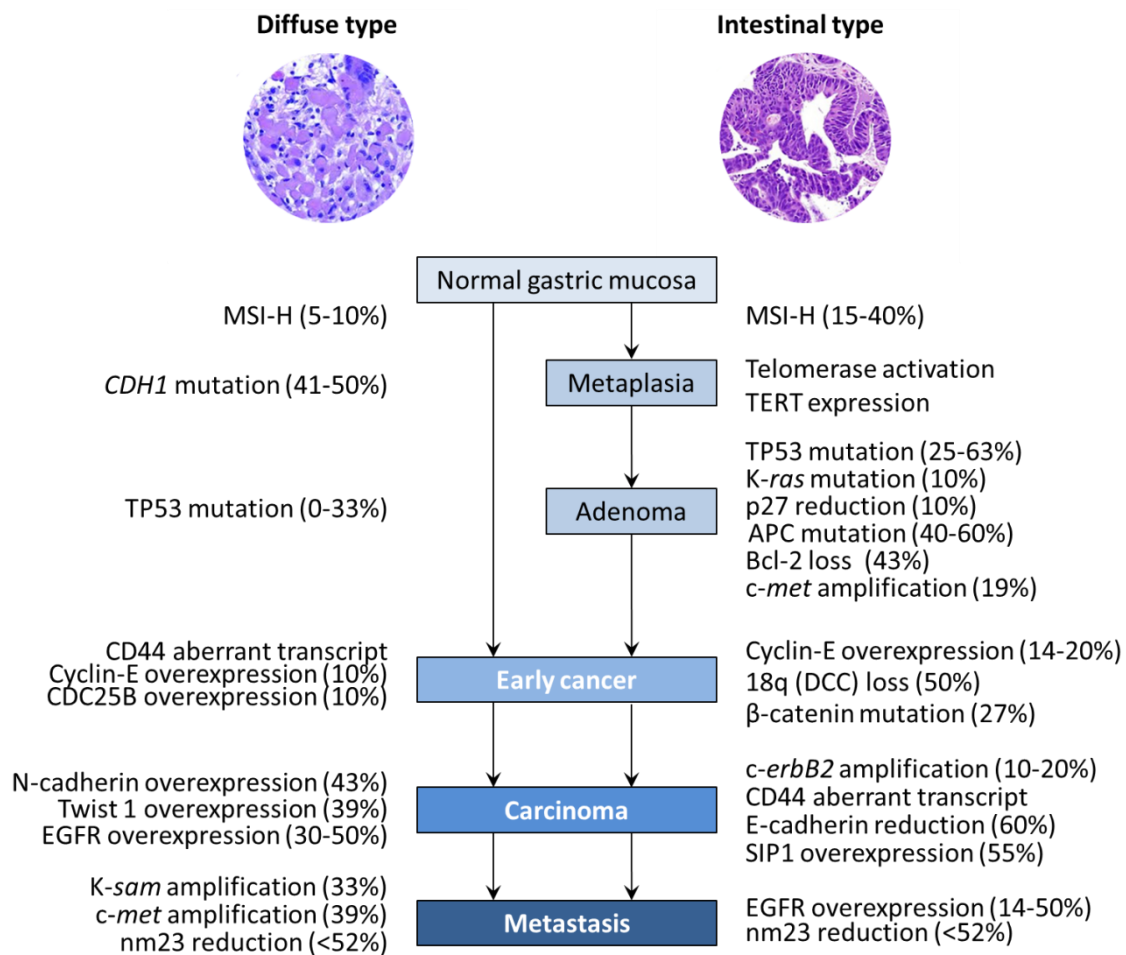
Figure 1.4 Molecular alterations associated with gastric carcinogenesis: The molecular changes differ between the two major types of gastric cancer: intestinal and diffuse type tumors. The alterations, such as mutation, overexpression or amplification, are ordered according to the stage of cancer development. Molecular changes in specific genes involved in cell adhesion, signal transduction, differentiation, development, gene transcription, and DNA repair have been identified. The percentages in parenthesis indicate the frequencies of the alterations observed when known. Abbreviations: *APC*, adenomatous polyposis coli; *Bcl-2*, B-cell CLL/lymphoma 2; *CD44*, CD44 antigen; *CDC25B*, cell division cycle 25B; *CDH1*, E-Cadherin; *c-erbB2*, *v-erb-b2* erythroblastic leukaemia viral Onkogene homologue 2; c-*MET*, *MET* proto-oncogene (hepatocyte growth factor receptor); DCC, deleted in colon cancer; *EGFR*, epidermal growth factor receptor; *K-ras*, *v-Kiras2* Kirsten rat sarcoma viral oncogene homologue; *K-sam*, encodes fibroblast growth factor receptor 2; MSI-H, microsatellite instability-high; nm23, nonmetastatic cells 1 (protein, NM23, expressed in); *p27*, Cyclin-dependent kinase inhibitor 1B; *p53*, tumor protein p53 (Li–Fraumeni syndrome); *SIP1*, SMAD-interacting protein 1; TERT, telomerase reverse transcriptase; *TWIST1*, twist homologue 1; (Modified from [35]).

1.1.4 Therapy

Surgery is the main therapeutic approach for the treatment of GC. Due to the late diagnosis, the often advanced stage of the disease and despite considerable improvements of surgical techniques, the 5-year survival remains very poor, even after complete resection of the tumor [55, 56]. Palliation of symptoms, rather than cure, is then often the primary goal of patient management. In order to improve the relapse-free and overall survival, neoadjuvant chemotherapy is evaluated in numerous clinical

studies. Multiple phase II and phase III studies indicate that neoadjuvant chemotherapy decreases tumor size and stage and significantly improves the progression-free and overall survival of patients [57-59]. For patients with advanced GC fluorouracil (FU)- and cisplatin-based combination chemotherapy has become the standard treatment [60].

The steady increase of knowledge about signal transduction and tumor biology has led to the development of new therapeutic regimens specifically targeting individual oncogenic pathway components [61]. A recent international clinical trial, the "ToGA"-study, evaluated the monoclonal antibody trastuzumab/Herceptin®, which is directed against the RTK HER2 in GC patients. The demonstrated efficacy led to the approval of trastuzumab for the treatment of metastatic gastric tumors exhibiting HER2 amplification or overexpression [61, 62].

1.2   E-cadherin

1.2.1   Cell-cell adhesion

Different types of cell adhesion molecules (CAMs) are located on the surface of the cell to allow interaction with neighboring cells. These proteins maintain a close physical association between cells, permit intercellular communication, and provide mechanical stability by formation of adherens junctions, tight junctions, gap junctions and desmosomes [63]. There are four major families of cell adhesion molecules, immunoglobulin (Ig), integrins, cadherins, and selectins [64-68].

1.2.2   The cadherin superfamily

The members of this superfamily of adhesion molecules are mainly involved in calcium dependent cell-cell adhesion and they play important roles in embryonic morphogenesis, cytoskeletal organization, migration, cell polarity and tissue integrity [69-71]. The majority of cadherins are single-pass transmembrane glycoproteins and are about 700-750 amino acids long. The large extracellular N-terminal fraction typically consists of 5-34 so-called cadherin repeats (EC). They are structurally related to immunoglobulin domains and comprise approximately 110 amino acid residues each [72]. The maintenance of a stable and functional conformation of the molecule requires calcium binding to short and highly conserved negatively charged amino acid sequences (DXD, DRE and DXNDNYPXF) located between neighboring ECs [73-77]. Furthermore, calcium is essential for the protection against the proteolytic degradation of cadherins [78-81].

Underpinned by cell sorting experiments, cadherins mediate cell adhesion mainly in a homophilic manner, meaning that the ECs of identical cadherins located on the membranes of adjacent cells

interact [82-85]. Thereby, the peptide sequence histidine-alanine-valine (HAV) within the most N-terminal EC1 contributes to adhesive binding and specificity and is responsible for trans-binding between cadherin monomers [72, 86]. Structural studies suggest that they associate in the plasma membrane to form dimers or larger oligomers, but the precise mechanism for their interaction is still controversial [87]. Some reports also revealed heterophilic interactions [88-91].

In humans, the cadherins represent a superfamily consisting of approximately 80 different members constituting at least six subfamilies [76, 92]. Based on their protein domain composition, genomic structure, and protein sequence classical or type-I cadherins, atypical or type-II cadherins, desmocollins, desmogleins, protocadherins and Flamingo cadherins can be distinguished [72, 74, 93].

1.2.3 E-cadherin, a classical cadherin

Classical cadherins, also referred to as type-I cadherins, represent the most important and best studied subfamily of cadherins [94]. It comprises approximately 20 members that show a common domain organization (Fig. 1.5). Their extracellular domain typically consists of five extracellular repeats [95]. The most prominent member of this family is E-cadherin. It was first described by Jacobs and co-workers in the early 1980s [96, 97] and is also referred to as L-CAM in chicken [98] and uvomorulin in mouse [99]. It is considered as an epithelial cell marker and is named after the tissue in which it was thought to be mainly expressed [95].

E-cadherin is a major constituent of the adherens junction protein complex. Its highly conserved cytoplasmic tail is connected to the actin filament network by the intracellular anchor proteins α-, β-, and γ-catenin (Fig. 1.5) [75, 93, 100]. Thereby E-cadherin binds to β-catenin which via α-catenin connects E-cadherin to actin [101]. Furthermore, p120-catenin binds to the juxtamembrane region of E-cadherin and stabilizes it at the cell surface [102-107]. The integrity of this so-called core is crucial for efficient cell-cell adhesion and phosphorylation of individual components e.g. by RTKs result in its disruption and the endocytosis of E-cadherin [100, 101, 108].
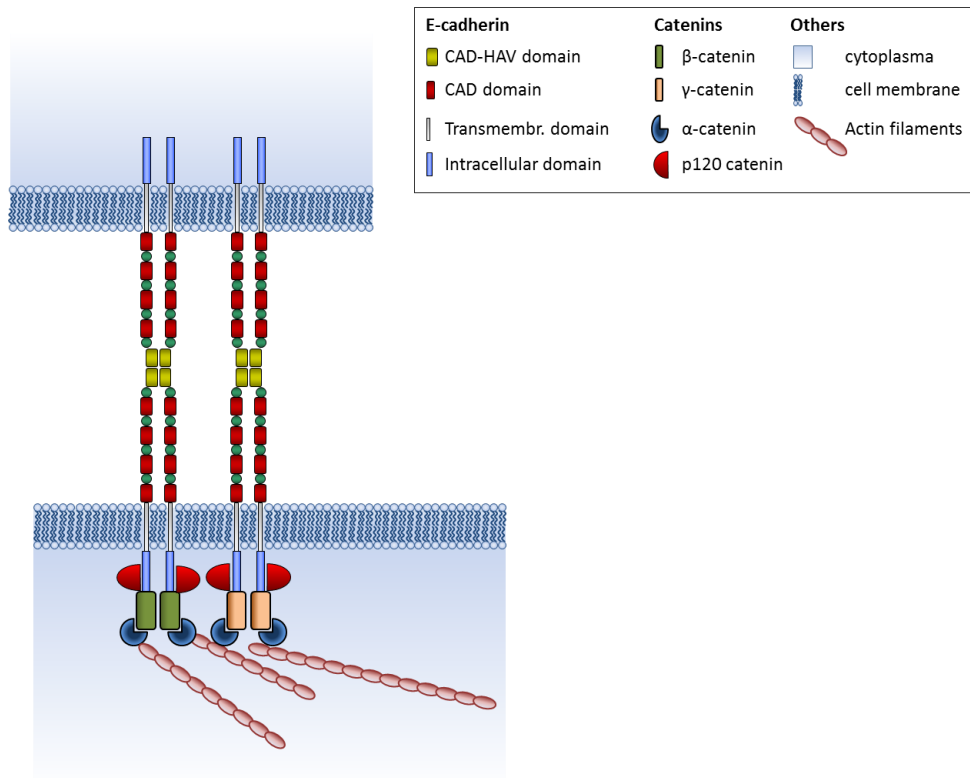
Figure 1.5 E-cadherin mediated cell-cell adhesion: E-cadherin molecules that are expressed on the plasma membrane of adjacent cells interact in a zipper-like fashion. The most amino-terminal cadherin domain on each E-cadherin molecule contains the histidine-alanine valine (HAV) motif that is thought to interact with E-cadherins of adjacent cells. Recent evidence indicates that cadherin molecules interact through their tips in cis and in trans in a highly flexible manner. The cytoplasmic core complex (CCC), consisting of α-catenin, β-catenin, γ-catenin and p120 catenin, links E-cadherin homodimers to the actin cytoskeleton (modified from [109]).

1.2.4   E-cadherin signaling

In addition to its adhesive function**,** E-cadherin also participates in signal transduction by interaction with multiple signaling molecules [110].

At the cell surface, crosstalk of E-cadherin with multiple RTKs such as the epidermal growth factor receptor (EGFR), vascular endothelial growth factor 2 (VEGFR2), hepatocellular growth factor receptor (c-*MET*) [109, 111-114], fibroblast growth factor receptor (FGFR), platelet-derived growth factor receptor (PDGFR) and transforming growth factor-β (TGFβ) receptor has been reported.

This crosstalk is often bidirectional, as several classes of RTKs can inhibit E-cadherin–dependent adhesion and E-cadherin can in turn inhibit for example the activation of EGFR, HER2/Neu, IGF-1R and c-Met [114, 115]. This occurs possibly by reducing the receptor mobility and the ligand-binding affinity [114]. For EGFR, these and earlier studies [116] found that the association with E-cadherin depends on the extracellular domain of E-cadherin but is independent of β-catenin, although β-catenin can also bind EGFR [112].

In the cell interior kinases of the SRC family, CSK, as well as phosphatases such as density-enhanced phosphatase DEP1, SHP2 and vascular endothelial protein Tyr phosphatase VE-PTP represent potential signaling partners. Furthermore, the homophilic engagement of E-cadherin regulates the activation of Rho GTPases Rac1 and Cdc42 [117-119] and Rho [120, 121] and it can for example prevent the transcriptional activity of β-catenin within the wnt/wingless signaling cascade by its recruitment to the membrane [122-130].

1.2.5   E-cadherin and cancer

Dedifferentiation is a hallmark of tumor progression and is often associated with the loss of E-cadherin function by a process called epithelial to mesenchymal transition (EMT). Alterations of the E-cadherin function have been documented in a variety of cancers [131-137] and are associated with increased invasive and metastatic potential [132, 133, 138-144]. E-cadherin is therefore regarded as tumor and invasion suppressor [145, 146]. Experiments, showing that the forced expression of E-cadherin results in a reversion of the invasive phenotype, further underline these findings [132, 141]. The mechanisms for E-cadherin inactivation comprise mutations, epigenetic and genetic silencing and transcriptional repression [138, 147-152]. Mutations of E-cadherin have been detected in samples of diffuse type GC [42], gynecologic cancers [153] and infiltrative lobular breast cancer [146, 154].

In diffuse type GC, inactivating mutations of the E-cadherin gene *CDH1* occur in approximately 50% of cases [42] and are detected early in tumor development. They are located predominantly in a hotspot region consisting of the exons 8-10 and often affect extracellular calcium-binding sites [42, 155]. Such mutations result in decreased adhesion and increased cellular motility [155-159] and diminish the tumor suppressive capacity of E-cadherin [160]. Furthermore, missense mutations or in-frame deletions affecting putative calcium binding sites of E-cadherin often lead to increased proteolytic activity accompanied by an abnormal cytoplasmic localization of E-cadherin [161]. E-cadherin deficiency was recently shown to initiate gastric signet ring-cell carcinoma in humans and mice [151].

1.3   The epidermal growth factor receptor (EGFR)

1.3.1   The HER-receptor family

EGFR, also known as ErbB1/HER1, is a member of a family of structurally related RTKs that includes ErbB2/HER2/Neu, ErbB3/HER3, and ErbB4/HER4 (Fig. 1.6) [162]. All four receptors share a common domain structure consisting of an extracellular ligand binding domain, a hydrophobic membrane-spanning region and a cytoplasmic tyrosine kinase domain harboring multiple tyrosine autophosphorylation sites [163, 164]. While EGFR and HER4 are fully functional receptors in terms of ligand binding and kinase activity, HER2 and HER3 are deficient receptors, as they cannot bind ligands and have defective tyrosine kinase activity [165-167].
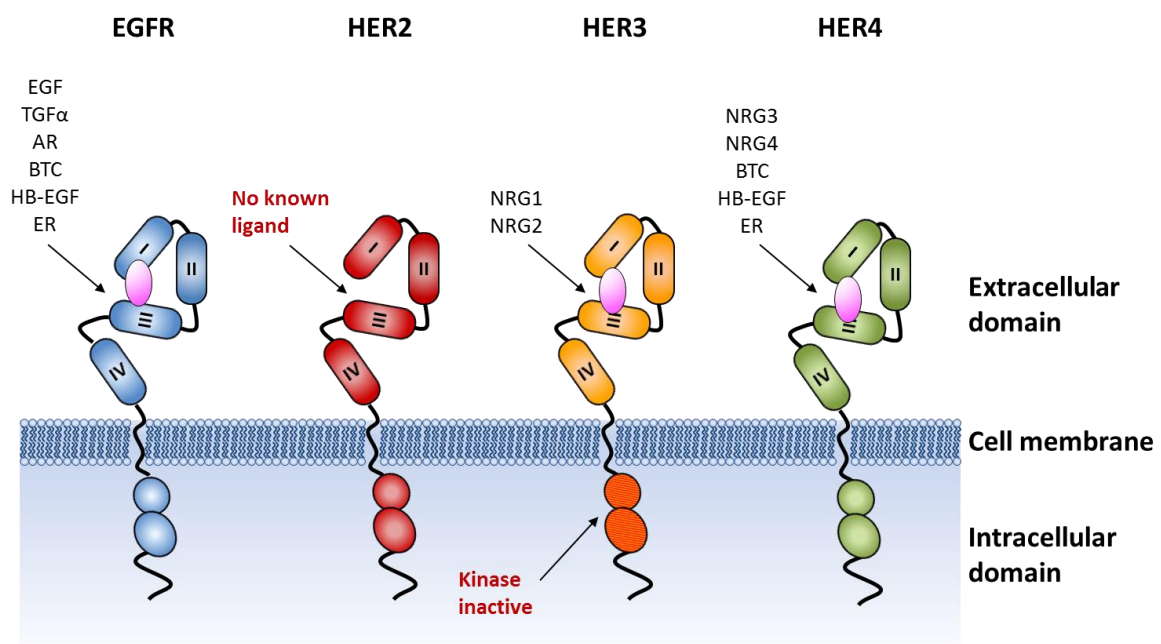
Figure 1.6 Structure and ligands of the HER-receptor family: Each member of the HER receptor family consists of an extracellular ligand-binding domain comprising four subdomains (I-IV), a transmembrane spanning helix and a cytoplasmic portion harboring a tyrosine kinase domain. Only EGFR and HER4 are fully functional in terms of ligand binding and kinase activity. ErbB3 has impaired kinase activity and no ErbB2 ligand has been detected so far.

Typically, receptor activation is induced by binding of ligands, which are growth factors of the EGF-family. They all share an EGF-like motif of 45–55 amino acids and six cysteine residues. According to their receptor affinity they can be divided into three groups [168]. The first group, including EGF, amphiregulin (AR), and transforming growth factor α (TGFα), exclusively binds to HER1. The second group comprises betacellulin (BTC), heparin-binding EGF (HB-EGF), and epiregulin (ER) [169], and exhibits dual specificity for EGFR and HER4. The third group is composed of the

neuregulins (NRG, also called heregulins, HRG) and includes two subgroups based on their capacity to bind HER3 and HER4 (NRG1 and NRG2) or only HER4 (NRG3 and NRG4) [170, 171]. So far, no ligand is known that binds to HER2. In addition to ligand-mediated EGFR induction, EGFR can also be transactivated by a multitude of G-protein-coupled receptors, integrins, and cytokine receptor [162, 169, 172].

1.3.2   Receptor activation

Crystal structures of the HER receptors reveal that their extracellular domain comprises four subdomains (I-IV), of which the domains I and III are involved in ligand binding. Ligand binding leads to the formation of a dimerization loop in subdomain II, which promotes receptor dimerization (Fig. 1.7). If no ligand is bound, intramolecular interactions between subdomain II and IV maintain the receptor in the so-called tethered state and prevent dimerization [173-175]. In contrast, the crystal structure of HER2 reveals a permanently activated conformation similar to that of receptors after ligand binding. Hence, despite its inability to bind ligands, HER2 is capable of dimerizing, possibly explaining why it is supposed to be the preferred dimerization partner [176]. Every single receptor can form dimers, either with identical receptors (homodimerization) or with any of the three other members of the HER family (heterodimerization) depending on which receptor proteins are expressed in a given cell. Due to their deficiency, HER2 and HER3 always require heterodimerization.

Dimerization leads to the activation of the intrinsic tyrosine kinase with subsequent autophosphorylation of key tyrosines located within the carboxy-terminal tail of the receptor [162, 164]. Phosphorylated tyrosine residues enable the recruitment and activation of proteins containing phosphotyrosine binding domains (PTBs) and Src-homology 2 domains (SH2), such as growth factor receptor-bound protein 2 (GRB2), SHC and PLCγ which in turn activate complex downstream signal transduction pathways (Fig. 1.7) [162, 164, 172].

Signal attenuation is predominantly achieved by the endocytosis of the receptor ligand complexes through clathrin-coated invaginations of the cell membrane. By distinct sorting pathways, the internalized receptor is either recycled back to the cell surface or upon ubiquitination is directed to the lysosomes for degradation [177, 178]. The rate of EGFR endocytosis is increased 5-10 fold following ligand activation, whereas the internalization rate of HER2, HER3 and HER4 remains unchanged after stimulation with ligands [179]. To compensate the lack of ligand-induced internalization and degradation, the other HER family members show higher constitutive turnover rates. Moreover, signal desensitization is induced by a plethora of transcriptional repressors and RNA-binding proteins such as LRIG, ARGOS or RALT [180] and ligand depletion, dephosphorylation and kinase inactivation represent alternative suppressive mechanisms attenuating ligand-induced signaling.

1.3.3 EGFR downstream signaling

Upon activation, EGFR can induce a variety of different downstream signaling pathways (Fig. 1.7). The ligand, the dimerization partner, as well as the individual signaling molecules recruited to the different autophosphorylation sites of the receptor determine which pathway is turned on and provide sufficient signaling complexity to regulate diverse processes like cell proliferation, differentiation, migration, and survival [162, 164, 172].
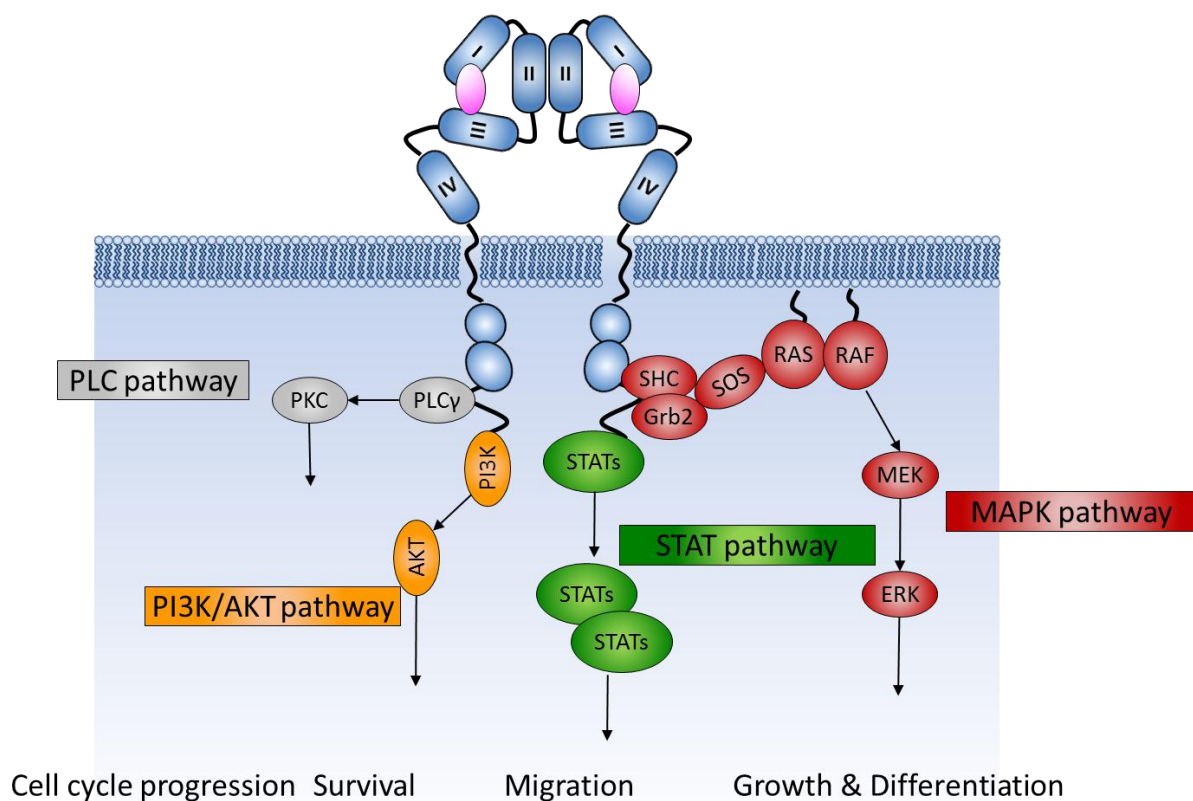
Figure 1.7 Activation and downstream signaling of EGFR: Binding of ligand to EGFR leads to receptor dimerization, autophosphorylation and activation of several downstream signaling pathways. Only selected signaling molecules are presented (modified from [181] and from [182]).

1.3.3.1 Ras-MAPK pathway

The Ras-MAPK (*mitogen-activated protein kinase*) pathway represents one of the most studied pathways downstream of EGFR. Upon EGFR activation, it can either be activated through the direct recruitment of GRB2 at the SH2-domain or through the indirect recruitment of GRB2 through the SHC adaptor. Via its SH3 domain, GRB2 recruits the nucleotide exchange factor Son of Sevenless

(SOS) to the plasma membrane, which in turn catalyzes the activation of Ras by facilitating the exchange of GDP by GTP [183]. Activated Ras then triggers the so-called MAPK cascade by recruitment and sequential activation of the cytoplasmic serine/threonine protein kinase Raf [184], MEK1/2 (mitogen-activated protein kinase kinase 1/2) and Erk1/2 (extracellular signal-regulated kinases 1/2). Finally, activated Erk1/2 translocates into the nucleus and induces various transcription factors regulating cell differentiation, cell proliferation, and cell death.

1.3.3.2   PI3K/Akt pathway.

Another key signaling pathway activated by EGFR is the phosphatidylinositol 3-kinase (PI3K)/Akt pathway. EGFR activates PI3K, which is the product of the *PIK3CA* gene, and mediates the formation of phosphatidylinositol-3,4,5-triphosphate (PIP3). PIP3 then activates Akt by binding at its pleckstrin homology (PH) domain. Activated Akt has several effects, both in the cytoplasm and the nucleus. It promotes cell survival and blocks apoptosis by a variety of routes, including inhibition of the proapoptotic BAD (BCL2 antagonist of cell death), procaspase 9 or the Forkhead (FKHR) family of transcription factors (FOXO) [185]. Moreover, the PI3K/Akt pathway also induces the expression of angiogenic factors such as VEGF or hypoxia inducible factor-1α (HIF1α) and activates the mammalian target of rapamycin (mTOR) [186].

1.3.3.3   Src kinase pathway

The cytosolic tyrosine kinase Src represents the first discovered tyrosine kinase and oncogene and is the prototypic member of a membrane-associated family of non-RTKs consisting of 12 members (Src, Fyn, Yes, Blk, Yrk, Fgr, Hck, Lck, Lyn, Brk, Srm, and Frk) [187, 188]. Src plays an important role in different cellular processes. It is involved in the regulation of proliferation, cytoskeleton, cell-matrix adhesion, motility and migration [189]. It is also involved in the EGFR signal transduction. Overexpression of Src was shown to enhance EGF-mediated proliferation and transformation in epithelial cells [190]. Phosphorylated residues on the cytoplasmic domain of EGFR serve as docking sites for Src, allowing direct physical interaction with EGFR, being either substrate or activator [191]. Alternatively interaction between EGFR and Src can be mediated by the adaptor molecule Shc or by C-terminal Src kinase (Csk)[192].

1.3.3.4   PLC-γ/ PKC pathway

Upon activation by EGFR, Phospholipase C-γ (PLC-γ) hydrolyses phosphatidylinositol 4,5-biphosphate to diacylglycerol (DAG) and inositol triphosphate (IP3). IP3 mediates calcium release from intracellular stores, affecting multiple Ca^{2+}-dependent enzymes. DAG is a cofactor for the

activation of protein kinase-C (PKC), which promotes cell-cycle progression, transformation, differentiation and apoptosis.

1.3.3.5 STAT signaling

Phosphorylated EGFR can directly or indirectly activate signal transducer and activator of transcription 1 (STAT1), STAT3 and STAT5. Upon phosphorylation, the activated STAT transcription factors translocate into the nucleus and directly regulate the expression of genes crucial for cell survival, proliferation, transformation and oncogenesis [193].

1.3.4   EGFR directed therapeutic options in cancer

As the activation of EGFR stimulates essential biological processes like cellular growth and proliferation, angiogenesis, motility and migration and apoptosis, its deregulation is implicated in the formation of many human cancers. Patients whose tumors exhibit alterations of EGFR tend to have a more aggressive disease and a poor clinical outcome [172]. Hyperactivation of the EGFR pathway is often promoted by the autocrine or paracrine overstimulation by ligands, protein overexpression, gene amplification and constitutive receptor activation by activating mutations.

EGFR represents one of these targets for therapeutic intervention and two distinct approaches for its inhibition are already approved for clinical use. The first is the use of monoclonal antibodies (mAbs) directed against the extracellular domain of EGFR. Antibodies such as cetuximab/Erbitux® or panitumumab/Vectibix™ are given intravenously and interfere with ligand binding thereby blocking receptor dimerization [194].

In contrast, small molecule tyrosine kinase inhibitors (TKIs), such as gefitinib/Iressa®, erlotinib/Tarceva® or lapatinib/Tyverb® are administered orally and compete reversibly with ATP in the tyrosine kinase domain thereby inhibiting EGFR autophosphorylation and downstream signaling [195].

EGFR inhibitors are often combined with chemotherapy to increase the therapeutic outcome. Furthermore, also combination with other selective compounds is evaluated extensively in order to overcome resistance to monotherapy often caused by compensatory pathways. EGFR inhibitors are currently approved in several countries for the treatment of advanced squamous-cell carcinoma of the head and neck (HNSCC), metastatic colorectal cancer (CRC), locally advanced or metastatic pancreatic cancer, advanced HER2-overexpressing breast cancer and metastatic non-small cell lung cancer (NSCLC).

Clinical phase II studies investigating the response of GC patients to treatment with cetuximab in combination with various types of chemotherapy showed a promising prolongation of the time to progression and acceptable response rates [196-199]. At present, a multinational phase III trial of

cetuximab plus chemotherapy is ongoing. However, reliable molecular biomarkers that would allow the identification of individuals who are likely to derive a clinical benefit from cetuximab treatment are still unknown.

1.4   Protein Microarrays

The adaption of concepts from genomic analysis has led to the development of protein microarrays that allow large scale analysis of many samples in a high throughput manner [200]. Expression profiling by protein microarrays allows the comprehensive characterization of cellular signaling networks and the identification of critical nodes or interactions. Furthermore, the functional and time resolved analysis of post translational modifications like protein phosphorylation provides essential information about the functional state and dynamic aspects of signaling pathways. These features are essential for the elucidation of tumor biology, the identification of drug targets or development of computer-based molecular models.

1.4.1   Array formats

In principle, protein microarrays consist of immobilized protein spots that are applied on a solid carrier in an array format [200]. Forward phase (FPPA) and reverse phase (RPPA) protein arrays represent the two major classes of protein arrays (Fig. 1.8). In the first case, each spot contains different capture antibodies that are fixed on a solid surface. FPPAs allow the measurement of multiple proteins within one heterogeneous protein sample. The signal detection is performed either by direct labeling of the bound protein or via an enzyme labeled secondary antibody similar to Western blot.

In contrast, in RPPA multiple test samples are immobilized within one array and one particular protein of interest is measured across multiple samples under identical experimental conditions. The signal detection is performed by use of specific primary and enzyme labeled secondary antibodies. Concomitant probing of multiple arrays with different antibodies provides a multiplexed readout.

Common approaches for the signal detection include fluorescence, colorimetric techniques based on silver-precipitation, chemiluminescence and label free Surface Plasmon Resonance. The image of the protein spot pattern can be captured and analyzed by microarray quantification software packages. For each spot, the signal intensity is proportional to the amount of protein.

1.4.2   Advantages

Protein microarrays provide high sensitivity in the femto- to attogram range and allow the multiplexed detection of multiple targets. Due to the miniaturization, only low sample volumes are needed.

Proteins of interest can be analyzed in denatured or native state circumventing problems with antigen retrieval. Protein-protein or protein-DNA interactions can be studied as well.

RPPA provides a high throughput capacity that allows the analysis of a high sample number within a reasonable period of time. The simplicity of the detection protocols and the automation of certain steps make it a robust and reproducible method. Furthermore, when an internal reference standard of known amounts of the investigated protein is included in the analysis, a direct and quantitative measurement of the phosphorylated end point can be attained within the linear dynamic range of the assay [201].
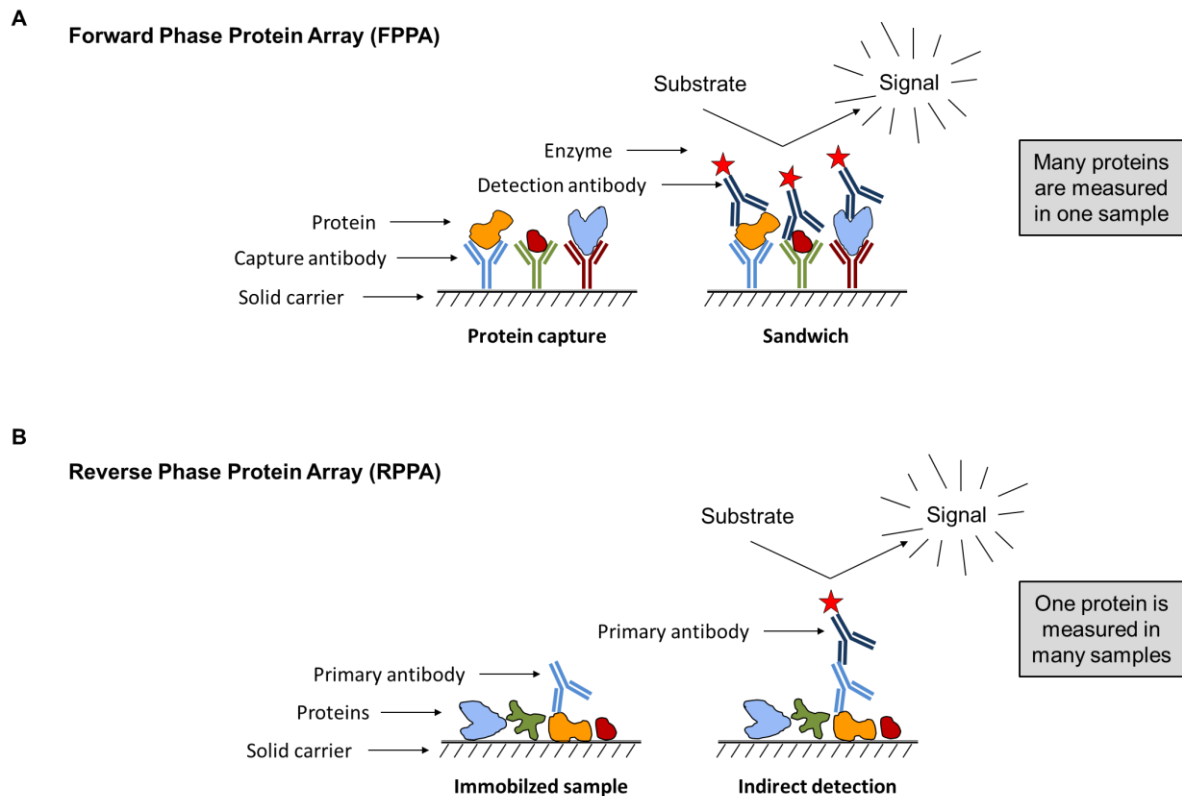
Figure 1.8 The principle of protein microarrays*: A: In forward phase protein microarrays, capture antibodies are immobilized on a solid carrier. Incubation with the sample is followed by the addition of enzyme-labeled secondary antibodies and signal detection. B: In RPPA, the samples are directly spotted and immobilized on a solid carrier, e.g. a nitrocellulose-coated glass slide that can be developed by immunodetection with a primary antibody and an enzyme-labeled secondary antibody similar to Western blot. Depending on the number of replicates and dilution steps, hundreds of samples can be spotted onto one slide. Concomitant probing of multiple slides with different antibodies allows analyzing a huge sample number under identical experimental conditions and provides a multiplexed readout.

1.4.3   Challenges

The detection of a vast range of different protein concentrations is one major analytical challenge for protein microarrays [200]. To facilitate the detection of low abundance proteins, the detection methods must have a much larger range of sensitivity compared to DNA microarrays. It is also important to block endogenous enzymes like peroxidases, biotin, avidin, alkaline phosphatase, which potentially interfere with detection amplification chemistries.

Targeted platforms measure and quantify only known proteins of interest. The availability of highly specific antibodies is therefore another limiting factor for the successful utilization of protein microarrays. Because the dot-blot format does not resolve protein fractions by molecular weight as in gel-based methods, it is crucial to thoroughly validate antibody specificity by detection of a single band in Western blot [202].

1.4.4   Applications & Sample types

Protein microarrays are used for the molecular profiling of cellular material and for the discovery of biomarkers, novel ligands and drugs [203]. It allows the assessment of post translational modifications, and thus the profiling of the activation state of known signaling pathways [204]. The monitoring of total vs. phosphorylated protein over time, before and after treatment, or between disease and non-disease state allows to infer the activity levels of proteins in a particular pathway in real time [200], facilitates the elucidation of dynamic aspects of signaling, and the testing of drug candidates [205].

Protein microarray-based techniques have already been used for extensive studies of a variety of different signaling pathways involved in malignant progression and tumor biology [201] using a variety of different sample types like serum, plasma, body fluids, cell culture supernatants, tissue culture lysates, resected tumor specimens [203].

1.5 Aim of the present study

Complex formation between E-cadherin and EGFR has been reported. Mutations within the extracellular domain of E-cadherin can result in reduced complex formation and enhanced ligand-dependent EGFR activation. These data point to an important role of E-cadherin as effector of EGFR signaling. Furthermore, clinical phase II studies investigating the response of gastric cancer patients to EGFR-inhibiting cetuximab treatment in combination with various types of chemotherapy showed a promising prolongation of the time to progression and acceptable response rates.

The aim of the present study was to characterize the impact of gastric carcinoma-derived E-cadherin mutations on EGFR signal transduction and on the anti-proliferative effect of cetuximab as a single agent on a panel of gastric cancer cell lines.

For this purpose, the present study addressed the following issues:

- To provide a better understanding of how gastric cancer-related mutation of E-cadherin affects EGFR signaling, the classical EGFR downstream signaling (Akt and MAPK pathway) was analyzed by reverse phase protein microarray. Phosphotyrosine specific antibodies as well as total protein antibodies were used to study protein phosphorylation and expression kinetics under long-term EGF stimulation in a cell culture model.

- To screen for additional proteins affected by enhanced EGFR activation due to mutant E-cadherin, a commercial forward phase protein microarray was applied using the same cell culture model. The activation levels of RTKs as well as intracellular signaling components were analyzed after EGF-stimulation. Screening results were confirmed by independent experiments and selected target proteins were further evaluated.

- To investigate the impact of E-cadherin on the anti-proliferative effect of cetuximab as a single agent and to identify potential biomarkers for the response, a panel of gastric cancer cell lines expressing different levels of EGFR was used. In approximation of the clinical situation, the activity of cetuximab was also tested in combination with chemotherapy in selected cell lines.

2 MATERIAL AND METHODS

2.1 Cell culture

2.1.1 Cell lines

For the investigation of E-cadherin mutation the originally E-cadherin negative cell line MDA-MB-435S (American Type Culture Collection (ATCC) No. HTM-129™) was already previously transfected with *wt* or *del 8* E-cadherin cDNA, and stable transfectants were established [155]. Although the MDA-MB-435S cell line derives from pleural effusion of a female with metastatic, ductal adenocarcinoma of the breast [206], gene expression analysis and single nucleotide polymorphism (SNP) array analysis revealed that it more closely resembles a melanoma cell line [207, 208]. Until now it is a matter of debate whether MDA-MB-435 is a breast cancer or a melanoma cell line.

In order to investigate the sensitivity to cetuximab, a panel of five gastric cancer cell lines was used. AGS cells derived from diffuse type adenocarcinoma of the stomach (AGS European Collection of Cell Cultures (ECACC), # 89090402) [209]. The signet ring cell carcinoma cell line KATOIII was isolated by pleural effusion (ECACC, # 86093004) [210]. MKN1 cells derive from lymph node metastasis of adenosquamous (Riken Biosource Center, # RCB1003) and MKN28 cells (Institut für klinische Pharmakologie, Med. Uni Wien) from lymph node metastasis of tubular gastric cancer [211]. MKN45 (II. Medizinische Abteilung, Klinikum rechts der Isar München) were isolated from liver metastasis of a diffuse type adenocarcinoma [211]. As a positive control for EGFR and E-cadherin expression the human epidermoid carcinoma cell line A431 was used (ATCC No. CRL - 1555™) [212].

2.1.2 Cultivation

Human cancer cell lines were cultured in an incubator at 37°C, 5% CO_2 and relative humidity of 95%. Cell lines MDA-MB-435S and A-431 were maintained in Dulbecco's Modified Eagle's Medium (DMEM, # 31966-021, Gibco) and cell lines MKN1, MKN28, MKN45, AGS and KATOIII were maintained in RPMI1640. All cell lines were cultured in the presence of 10% (v/v) fetal calf serum (FCS, # 3302-P260317, PAN Biotech) and 1% penicillin/streptomycin (v/v), in order to avoid bacterial contamination (10,000 units/ml penicillin G sodium/10,000 μg/ml streptomycin sulphate; # 15140-122, Gibco). Culture medium of transfected cells was additionally supplemented with Geneticin G418 sulfate (600 mg/l, # 11811-031, Gibco), which served as selection antibiotic to only allow growth of transfected cells.

2.1.3 Passaging

In order to keep cells in the phase of exponential growth, they were split at least twice a week, when they reached a confluence of about 70-80%. Therefore, culture medium was aspirated and cells were washed with PBS (without Ca^{2+}/Mg^{2+}, # H15-002, PAA Laboratories) to completely remove remaining FCS, which inhibits enzymatic activity of Trypsin/EDTA (# L11-004, PAA Laboratories). Then, cells were detached with 0.5 or 1 ml Trypsin/EDTA, depending on the size of the culture flask, for approximately 5 min at 37 °C. Finally, cells were harvested in culture medium and split in an appropriate ratio in a new tissue culture flask. All reagents were equilibrated at 37°C in a water bath prior to use. If cells were seeded for an experiment, detached cells were transferred to a falcon tube and the cell count was determined with the CASY cell counter. The demanded cell number was then pipetted in a separate culture vessel and remaining cells were transferred to a new tissue culture flask for cultivation as described above.

2.1.4 Cryopreservation

For long-term storage, aliquots of every cell line were stored in liquid nitrogen at -196°C. Stocks were frozen at early passage numbers, in order to ensure constant quality of the cells. Briefly, after removal of the cell culture medium, the cells were washed with PBS and detached with Trypsin/EDTA. Trypsin was inactivated by addition of FCS-containing culture medium and $5x10^5$ cells were suspended in 1 ml culture medium containing 10% (v/v) FCS and 10% (v/v) cryo-protective DMSO (# 20385, Serva). The aliquots were transferred to a freezing container filled with 100% isopropyl alcohol and stored at -80°C over night to achieve a cooling rate of about 1°C/min. The next day, the vials were directly transferred to liquid nitrogen.

2.1.5 Thawing

As cells with high passage numbers may change growth behavior and morphology, fresh cells were thawed after 30 passages. Frozen cells were briefly thawed at 37°C in a water bath, and the cells were transferred to 10 ml of culture medium containing 10% FCS. In order to remove the cytotoxic DMSO, cells were centrifuged at 1000 rpm for 5 min and the pellet was suspended in fresh culture medium. All reagents were equilibrated at 37°C in a water bath prior to use, and cells were cultured as described above.

2.1.6 Mycoplasma detection assay

A mycoplasma detection assay was routinely performed after thawing of cells, in order to document the absence of contaminations. Usually, cell culture contaminations with prokaryotic mycoplasma remain undetected for a long time, but can have severe effects on cultured cells. They interfere with cell metabolism and thereby impair cell growth. Further they can disturb cellular signaling and by destabilizing chromosomes they can induce apoptosis and facilitate acquisition of mutations. Hence, it is crucial to make sure the used cells are free of contaminations.

A nested polymerase chain reaction (PCR) protocol (Takara Bio Inc., Saint-Germain en Laye, France) allows detection of multiple mycoplasma strains from cellular supernatants (Table 1).

Table 1 Mycoplasma that can be detected (amplicon size)

Strain	1st PCR (bp)	2nd PCR (bp)
M. hyopneumoniae	681	237
M. neurolyticum	501	196
M. fermentans	491	195
M. hyorhinis	448	211
M. orale	423	179
M. arthritidis	408	157
M. salivarium	403	151
M. hominis	370	147
M. arginini	369	145

Prior to collection of the supernatants, cells should have grown at least 3 days to a confluence of about 90%. After boiling at 96 °C for 5 min and removal of debris by centrifugation at 13,000 rpm for 5 s, 10 µl of each supernatant are used as template for the first PCR. Then, 1 µl of the first PCR product is used as template for the second PCR. Reagents for both PCRs were mixed according to Table 2 and DNA was amplified following the indicated cycler program (Table 3).

Table 2 PCR mixes

Reagent	1st PCR	2nd PCR
aqua dest.	24.5 µl	33.5 µl
10×Buffer (15 mM Mg^{2+})	5 µl	5 µl
dNTPs (1.25 mM each; # 803-0007, Applied Biosystems)	8 µl	8 µl
Primer-Mix 1	2 µl	2 µl
Taq-Polymerase (5,000 U/ml; # 27079906, GE Healthcare)	0.5 µl	0.5 µl
template	10 µl	1 µl
FINAL VOLUME	**50 µl**	**50 µl**

Table 3 Thermo cycler program

Temperature (°C)	Time (min)	Cycles
94	4	-
94	0.5	35
55	2	
72	1	
72	7	-
4	∞	-

To ensure technical correctness and reagent purity, a positive control and negative control (without template) sample were included in the analysis. After the second PCR, 10 µl of its product were mixed with 5x DNA loading buffer, loaded onto a 1.5 % agarose gel (# 840006, Biozym) containing 0.1 µg/ml ethidium bromide (# 0492, Amresco) and separated at 120 V for 30 min. Finally, DNA fragments were visualized at a wavelength of 312 nm by use of an Eagle Eye II UV- trans-illuminator (Stratagene, La Jolla, USA).

2.2   Protein extraction

For protein extraction from gastric cancer cells, L-CAM buffer was freshly prepared prior to lysis from a 10x stock. Table 4 and 5 show the components and their concentration of the stock solution and the lysis buffer. MDA-MB-435S cells were extracted by use of the commercial lysis buffer # 6 (R&D Systems Europe, Abingdon, United Kingdom).

Table 4 Composition of the L-CAM lysis buffer stock solution (10x)

Component	Cat. No	Supplier
140 mM NaCl	# 1.06404.5000	Merck, Darmstadt, Germany
47 mM KCl	# 1.04936.0500	Merck, Darmstadt, Germany
7 mM MgSO4	# 80309	Sigma, Steinheim, Germany
12 mM CaCl2	# 1016	Sigma, Steinheim, Germany
10 mM Hepes pH 7.4	# 3375	Sigma, Steinheim, Germany

Cells were seeded at densities of 2×10^5 to 2×10^6 cells per 10 cm tissue culture dish and incubated at 37°C and 5% CO_2 until they attached to the surface. Subsequent to starvation for 16 h, cells were stimulated with 100 ng/ml EGF, Sigma-Aldrich Biochemie GmbH, Hamburg, Germany) for the indicated period of time. For experiments with cetuximab (Merck, Darmstadt, Germany), 24 h after seeding, cetuximab was added at concentrations between 0 and 200 µg/ml to the culture medium. After additional 48 h of treatment, the cells were lysed. After three consecutive washing steps with

ice-cold PBS without Ca^{2+}/Mg^{2+} (PAA Laboratories GmbH, Cölbe, Germany), lysis was performed on ice with 100-200 µl of the above mentioned lysis buffers # 6. Subsequent to 30 min of incubation at 4°C to ensure efficient protein extraction and centrifugation at 13000 rpm (4°C) for 10 min, lysates were denatured for 5 min at 95°C. Aliquots were used for the determination of the protein concentrations (see 2.3) and samples designated for use in Western blot were mixed with Laemmli buffer prior to denaturation. Finally, samples were immediately snap frozen in liquid nitrogen for long term storage at −80°C.

Table 5 Composition of the L-CAM lysis buffer (1x)

Component	Cat. No	Supplier
10 % (v/v) 10 x L-CAM	-	-
1 % (v/v) Triton X-100	# 648462	Merck, Darmstadt, Germany
2 mM PMSF	# 7626	Sigma, Steinheim, Germany
2 mM Na_3VO4	# 6508	Sigma, Steinheim, Germany
19 µg/ml Aprotinin	# 6279	Sigma, Steinheim, Germany
20 µg/ml Leupeptin	# 2032	Sigma, Steinheim, Germany
10 mM $Na_4P_2O_7$ x10 H2O	# 221368	Sigma, Steinheim, Germany
10 mM NaF	# 7920	Sigma, Steinheim, Germany

2.3   Bradford Protein assay

The total protein concentration of cellular lysates was determined by use of the Bradford protein assay. This method is based on an absorbance shift of a Coomassie Brilliant Blue G-250 solution from 465 nm (brown) to 595 nm (blue) due to protein binding, This shift corresponds to the protein content of the sample. Briefly, one part of Protein Assay Dye Reagent Concentrate (# 500-0006, Bio-Rad) was diluted with four parts aqua dest. Dilutions of known concentration (1.48 µg/ml, 4.44 µg/ml, 7.4 µg/ml, 10.36 µg/ml) of Protein Standard II (1.48 mg BSA/ml, # 500-0007, Bio-Rad) were prepared in this reagent for later calculation of a standard curve. For each sample 2 µl of protein extract were added to 998 µl Protein Assay Dye Reagent (dilution 1:500) and after 5 min of incubation at room temperature, absorbance was measured at 595 nm in a UV/VIS spectrophotometer. Finally, standard curve was used for calculation of the relative protein concentrations of the samples.

2.4   SDS-polyacrylamide gel electrophoresis and Western blot analysis

Between 10 and 30 µg of total proteins were separated by SDS-polyacrylamide gel electrophoresis under reducing conditions and transferred to PVDF (GE Healthcare, München, Germany) or nitrocellulose membranes (Schleicher & Schuell, Dassel, Germany). After 1 h of blocking, the

membranes were probed with appropriate primary antibodies overnight at 4°C (Table 7). Detection was performed with horseradish peroxidase-conjugated secondary antibodies using enhanced chemiluminescence (Amersham, Braunschweig, Germany). For signal quantification, blots were scanned and densitometric analysis was performed using Scion Image Software V. beta 4.0.2 (Scion Corporation, Frederick, MD, USA).

2.4.1 Buffers and solutions for Western blot analysis

Gel formulations for SDS-PAGE

Component	Stacking gel	Separation gel (10%)
Aqua dest.	3.05 ml	7.33 ml
0.5 M Tris (pH 6.8)	-	3.75 ml
1 M Tris (pH 8.8)	1.25 ml	-
40 % Acrylamid/Bis (# 161-0148, Bio-Rad)	0.63 ml	3.75 ml
20 % SDS (# A0675.1000, AppliChem)	25 µl	75 µl
10 % APS (# A7460, Sigma-Aldrich)	40 µl	90 µl
TEMED (# 161-0801, Bio-Rad)	4 µl	9 µl

5 × Laemmli buffer:

Component	Cat. No	Supplier
60 mM 1.25 M Tris-HCl (pH 6.8)	-	-
8.7 % (v/v) Glycerol	# 1.04092.1000,	Merck, Darmstadt, Germany
720 mM 2-Mercaptoethanol	# 7154	Sigma, Steinheim, Germany
2 % (w/v) SDS	# 151213	USB
80 µg/ml Bromphenol blue	# 5525	Sigma, Steinheim, Germany

10 × SDS running buffer:

Component	Cat. No	Supplier
0.25 M Tris base	# 75825	UBS, Cleveland, Ohio, USA
1.92 M Glycine	# 1.04201.1000	Merck, Darmstadt, Germany
1 % (v/v) 20 % SDS solution	# A0675.1000	AppliChem, Darmstadt, Germany

The buffer was stored at room temperature

10 × Transfer buffer:

Component	Cat. No	Supplier
0.25 M Tris base	# 75825	UBS, Cleveland, Ohio, USA
1.92 M Glycine	# 1.04201.1000	Merck, Darmstadt, Germany
1 % (v/v) 20 % SDS solution	# A0675.1000	AppliChem

The buffer was stored at room temperature. For use 100 ml of 10 x transfer buffer were diluted with 700 ml aqua dest. and 200 ml methanol (# 1.06009.1000, Merck).

10 × TBS (pH 7.3):

Component	Cat. No	Supplier
0.5 M Tris base	# 75825	UBS, Cleveland, Ohio, USA
1.5 M NaCl	# 1.06404.5000	Merck, Darmstadt, Germany

The pH was adjusted, the buffer was autoclaved and stored at room temperature. For a ready use solution of TBST, 1 x TBS was supplemented with 0.1% v/v Tween-20 (# 8.22184.1000, Merck). The buffer was stored at room temperature.

Blocking buffer:

TBST supplemented with the indicated percentage of non-fat dried milk (# 60219, Töpfer) or BSA (# 3912, Sigma). The buffer was prepared freshly before use and stored at 4 °C for.

2.4.2 Antibodies

Table 6 Comprehensive information about the antibodies used in the present study

Protein	Cat.Nr.	Species	Dilution	Blocking/Diluent	Source
EGFR	# 2232	Rabbit	1:2,000	5% BSA	CST, Danvers, USA
pEGFR (Y1068)	# 447886	Rabbit	1:2,000	TBST	Invitrogen,Carlsbad, USA
pEGFR (Y1086)	# 2220	Rabbit	1:2,000	TBST	CST, Danvers, USA
pMET (Y1234/Y1235)	# 3077	Rabbit	1:1,000	5% non-fat dried milk	CST, Danvers, USA
Erk1/2	# 9102	Rabbit	1:1,000	5% BSA	CST, Danvers, USA
pErk1/2 (Y204/T202)	# 9101	Rabbit	1:1,000	5% BSA	CST, Danvers, USA
Akt	# 9272	Rabbit	1:1,000	5% BSA	CST, Danvers, USA
pAkt (S473)	# 9271	Rabbit	1:1,000	5% BSA	CST, Danvers, USA
pSrc (Y416)	# 2101	Rabbit	1:2,000	10%non-fat dried milk	CST, Danvers, USA
pSrc (Y529)	# 2105	Rabbit	1:2,000	10%non-fat dried milk	CST, Danvers, USA
E-cadherin	# 610182	Mouse	1:5,000	5% non-fat dried milk	BD,Pharmingen, USA
β-catenin	# 610154	Mouse	1:2,000	5% non-fat dried milk	BD Biosciences
β-actin	A1978	Mouse	1:5,000	5% non-fat dried milk	Sigma
α-tubulin	T9026	Mouse	1:5,000	5% non-fat dried milk	Sigma
anti-mouse IgG-HRP	# NA931	Sheep	1:10,000	5% non-fat dried milk	GE Healthcare
Anti-rabbit IgG-HRP	# 7074	Goat	1:10,000	5% non-fat dried milk	CST, Danvers, USA

2.4.3 Stripping

Blots to be stripped were rinsed with TBST, placed in Restore™ Western Blot Stripping Buffer (# 21059, Pierce) and incubated for 15 min at room temperature. Thereafter the blots were washed again 3x10 min in TBST and subjected to immunodetection. Membranes that were not stripped immediately after chemiluminescent detection were stored in PBS at 4°C until the stripping procedure was performed.

2.5   Protein microarrays

2.5.1   Reverse Phase Protein Microarray

2.5.1.1   Spotting

Protein lysates were printed in triplicates and in a miniature dilution curve (starting from 2 µg/µl, 1:2, 1:4, 1:8, 1:16, and buffer) onto "Oncyte Avid" nitrocellulose film slides (Grace Bio-Labs, Bend, OR, USA) with the BioOdyssey™Calligrapher™ MiniArrayer (Biorad, Muenchen, Germany). Serial dilution of the samples (resulting in 3*6 =18 data points per sample) ensured the robustness of the experimental design and the signal detection in the linear dynamic range. Miniaturization minimized the required amounts of sample.

2.5.1.2   Signal detection

Immunodetection was performed similar to Western blot, using the ECLPlus and ECLadvance Western Blot Detection Systems (GE Healthcare Europe, Muenchen, Germany). Briefly, after equilibration of the slides for 5 min in TBST, they were blocked in a peroxidase blocking solution (Dako, 3ml per slide) at room temperature, and after 3 consecutive washing steps in TBST for 2 min, slides were blocked in 5% milk powder to prevent unspecific antibody binding. The specific antibodies were then applied at the concentrations listed in table 2 and slides were incubated overnight at 4°C. The antibodies used were tested for their specificity in Western blot prior to use in RPPA, which is crucial due to the lack of size discrimination in RPPA. The next day, slides were washed in 3 consecutive steps with TBST for 15 min and the adequate secondary antibodies were added for 1 h (see table 2). After a final washing step, each slide was submerged for 3 min in 250 µl of an ECL-mixture (2:1 ECL Plus: ECL advanced). Finally, slides were exposed to an X-ray film and chemiluminescent signals were detected.

2.5.1.3   Signal quantification

Developed films were scanned with a resolution of 1200 dpi (Scanjet 3770, Hewlett-Packard, Hamburg, Germany) and greyscale images were saved in TIFF format. Density of protein spots was analyzed by the microarray data processing software Microvigene 3.5.0.0 (VigeneTech, Carlisle, MA, USA).

2.5.1.4   Data interpretation

For compensation of unequal loading and to ensure proper data evaluation, relative expression levels of proteins were calculated by normalization to arrays probed in parallel with antibodies directed against the HKPs α-tubulin (mouse monoclonal Ab # T6199, Sigma-Aldrich Chemie GmbH, Steinheim, Germany; dilution 1:10,000) and β-actin (mouse monoclonal Ab # A1978, Sigma-Aldrich Chemie GmbH; dilution 1:7,000). To validate this approach, data of 72 samples obtained from normalization with HKPs were compared with data obtained from normalization with a total protein stain, Fast Green FCF (# 44715, Sigma-Aldrich). To allow statistical analysis, three individual biological replicates were analyzed.

2.5.2   Forward Phase Protein Microarray

For the screening of protein phosphorylation, two commercial forward phase protein microarrays were used (Human Phospho-Kinase Array Kit # ARY003 and Human Phospho-RTK Array Kit # ARY001, R&D Systems). Both represent rapid, sensitive, and economical tools to simultaneously detect the relative levels of protein phosphorylation sites without performing numerous experiments. Capture and control antibodies are spotted in duplicate on nitrocellulose membranes.

2.5.2.1   Signal detection

The assays were performed according to the manufacturers´ instructions. After 1 h of blocking the membranes with the provided array buffer, 100 µg of the protein lysates were pipetted to the membranes and incubated overnight at 2-8°C on a rocking platform shaker. Subsequent to washing a total of 3 times with the provided wash buffer, a cocktail of biotinylated detection antibodies was pipetted on the membranes and incubated for 2 h at room temperature on a rocking platform. After another washing step the HRP-conjugated streptavidin solution was added to each well and incubated for 30 min at room temperature on a rocking platform. After a final round of washing, signal detection was performed by exposure of the membranes to a film.

2.5.2.2   Signal quantification

The developed films were scanned with a resolution of 1200 dpi (Scanjet 3770, Hewlett-Packard, Hamburg, Germany) and greyscale images were saved in TIFF format. Density of protein spots was analyzed as described in 2.5.1.3. The signals were identified by placing the transparency overlay on the array image and aligning it with the positive control spots on each membrane. The signal intensity of the capture spots corresponds to the amount of phosphorylated bound protein. For signal

quantification, an averaged background signal deriving from negative control spots was subtracted from each capture spot and signals were normalized to the positive control spots.

2.6   Flow Cytometry analysis

Cells were seeded at a density of 6 x 10^5 cells per 10-cm tissue dish and cultured for 48 h. After washing with PBS (without Ca^{2+}/Mg^{2+}), cells were detached using 1.5 ml Versene (Invitrogen/Gibco) for 15 min at 37°C. Detached cells were resuspended in-ice cold washing buffer (consisting of PBS (without Ca^{2+}/Mg^{2+}), 0.1% (w/v) sodium azide (Merck, Darmstadt, Germany), and 0.1% (w/v) bovine serum albumin (BSA; Sigma-Aldrich, Steinheim, Germany). After two additional washing steps (each comprising (i) resuspension of cells in washing buffer, (ii) sedimentation at 310 x g (4°C) for 5 min and (iii) removal of the supernatant), cells were incubated with 50 µl of monoclonal antibody directed to EGFR (Ab-1, clone 528, Thermo Fisher Scientific, Ulm, Germany; 2.5 µg/ml) or E-cadherin (SHE78-7, Takara Bio Inc., Shiga, Japan; 5 µg/ml) in 96-well microtiter plates. Additionally, an isotype control antibody (IgG2a, clone PPV-04, Exbio, Prague, Czech Republic, distributed by BIOZOL (Eching, Germany); 5 µg/ml) was routinely applied. After incubation for 1 h at 4°C, the cells were washed twice as described before and incubated with 50 µl of the secondary antibody solution (Alexa Fluor 647 F(ab)2-fragment (H+L), Invitrogen, 5 µg/ml) for 1 h (4°C) in the dark. Two washing steps were performed to remove unbound secondary antibodies. The cells were then resuspended in 200 µl of the washing buffer and subsequently analyzed using a FACSCanto flow cytometer (BD Bioscience, Heidelberg, Germany). For live-dead discrimination of the cells, 2 µg/ml propidium iodide was added to each sample directly before measurement.

2.7   Immunofluorescence staining

In total, 1 x 10^5 cells per 6-well were grown on cover slips for 48 h. After two washing steps with PBS (with Ca^{2+}/Mg^{2+}) (PAA Laboratories), the cells were fixed and permeabilized with ice-cold methanol (Merck) for 6 min at room temperature. Subsequently, the cells were washed thrice with PBS (with Ca^{2+}/Mg^{2+}) and then incubated with primary monoclonal antibodies directed to EGFR (10 µg/ml, Ab-1, clone 528, Thermo Fisher Scientific, Ulm, Germany) or E-cadherin (8 µg/ml, HECD-1, Alexis Biochemicals, Lörrach, Germany) for 16 h (4°C). Unbound primary antibodies were removed by washing twice with PBS (with Ca^{2+}/Mg^{2+}) before the polyclonal FITC-conjugated secondary antibody (Zymax Grade, Invitrogen) was added; the samples were incubated for 1 h in the dark to visualize the marked proteins (for EGFR detection: 10 µg/ml; for E-cadherin detection: 7.5 µg/ml). Additionally, cell nuclei were stained using the DNA-binding fluorescent dye DAPI (Sigma-Aldrich; 20 µg/ml). Finally, the cells were washed once with PBS (with Ca^{2+}/Mg^{2+}), transferred into distilled H_2O and embedded in Vectashield mounting medium (Vector Laboratories, Burlingame, USA). The cells were

analyzed using an Axiovert 200M epifluorescence microscope (Carl Zeiss AG, Jena, Germany) coupled with an apotome and the high-resolution camera AxioCam MRc. For magnification, a 63x DIC water immersion objective was used. Image analysis was performed with AxioVision Rel. 4.6 software from Zeiss.

2.8   XTT cell proliferation assay

To determine the cellular sensitivity towards cetuximab alone and in combination with chemotherapy, a modified US National Cancer Institute (NCI, Bethesda, MD, USA) protocol for *in vitro* cancer screens was used [213]. The XTT cell proliferation kit II (Roche Diagnostics, Mannheim, Germany) was used according to the manufacturer's instructions to assess growth inhibitory effects. According to the individual doubling times of the different cell lines, cells were plated at densities between 1×10^3 and 4×10^3 cells per well in 75 µl of culture medium. After 24 h of incubation at 37°C and 5% CO_2, cetuximab was added at concentrations between 0 and 200 µg/ml in 25 µl of culture medium. 5-FU and cisplatin combination chemotherapy was applied at levels achievable in tumor tissues (0.5 µg/ml cisplatin and 0.05 µg/ml 5-FU; [214]). Additionally, a five-fold increase in the concentration was used to enhance the growth inhibition. When chemotherapy and cetuximab were combined, cetuximab was applied at a concentration of 100 µg/ml, which is comparable to the active drug concentrations achieved in cancer patients [215-217].

Subsequent to 48-hof incubation, 50 µl of the XTT labeling mixture were added per well, and after 2 h at 37°C and 5% CO_2, the absorbance of the samples was measured at a wavelength of 492 nm and a reference wavelength of 620 nm using a microplate reader (Asys Expert Plus, Biochrom, Berlin, Germany). A growth control (GC) and an isotype control antibody (ISO) were used to confirm the specificity of the measured effects. Cetuximab specific effects were confirmed by using a IgG1κ isotype control antibody (Southern Biotech, Birmingham, USA, distributed by Biozol) and a solvent control for cells grown without antibody (8.48 mg/ml NaCl, 1.88 mg/ml Na2HPO4•7H$_2$O, 0.41 mg/ml NaH2PO4•H$_2$O). Furthermore, untreated cells were included to monitor growth characteristics.

2.9   Statistical analysis

2.9.1   RPPA experiments

For RPPA experiments, comparison between cell lines was performed at a significance level of p=0.05 by use of mixed linear models and spline functions for approximation of temporal trends with the statistical software package R (The R Foundation for Statistical Computing, Vienna, Austria).

Comparison between cell lines was calculated over the entire observation period for expression data and around peaks for activation data (0-30 min for EGFR and Akt, 0-45 min for Erk1/2).

In addition to the analysis performed in the present study, RPPA data are also analyzed by state of the art bioinformatics, in order to gain further insights into the biology underlying the observed protein activation profiles. This analysis is currently ongoing at the Institute of Bioinformatics and Systems Biology at the Helmholtz Zentrum München.

2.9.2 Cetuximab sensitivity

For the cetuximab studies the distribution of data is presented as the means ± SD. Pairwise comparisons were performed using two-sided Welch's t-tests at a significance level of 0.05 with the statistical software package R (The R Foundation for Statistical Computing, Vienna, Austria). A summary of all statistical data is presented in supplementary tables 2-8. Bivariate relationships were analyzed by the Spearman rank correlation test using SPSS, version 19.0 (SPSS, Inc, Chicago, IL, USA). Two-side p-values below 0.05 were considered to be statistically significant.

3 RESULTS

3.1 Analysis of EGFR downstream signaling by RPPA*

3.1.1 Establishment and validation of the RPPA protocol

The protocol established for the present study is depicted in Fig. 3.1. First, the specificity of the chosen antibodies had to be assessed by Western blot, because the dot-blot format of the RPPA does not allow size discrimination, which would allow protein identification. The antibody specificity was determined on the E-cadherin-negative MDA-MB-435S carcinoma cell line after stable transfection with the empty vector (*pBat*), *wt* or *del 8* E-cadherin, which were used later in the RPPA experiments. Protocols have been optimized for all eleven antibodies used in the present study. As illustrated in Fig. 3.2, all antibodies showed specific bands at the expected molecular weight in the Western blot analysis. Several characteristic bands were observed for E-cadherin and the extracellular signal-regulated protein kinase (Erk1/2).
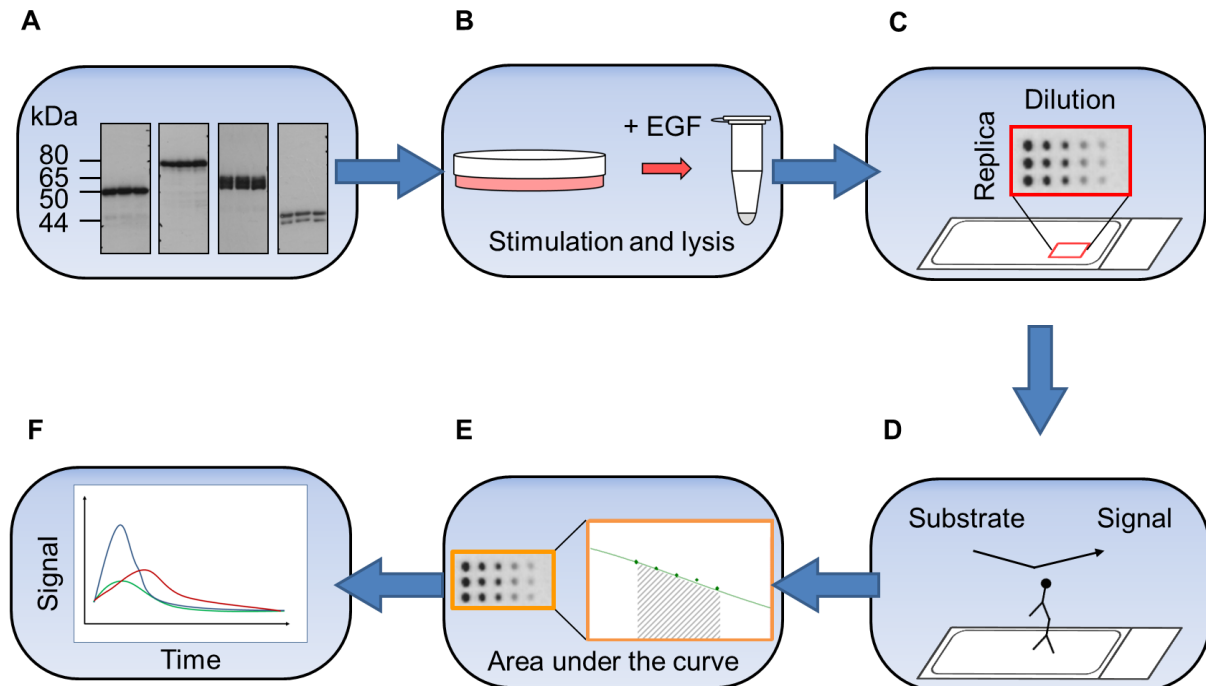
Figure 3.1 The established RPPA workflow: A: Prior to use in RPPA, the specificity of each antibody has to be demonstrated by exhibiting only specific bands at the expected molecular weight in Western blot. B: Cells are grown, stimulated with EGF and lysed according to a standardized protocol. C: The samples are directly spotted in an array format (3 replica and 6-point dilution) onto nitrocellulose-coated glass slides. D: Each slide is developed by use of a specific antibody and the signal detection is performed by indirect chemiluminescence similar to Western blot. E: The commercially available microarray processing software Microvigene is used for signal quantification. F: Finally, the generated data can be interpreted.

38
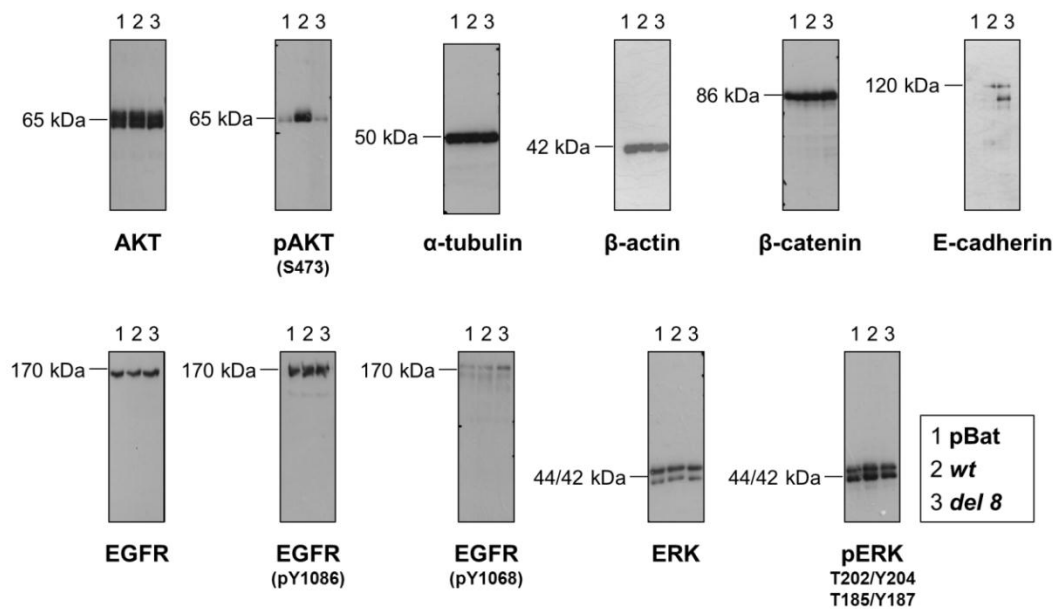
Figure 3.2 Antibody validation by Western blot: As the RPPA does not resolve protein fractions by molecular weight as in gel-based methods, it is crucial to validate the antibody specificity. The specificity of the 11 antibodies that were used in this study were tested by Western blot analysis with the same cellular lysates (of *pBat*, *wt* and *del 8* cells) that were used afterwards in the RPPA. As illustrated, all antibodies exhibited the specific and expected bands and were therefore approved for use in RPPA.

To validate this approach, data of 72 samples obtained from normalization with housekeeping proteins were compared with data obtained from normalization with a total protein stain, Fast Green FCF. A Spearman´s rank coefficient of r_s=0.890 was achieved, which indicates a strong correlation and validates the chosen approach (Fig. 3.3A). To assess the reproducibility of the established RPPA protocol, a total of 12 differently treated samples (*pBat, wt* and *del 8* cells, either starved, EGF stimulated or grown in FCS-containing culture medium) was spotted either twice on the same slide for intra-slide comparison or repeatedly on two individual slides for inter-slide comparison. Subsequently, slides were probed with an antibody directed against pEGFR Y1086 and signals were compared by the Spearman´s rank correlation (Fig. 3.3B and C).
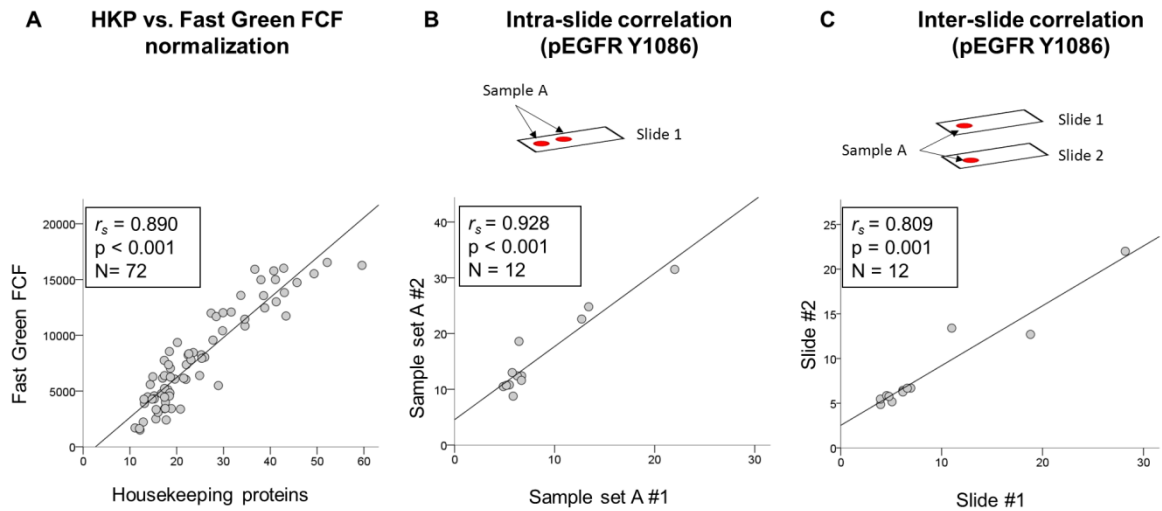
Figure 3.3 Assessment of the reproducibility and the reliability of the established RPPA protocol: A: Normalization with α-tubulin and β-actin was validated by comparison to normalization with the total protein stain, Fast Green FCF. The Spearman´s rank correlation coefficient indicates equal results of both approaches and validates the chosen approach. The reproducibility of the RPPA was assessed by comparison of 12 differently treated samples by intra-slide (B) or inter-slide comparison (C). Coefficients of correlation of rs=0.928 for the intra-slide and rs=0.809 for the inter-slide comparison indicate a high reproducibility of the established protocol.

A coefficient of correlation of r_s=0.928 for the intra-slide (Fig. 3.3B) and of r_s=0.809 for the inter-slide comparison (Fig. 3.3C) were achieved and indicate the high reproducibility of the established protocol. Taken together, a RPPA protocol that provides high robustness and reproducibility was successfully established for the analysis of the EGFR signaling pathway.

3.1.2 Characterization of the E-cadherin and β-catenin expression profiles under EGF stimulation

Together with E-cadherin, β-catenin represents a major constituent of the adherens junction (AJ) complex, which is responsible for the mediation of cell-to-cell adhesion. As an important mediator of the bidirectional crosstalk between E-cadherin and EGFR, the expression profile of β-catenin was monitored by RPPA as well. The E-cadherin expression profiles of the E-cadherin-negative MDA-MB-435S carcinoma cell line after stable transfection with the empty vector (*pBat*), *wt* or *del 8* E-cadherin under EGF stimulation were monitored over time by RPPA. The detected E-cadherin expression profiles differed significantly between all cell lines (Fig. 3.4A, supplementary table 1). This is due to the detection of an additional band in *del 8* cells as mentioned above. However, E-cadherin expression in both E-cadherin-positive cell lines remained almost unchanged and no direct response to EGF stimulation could be detected. Similar to E-cadherin, the expression of β-catenin remained almost unchanged by EGF stimulation and no relevant differences between the cell lines were observed (Fig. 3.4B).
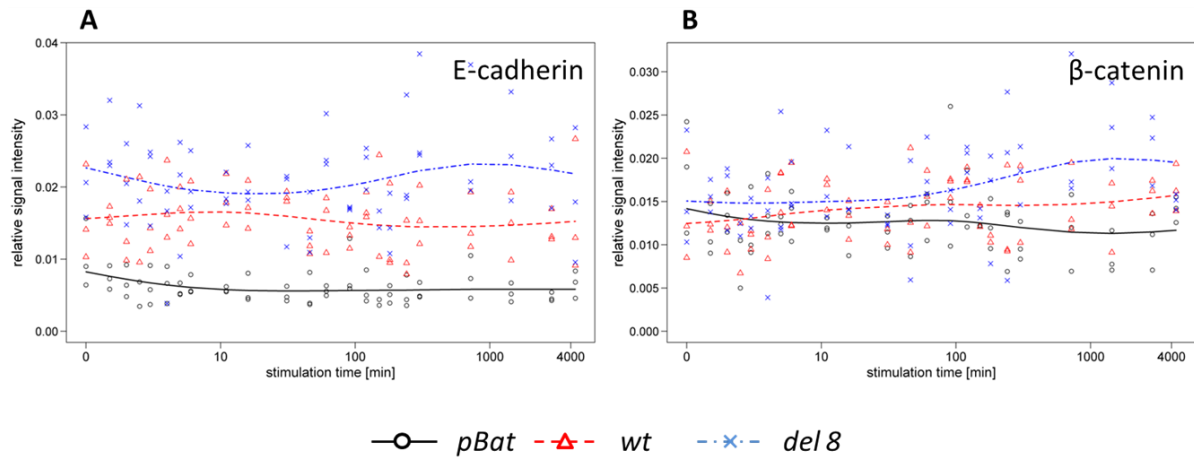
Figure 3.4 E-cadherin and β-catenin expression under long-term EGF stimulation: The changes over time as determined by RPPA of E-cadherin (A) and β-catenin (B) expression are shown for 4320 min (72 h) under EGF stimulation. The figure shows signal intensities (y-axis) of three biological replicates (*pBat*: black circles; *wt*: red triangles; *del 8*: blue crosses) and an approximation of the mean expression profile over time for all cell lines (x-axis [min]; *pBat*: black full line; *wt*: red dashed line; *del 8*: blue chain dotted line). The statistical evaluation of the present results is summarized in Supplementary Table 1.

3.1.3 Impact of E-cadherin mutation on the ligand-dependent EGFR activation

To investigate the effects of the E-cadherin status on the expression and ligand-dependent activation of EGFR, the chosen cell panel was analyzed under long-term EGF stimulation by RPPA.

Detection of phosphorylated tyrosine residues Y1068 and Y1086 of EGFR was used to determine the receptor activation levels. All three cell lines exhibited rapid EGFR phosphorylation at both sites with a maximum at one minute of EGF stimulation. After 5 min, a decline to base line activity was observed (Fig. 3.5A and B). Activation levels differed significantly between all cell lines (Supplementary table 1) and *del 8* cells exhibited the strongest receptor activation. Although individual statistically significant differences between the expression profiles were observed, their informative value remains elusive. Overall, the protein expression seems to be unchanged by EGF stimulation in all cell lines (Fig. 3.5C).

Taken together, these findings indicate a rapid ligand-dependent activation of EGFR in all cell lines, subsequently followed by a decline to base line activity without any recurrence of activation under long-term EGF stimulation. In agreement with previous studies of our group, the in frame deletion of exon 8 of E-cadherin led to enhanced activation of EGFR compared to *wt* cells [218].
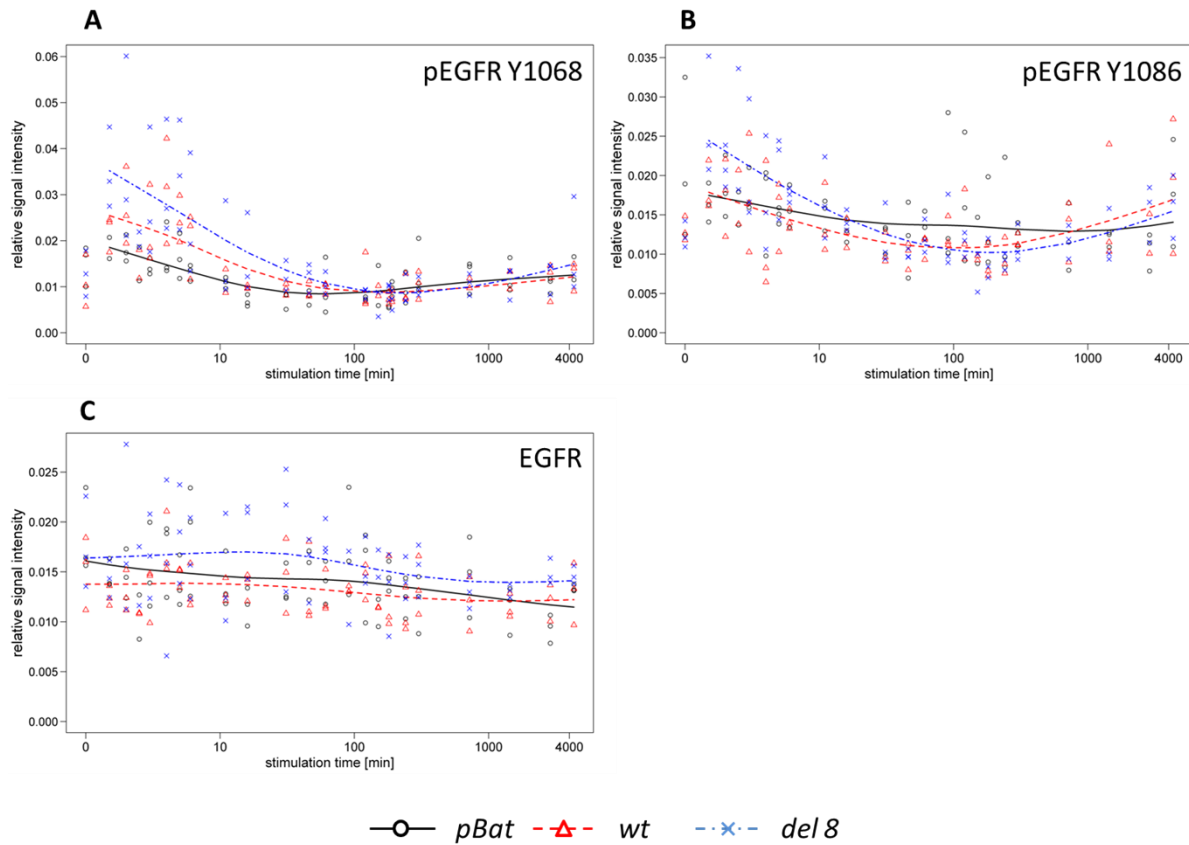
Figure 3.5 EGFR activation and expression under long-term EGF stimulation: The changes over time as determined by RPPA of EGFR activation (A, B) and expression (C) are shown for 4320 min (72 h) under EGF stimulation. The figure shows signal intensities (y-axis) of three biological replicates (*pBat*: black circles; *wt*: red triangles; *del 8*: blue crosses) and an approximation of the mean expression profile over time for all cell lines (x-axis [min]; *pBat*: black full line; *wt*: red dashed line; *del 8*: blue chain dotted line). The statistical evaluation of the present results is summarized in Supplementary Table 1.

3.1.4 Impact of E-cadherin mutation on the EGFR downstream signaling

Outside-in signal transduction via EGFR can occur through different pathways. Of major importance are the PI3K/Akt pathway and the Erk1/2 cascade, also referred to as mitogen activated protein kinase (MAPK) cascade. The impact of E-cadherin mutation on the expression and activation of Akt and Erk1/2, as major representatives of their respective pathways, was analyzed in the chosen cell panel under long-term EGF stimulation.

The activation of Akt was determined by detection of the phosphorylated serine residue S473 located within the activation loop of the protein [219]. While activation with a maximum at five min of stimulation could be shown in *wt* and *del 8* cells, no activation was detected in the E-cadherin-negative *pBat* cell line (Fig. 3.6A). The difference between the activation profiles of *del 8* and *pBat* cells was statistically significant (Supplementary table 1). Akt expression remained constant over the entire observation period and no significant differences between the cell lines were detected (Fig. 3.6B).

Activation of Erk1/2 was determined by simultaneous detection of the phosphorylated key residues in the activation loop [220] of Erk1 (T202/Y204) and Erk2 (T185/Y187). It reached a maximum at ten to fifteen min of stimulation (Fig. 3.6C). No significant differences were found between *pBat* and *wt* cells, but Erk1/2 activation in *del 8* cells was significantly enhanced compared to *pBat* and *wt* cells (Supplementary table 1). Although individual statistically significant differences between Erk1/2 protein expression profiles were observed, their informative value remains elusive. Overall, the protein expression seems to be unchanged by EGF stimulation in all cell lines (Fig. 3.6D).
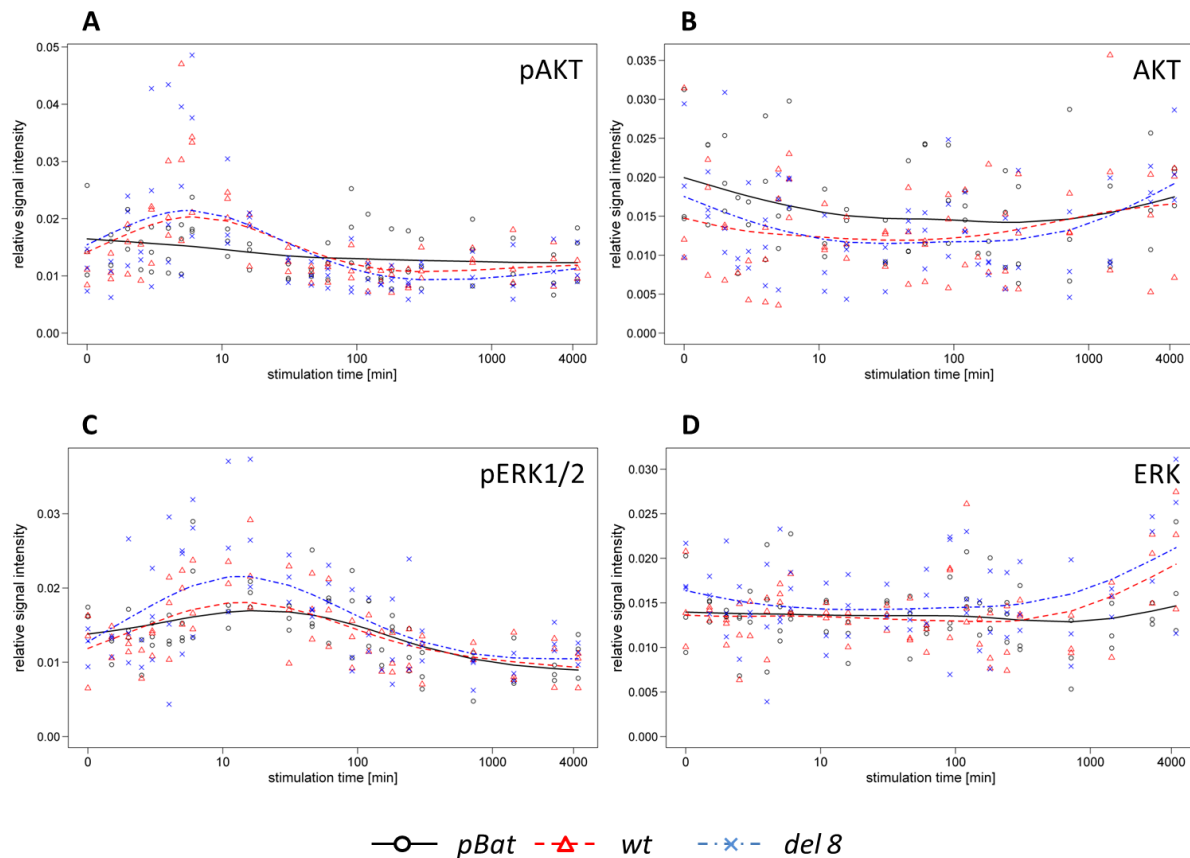
Figure 3.6 Activation and expression of Akt and Erk1/2 under long-term EGF stimulation: The changes over time as determined by RPPA of Akt and Erk1/2 activation (A,C) and expression (B,D) are shown for 4320 min (72 h) under EGF stimulation. The figure shows signal intensities (y-axis) of three biological replicates (*pBat*: black circles; *wt*: red triangles; *del 8:* blue crosses) and an approximation of the mean expression profile over time for all cell lines (x-axis [min]; *pBat*: black full line; *wt*: red dashed line; *del 8:* blue chain dotted line). The statistical evaluation of the present results is summarized in Supplementary Table 1.

Taken together, EGF stimulation led to efficient activation of Akt as well as Erk1/2 in all investigated cell lines, with the exception of Akt in *pBat* cells. The activation maxima could precisely be determined. While activation of Akt occurred rapidly after 5-10 min, maximal activation of Erk1/2 was observed later after 10-15 min. In both cases, the activation was independent of protein expression levels. Ligand-dependent non-recurring activation of Erk1/2 as well as Akt was subsequently followed by decline to base line activity. While no influence of E-cadherin mutation on the activation of Akt

could be detected, enhanced activation of Erk1/2 was found in *del 8* cells. Fig. 3.8 illustrates experimental data, including time information, of previous reports and of the present study showing how the enhanced activation of EGFR is transduced by increased binding of the adapters GRB2 and SHC and Erk1/2 in cells harboring somatic mutation of E-cadherin within the extracellular domain.
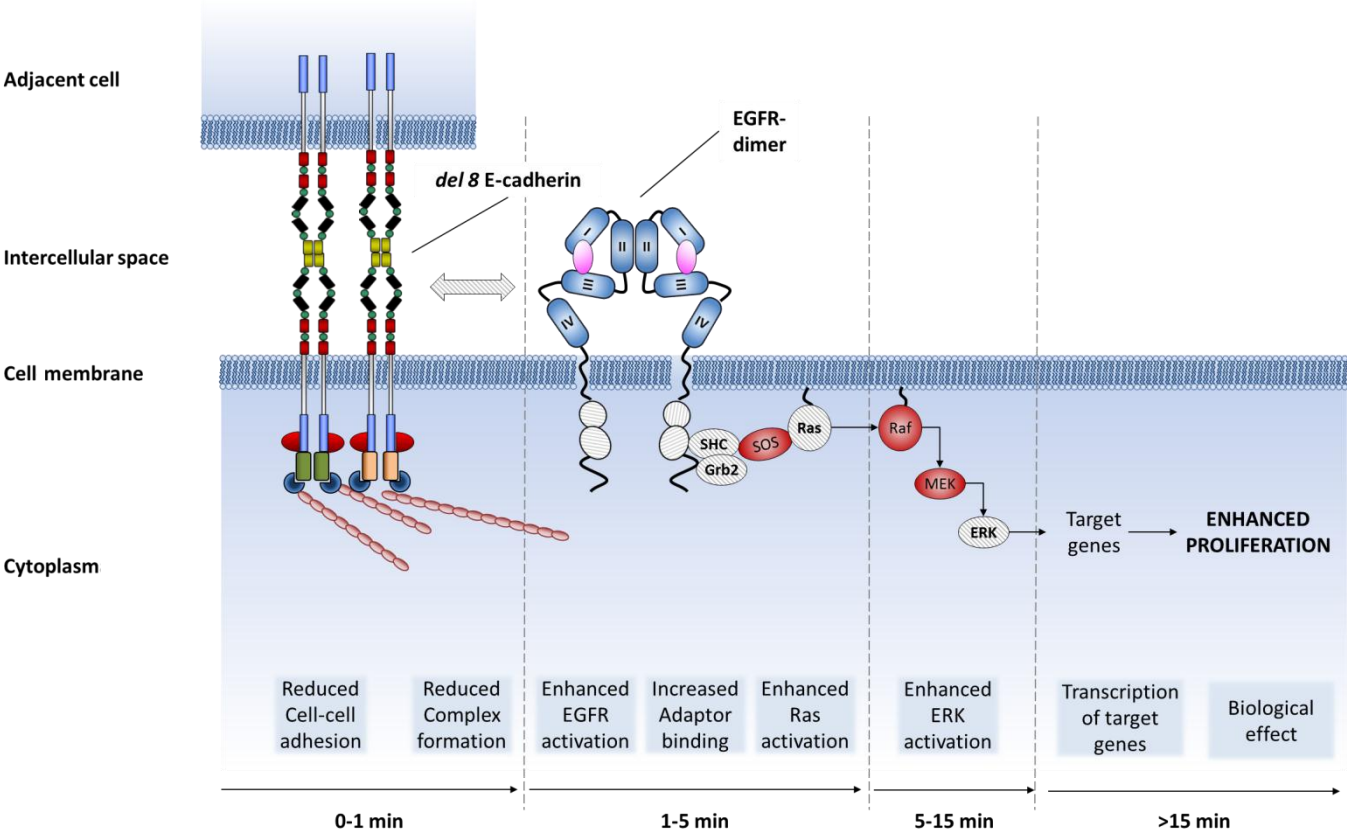
Figure 3.8 Deregulation of EGFR and Erk1/2 signaling by mutation of E-cadherin: This illustration summarizes data of the previous [218] and the present study that indicate deregulation of EGFR and Erk1/2 signaling in cells harboring somatic mutation of E-cadherin within the extracellular domain. Due to such a mutation, changes in the interaction of E-cadherin with EGFR lead to enhanced signaling that is transduced through Erk1/2. Proteins that have been investigated experimentally are shown grey-shaded.

3.2 Analysis of EGFR signaling by forward phase protein microarrays

Multiple studies reveal an important role of E-cadherin in EGFR signal transduction. In order to elucidate the impact of E-cadherin mutation on EGFR-mediated signaling apart from the classical signaling pathway, *wt* and *del 8* cells were analyzed after EGF stimulation by two different commercial FPPAs. The use of phosphospecific antibodies within the arrays allowed determining the activation levels of multiple RTKs and intracellular signaling proteins simultaneously.

3.2.1 RTK proteome profiler

The human Phospho-RTK antibody array was used for the analysis of 42 RTKs in *wt* and *del 8* cells. Protein lysates of the respective cell lines were analyzed after serum starvation and after 1 min of EGF stimulation. As illustrated in Fig. 3.9, the previously detected enhanced activation of EGFR in *del 8* cells could be confirmed by this alternative approach. Furthermore, activation of five additional RTKs (c-RET, EPHA4, EPHB2, HER2 and MSPR) could be detected. Of these, only HER2 showed an EGF-dependent increase of activation in both investigated cell lines, whereas the remaining receptors did not respond to EGF stimulation. Differential activation between *wt* and *del 8* cells was found in none of the detected RTKs.
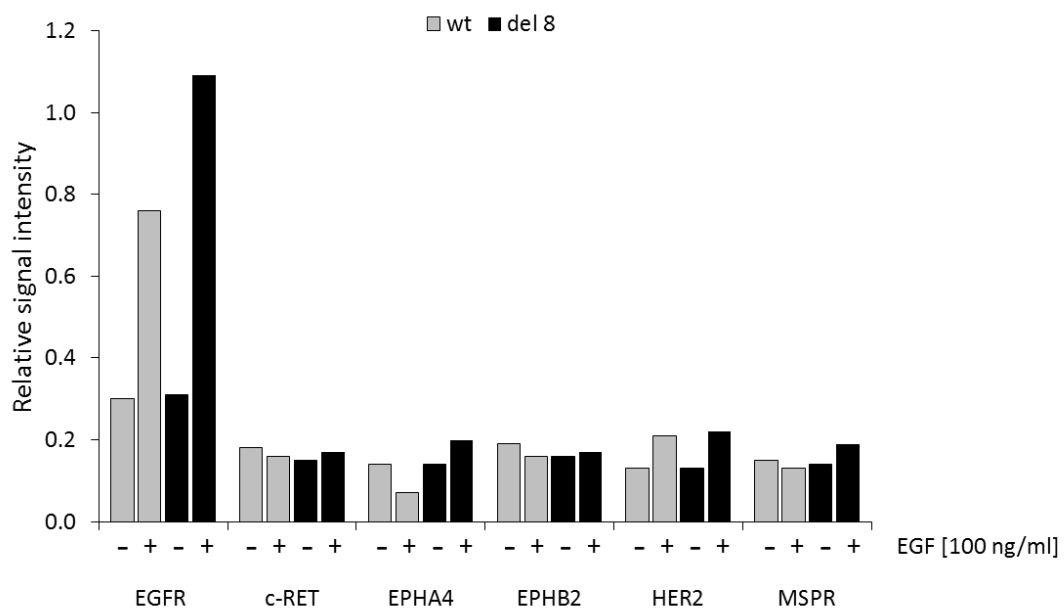
Figure 3.9 EGFR-mediated transactivation of RTKs: The commercial RTK Proteome Profiler protein microarray was used to assess co-activation of multiple RTKs. Activation of six RTKs was detected after starvation and EGF-stimulation. Two of them (EGFR, HER2) showed EGF-dependent induction of activation. EGFR-mediated differential activation was only found for EGFR. Hence, the previous findings showing enhanced EGFR activation after EGF-stimulation in cells harboring mutation of E-cadherin could be confirmed by an alternative approach.

3.2.2 Phospho-kinase proteome profiler

In addition to the detailed time-resolved monitoring of protein activation and expression by RPPA, the human phospho-kinase antibody array was used for the analysis of 46 different intracellular signaling proteins. The purpose of this screening approach was to identify signaling proteins that are differentially activated between *wt* and *del 8* cells in an EGF-dependent manner, in order to evaluate the impact of E-cadherin mutation. Protein lysates of *wt* and *del 8* cells were analyzed after serum starvation and after 1 and 60 min of EGF stimulation, in order to cover early as well as late downstream effects. Additionally, samples of both cell lines grown in cell culture medium containing FCS were investigated.

In order to facilitate the evaluation of the screening results, a two-colored heat map was prepared to order proteins according to their activation patterns. Proteins were classified as "EGF-dependent" and "differentially activated", when their activation levels after EGF stimulation in *wt* cells differed from the unstimulated *wt* sample and when they exhibited differential activation between *wt* and *del 8* cells at both time points of stimulation. Proteins that showed differential regulation between *wt* and *del 8* in FCS-containing medium were grouped as FCS-dependent differentially regulated. Only differences greater than 30 % were considered (Fig. 3.10A).

16 proteins show EGF-dependent differential regulation between the two investigated cell lines. Interestingly, these include three members of Src family kinases (Src, Yes and Fgr). Eight proteins, including Src and Yes, exhibit differential activation after EGF stimulation as well as in FCS containing medium. As a prototypic member of this family and because of its known interaction with E-cadherin and EGFR and its prominent role in cancer, Src was chosen as target for further analysis.

The detailed activation profile of Src that was detected in the forward phase protein microarray experiment is depicted in Fig. 3.10B. *Wt* cells show a time-depending increase in activation with EGF-stimulation, whereas the signals in *del 8* cells remain at basal level. At both time points of stimulation, there are obvious differences in the activation levels between *wt* and *del 8* cells. Analysis of Src activation in samples of both cell lines grown in FCS-containing medium reveals a similar result.

A

+EGF	+FCS	Protein (phosphorylation)
		AKT (S473)
		AKT (T308)
		AMPKα2 (T172)
		CREB (S133)
		ERK1/2 (T202/Y204, T185/Y187)
		FAK (Y397)
		GSK3αβ (S21/S9)
		HCK (Y411)
		HSP27 (S78/S82)
		LYN (Y397)
		MEK1/2 (S218/S222, S222/S226)
		p27 (T157)
		p70S6 (T229)
		PLC γ-1 (Y783)
		STAT2 (Y689)
		STAT5a (Y699)
		STAT5a/b (Y699)
		STAT5b (Y699)
		STAT6 (Y641)
		TOR (S2448)
		AMPKα1 (T174)
		CTNNB1
		FYN (Y420)
		JNK pan (T183/Y185, T221/Y223)
		LCK (Y394)
		p27 (T198)
		p38α (T180/Y182)
		p70S6K (T389)
		PXN (Y118)
		PYK2 (Y402)
		CHK2 (T68)
		eNOS (S1177)
		FGR (Y412)
		JUN (s63)
		MSK1/2 (S376/S360)
		p53 (S15)
		p53 (S392)
		p53 (S46)
		p70S6K (T421)
		RSK1/2 (S221)
		RSK1/2/3 (S380)
		SRC (Y419)
		STAT1 (Y701)
		STAT3 (Y705)
		STAT4 (Y693)
		YES (Y426)

Differential activation
- Yes
- No

B

Src activation profile

□ wt ■ del 8

(Rel. Signal intensity vs. serum-starved, 1 min, 60 min, FCS; EGF [100ng/ml])

Figure 3.10 Results of the Phospho-kinase Proteome Profiler protein microarray: A: The commercial protein microarray was used to assess the activation pattern of 46 intracellular proteins simultaneously by detection of site specific phosphorylations. Differential activation between *wt* and *del 8* cells dependent on EGF and FCS was defined as criteria for unbiased target selection. Proteins meeting the criteria are colored yellow. Ranking of proteins according to the selection criteria resulted in a list of eight proteins showing differential activation after EGF stimulation as well as in the presence of FCS; B: The Src activation profile detected by protein microarray is characterized by reduced activation in *del 8* cells under EGF-stimulation as well as in FCS- containing culture medium.

3.3 Analysis of the impact of E-cadherin mutation on EGF-dependent Src activation

3.3.1 Reproduction of protein microarray data

The stimulation periods of 1 and 60 min in the phospho- kinase protein microarray experiment were chosen arbitrarily to cover early as well as late downstream events. Furthermore, due to the limited sample capacity of the commercial protein microarray kit only *wt* and *del 8* cells were analyzed.

To evaluate the effects of the E-cadherin status on the EGF-dependent Src activation as accurately as possible, the time dependent activation profile of Src was assessed by Western Blot. An optimal stimulation time of 5 min was established (data not shown), which was used for further testing. Furthermore, the *pBat* cell line was again included in all experiments.

Figure 3.11 illustrates that the previous results generated by protein microarray showing differential Src activation after EGF-stimulation and in FCS containing medium could be confirmed on a set of independently prepared cellular lysates by Western blot.
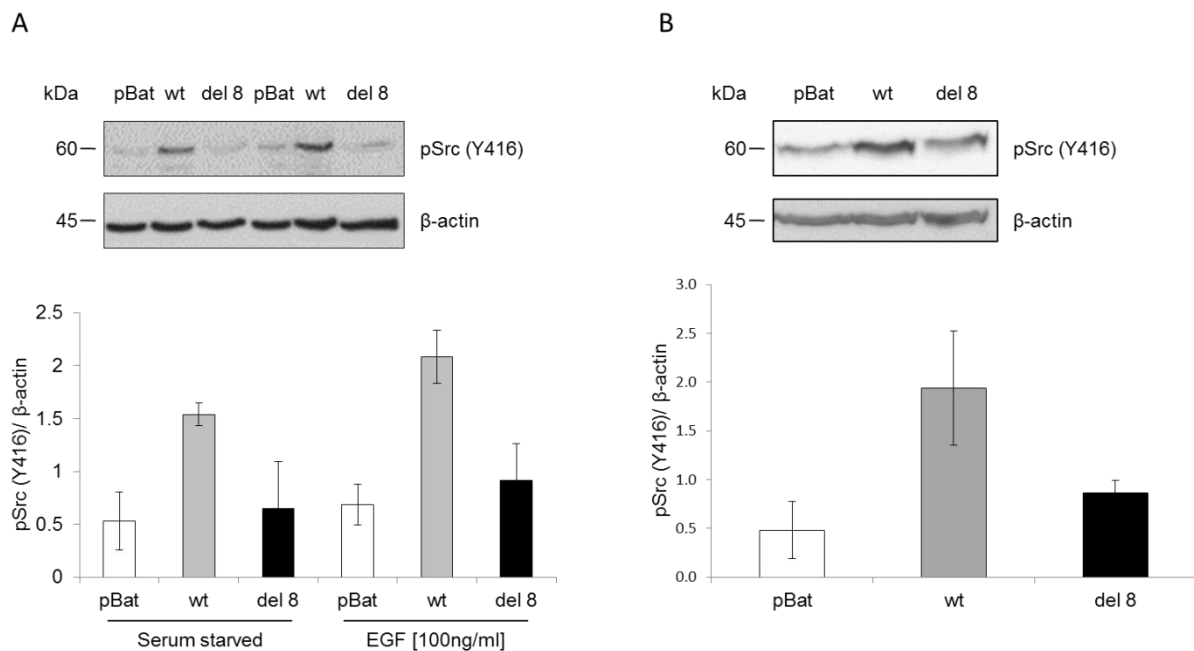
Figure 3.11 Reproduction of the protein microarray results by Western blot: A: In order to validate the screen findings, the detected activation profile under the determined optimal EGF-stimulation time was reproduced; B: Data of Src activation in FCS-containing culture medium could successfully be reproduced by Western Blot as well.

3.3.2 Analysis of an antagonistic Src phosphorylation site

Src contains several functional domains regulating its activity [189, 221]. Whereas phosphorylation of Y416 is a prerequisite for maximal kinase activity, phosphorylation of the negative-regulatory Y529 leads to the inhibition of the catalytic activity [222, 223]. In order to investigate whether enhanced phosphorylation of Y529 is the reason for the low activation levels in *del 8* cells, Western blot was performed. As illustrated in Fig. 3.12, a similar phosphorylation profile as for Y416 was detected. These data indicate that enhanced phosphorylation of the negative-regulatory Y529 residue of Src is not the cause for the observed reduced activity in *del 8* cells.

pSrc Y529
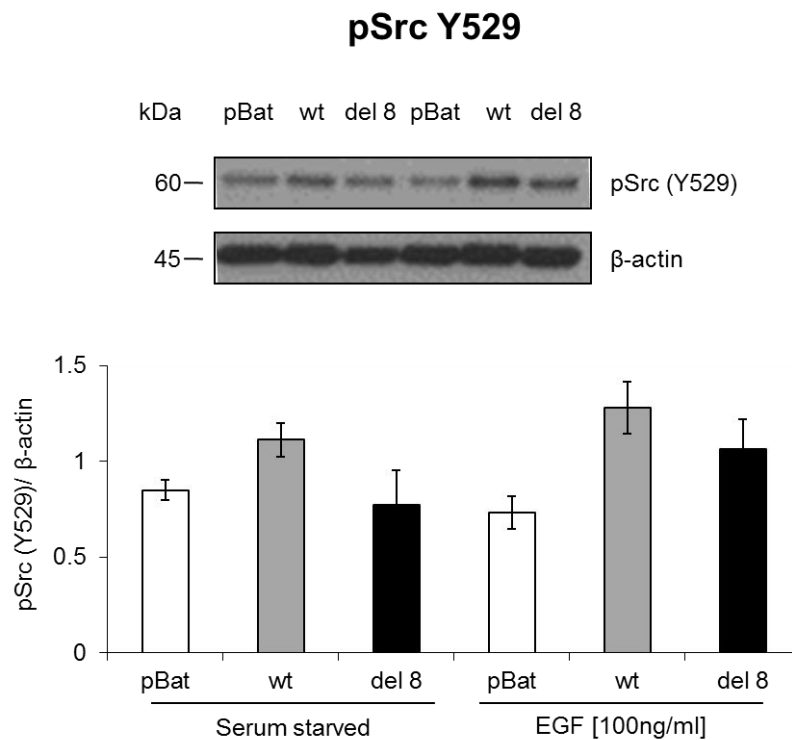
Figure 3.12 Evaluation of the phosphorylation levels of the negative-regulatory tyrosine Y529: Phosphorylation of the tyrosine residue Y416 within the activation loop of Src can be suppressed by phosphorylation of Y529 in the C-terminus of the protein. To assess whether elevated phosphorylation of Y529 is the reason for the reduced activation in *del 8* cells, Western blot was performed.

3.3.3 Evaluation of the regulatory mechanism in FCS-containing medium

As shown before, EGF dependent differential regulation could be determined after starvation and specific activation of the EGFR pathway by EGF stimulation. In addition, similar differences between *wt* and *del 8* cells in Src activation were determined in FCS-containing medium. To examine the

contribution of EGFR to the detected activation levels in FCS- containing medium, the EGFR-inhibiting monoclonal antibody cetuximab was used.

As depicted in Fig. 3.13 the differential regulation between *wt* and *del 8* cells at tyrosine residue Y416 as well as Y529 is abrogated upon EGFR inhibition. These data suggest that, despite the complex composition of FCS, EGFR is the major contributor of the differential activation observed.
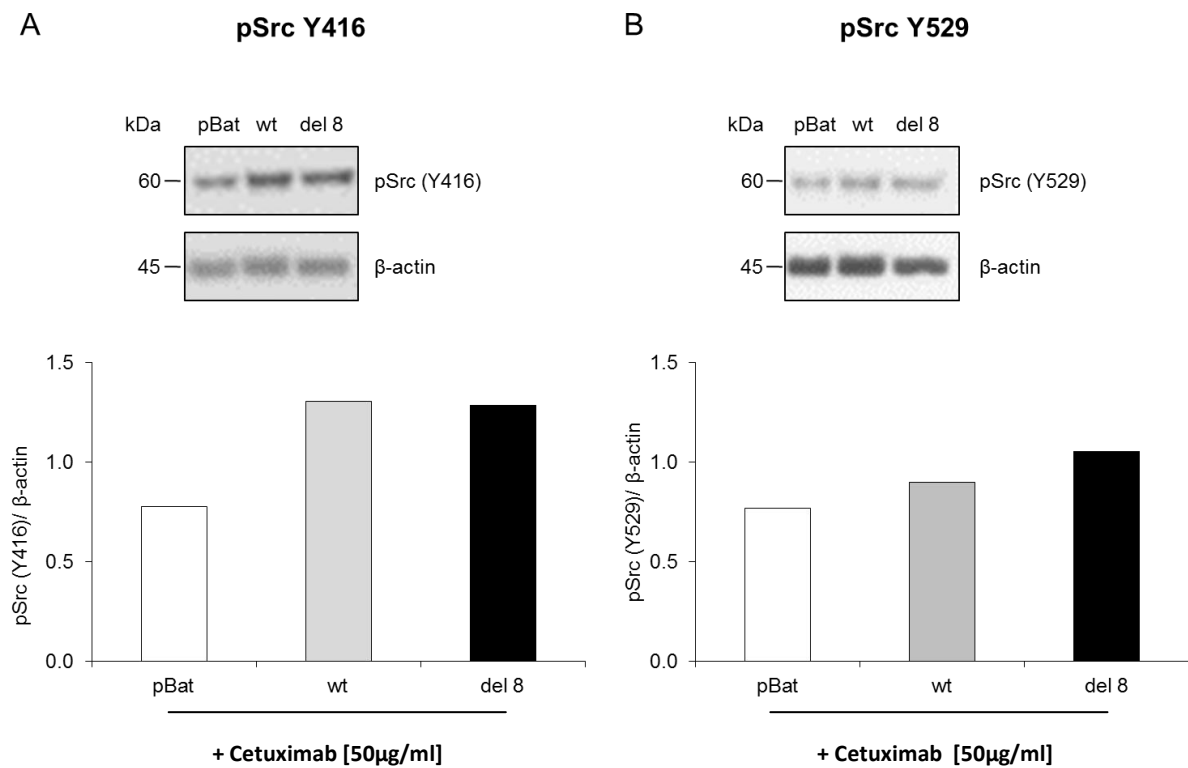
Figure 3.13 Evaluation of the regulatory mechanism in FCS-containing medium: To investigate the contribution of EGFR to the observed activation profile of Src in the presence of FCS, the EGFR-inhibiting monoclonal antibody cetuximab was used. As depicted, the differential activation between *wt* and *del 8* cells is abrogated by cetuximab at both investigated tyrosine residues (A: Y416; B: Y529) suggesting that also in the presence of FCS EGFR is the major contributor to Src regulation.

3.4 Analysis of cetuximab sensitivity of gastric cancer cell lines*

3.4.1 EGFR expression, localization and activation

To investigate whether the total or activated EGFR expression levels modify the cetuximab responsiveness of gastric cancer cell lines and to assess a possible relationship between the abundance and activation of the receptor, we characterized a panel of five human gastric cancer cell lines (AGS, KATOIII, MKN1, MKN28 and MKN45) by immunoblot, flow cytometry and immunofluorescence analysis.

First, we examined the expression level and subcellular localization of EGFR in the different cell lines. Western blotting revealed the following descending order of total cellular levels of EGFR: MKN1 > MKN28 > KATOIII > AGS > MKN45 (Fig. 3.14A). The differences in the expression of EGFR between the MKN1 cell line and all other cell lines (except MKN28) were significant.

Flow cytometry analysis of the surface localization of EGFR revealed a slightly different order of EGFR expression: MKN1 > MKN28 > KATOIII = MKN45 > AGS (Fig. 3.14B). The subcellular staining pattern of EGFR in the various cell lines was visualized by immunofluorescence (Fig. 3.14C). EGFR staining was localized predominantly at the plasma membrane, with the strongest intensity at cell-cell contacts, in the cell lines KATOIII, MKN28 and MKN45, with a distribution pattern similar to that in the A431 control cells. In contrast, EGFR staining was distributed evenly throughout the whole cells in the MKN1 cell line. Very faint EGFR signals were detectable in the AGS cell line at residual cell-cell contacts.

Next, we examined the activation level of EGFR in the gastric cancer cell lines and investigated a possible relationship between total and active EGFR expression levels. Western blot analysis that detected phosphorylation of EGFR on tyrosine residue Y1068 revealed the following order of EGFR activation levels: KATOIII > MKN45 > AGS = MKN1 > MKN28 (Fig. 3.14D). The differences in the activation of EGFR between the KATOIII cell line and all other gastric cancer cell lines were significant.

Together, these findings demonstrate differences in the expression and localization of EGFR in the investigated cell lines and suggest that the expression and activation of EGFR are not correlated in this gastric cancer cell line model.
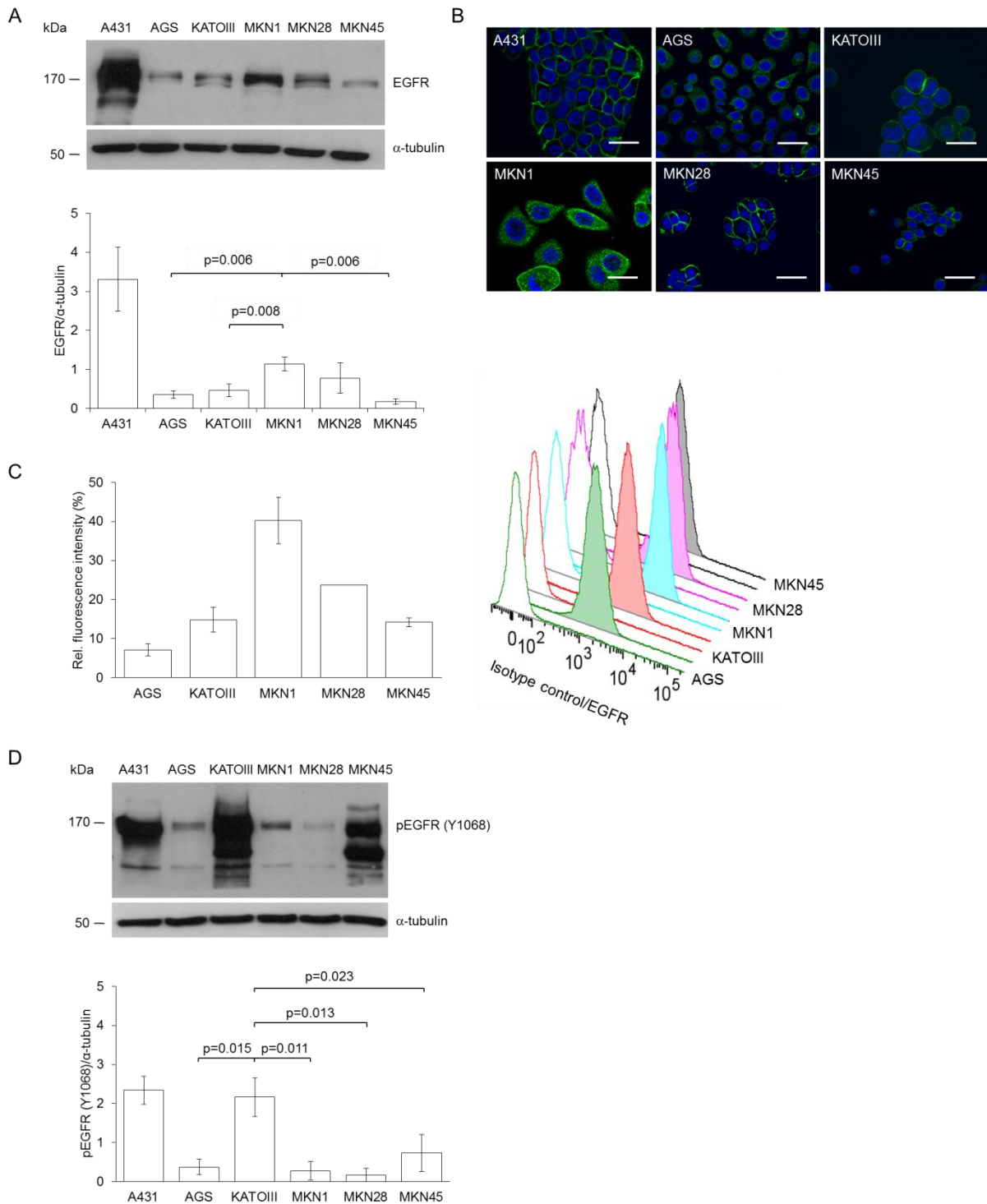
Figure 3.14 EGFR expression, localization and activation: The expression, localization and activation of EGFR were studied in the gastric cancer cell lines AGS, KATOIII, MKN1, MKN28 and MKN45. A431 cells were used as positive controls. A: EGFR expression was detected in the total lysates of the cells by Western blotting, using staining of a-tubulin as a loading control. The results presented are representative of three independent experiments. Mean expression levels of EGFR were quantified using densitometric analysis and calculated in relation to the expression of a-tubulin (±SD). B: EGFR was visualized by immunofluorescence. Scale bar: 50 μm. C: Flow cytometry analysis revealed surface localization of EGFR in all cell lines. The mean relative fluorescence intensities of two independent experiments are shown (±SD). D: Phosphorylated EGFR (pEGFR, pY1068) was detected in total lysates of cells by Western blot using a-tubulin as a loading control. The depicted results are representative of three independent experiments. The mean expression levels of pEGFR were quantified using densitometric analysis and were calculated in relation to the levels of a-tubulin (±SD). A summary of statistical data is presented in Supplementary Table 2 and 3.

3.4.2 Cetuximab responsiveness of gastric cancer cell lines

To determine the efficacy of cetuximab as a monotherapy in the gastric cancer cell line model, cells were treated with varying concentrations of the therapeutic agent. The metabolic activity of the cells as surrogate marker for cell viability was investigated by the XTT cell proliferation assay.

The concentration-response curves are shown in Fig. 3.15. The viability of MKN1 and MKN28 cells was significantly reduced by cetuximab in a concentration-dependent manner (Fig. 3.16A, B). At a cetuximab concentration of 1 µg/ml, significant effects on cell viability were found (MKN1: $p=0.038$, MKN28: $p=0.009$). Increasing the concentration of cetuximab to a maximum of 200 µg/ml resulted in a further significant gradual reduction of metabolic activity. Therefore, the MKN1 and MKN28 cell lines were classified as cetuximab-responsive cell lines.

In contrast, cell lines AGS, KATOIII and MKN45 were classified as cetuximab-nonresponsive cell lines, because no significant concentration-dependent reduction of metabolic activity was found up to a concentration of 100 µg/ml cetuximab (Fig. 3.16C, D, E), which is comparable to the active drug concentrations achieved in cancer patients [215-217]. The strongest effects of the drug were observed at the maximal dose of 200 µg/ml cetuximab, which is above the clinical threshold value.

These findings demonstrate the activity of cetuximab as a single agent in two gastric cancer cell lines (MKN1, MKN28) and indicate that all of the other considered cell lines are nonresponsive (AGS, KATOIII and MKN45).
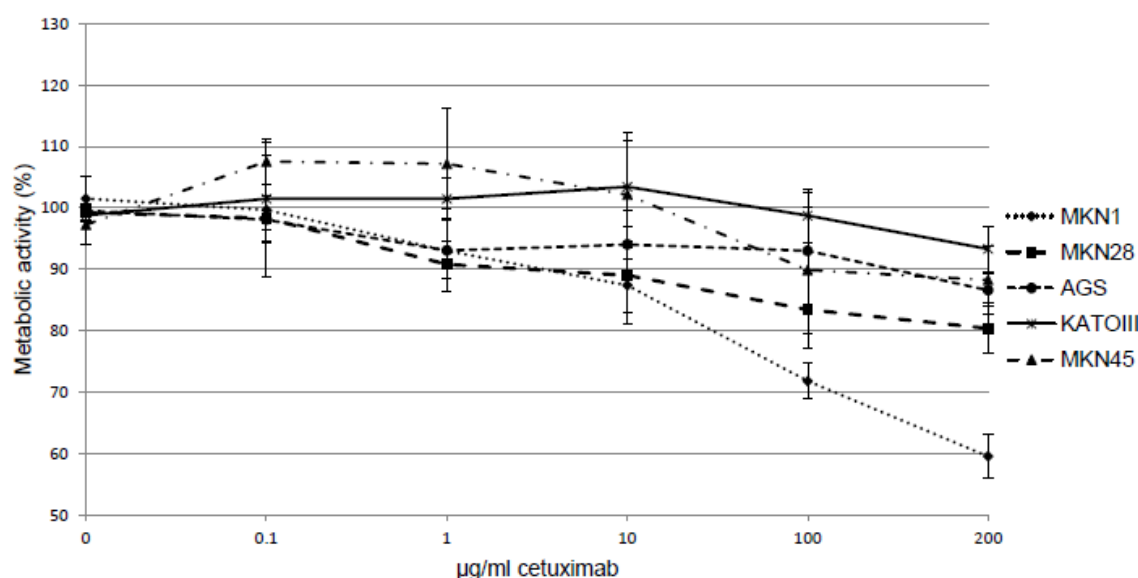
Figure 3.15 Cetuximab responsiveness of gastric cancer cell lines: The effect of cetuximab on the metabolic activity of gastric cancer cell lines was determined by XTT assay. The cell lines MKN1, MKN28, MKN45, AGS and KATOIII were treated with increasing doses of cetuximab and growth inhibitory curves were determined. Results represent means ±SD of three individual experiments.
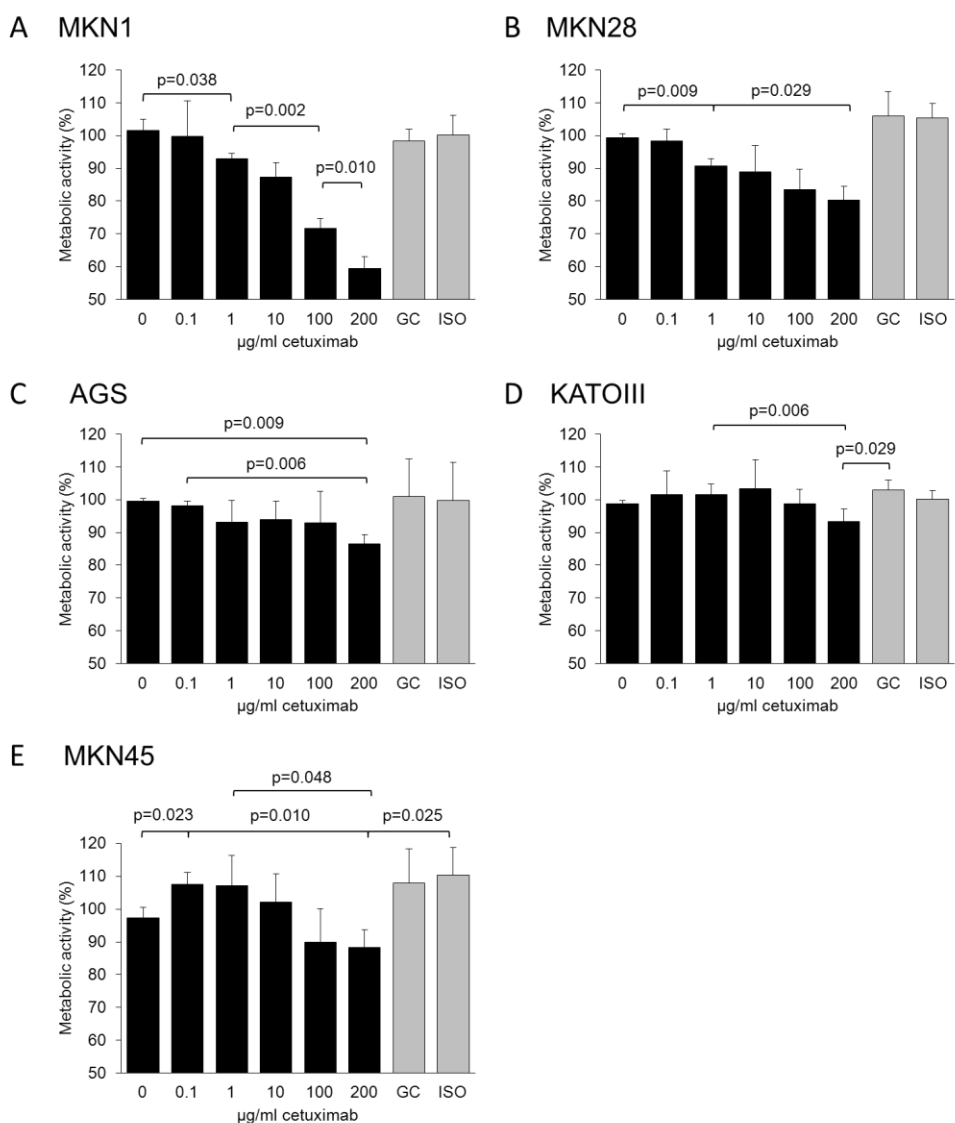
Figure 3.16 Cetuximab responsiveness of gastric cancer cell lines: The effect of cetuximab on the metabolic activity of gastric cancer cell lines was determined by XTT assay. The cell lines A: MKN1, B: MKN28, C: AGS, D: KATOIII and E: MKN45 were treated with increasing concentrations of cetuximab. The depicted results are representative of three independent experiments. The metabolic activity was normalized to that of the untreated control. A growth control (GC) and an isotype control antibody (ISO) were used to confirm the specificity of the measured effects. A summary of statistical data is presented in Supplementary Table 4.

3.4.3 Effect of cetuximab combined with chemotherapy on the viability of gastric cancer cells

In an approximation of the clinical situation, the activity of cetuximab was also assessed in combination with chemotherapy. Fluorouracil (FU) - and cisplatin-based combination chemotherapy is the standard treatment for patients with advanced gastric cancer [60]. Therefore, the effect of cetuximab in combination with 5-FU and cisplatin on cell viability was tested in the cetuximab-sensitive MKN1 cell line and in the cetuximab-resistant KATOIII cell line with the XTT assay.

Cetuximab at a concentration of 100 µg/ml was used alone or in combination with two different concentrations of 5-FU and cisplatin. The viability of the MKN1 cells was reduced by approximately 40% by cetuximab alone (Fig. 3.17A), which is within the same range as described above (Fig. 3.16A). In contrast, cetuximab showed no activity in KATOIII cells (Fig. 3.17B), as observed previously (Fig. 3.16B).

Clinically relevant concentrations of 5-FU (0.05 µg/ml) and cisplatin (0.5 µg/ml) [214] showed no effect on cell viability in either cell line. Therefore, a five-fold-increased concentration of the combination chemotherapy was used. The effect was an approximately 80% inhibition of MKN1 cell growth and no reduction of KATOIII cell viability. The addition of cetuximab to the chemotherapy combination regimen had a dramatic effect: MKN1 cell viability was reduced below the viability measured at the starting point, which indicates not only that cell growth was inhibited but also that cell death occurred. In KATOIII cells, cetuximab seemed to sensitise cells to chemotherapy because an approximately 50% reduction of cell viability was observed.

These results suggest that the combination of cetuximab, 5-FU and cisplatin in clinically relevant doses did not improve the treatment outcome compared with cetuximab monotherapy. Importantly, the classification of responder and non-responder cell lines that was initially based on the activity of cetuximab as a single agent remained valid under combination therapy conditions. However, when five-fold-higher concentrations of the chemotherapeutic drugs were used, the combination of cetuximab, 5-FU and cisplatin was more efficacious than the cetuximab monotherapy in the MKN1 cell line (80% vs. 40-50% reduction of cell viability) and the KATOIII cell line (50% vs. 0% reduction of cell viability).
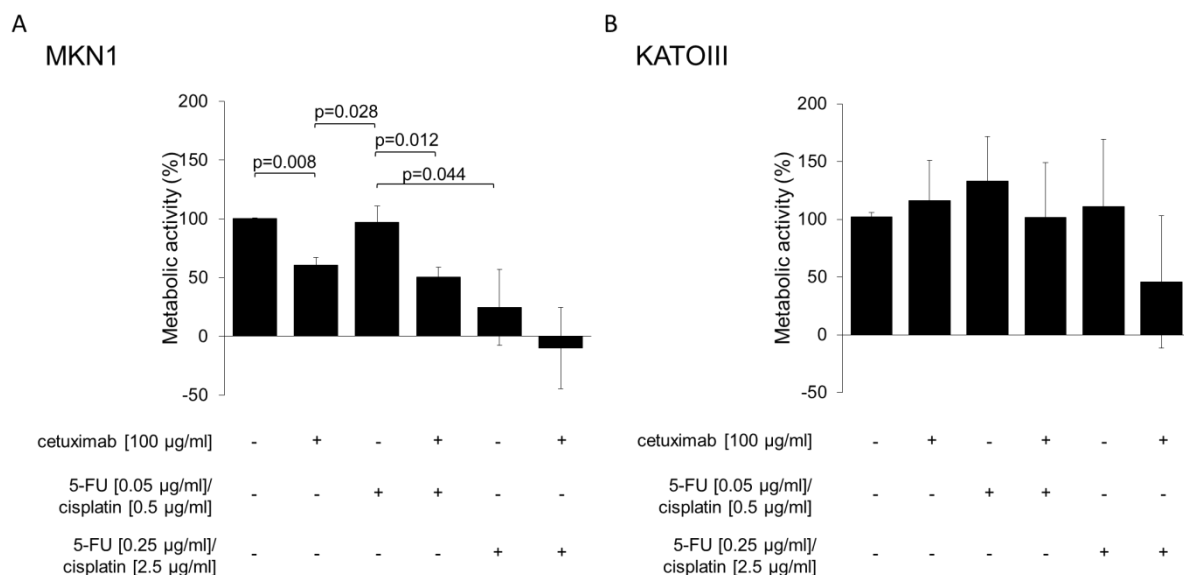
Figure 3.17 Effect of cetuximab combined with chemotherapy: The effects of cetuximab in combination with chemotherapy on a cetuximab-sensitive (A: MKN1) or cetuximab resistant (B: KATOIII) cell line were determined by XTT assay. Cetuximab was used at a concentration of 100 µg/ml alone or in combination with two different concentrations of 5-FU and cisplatin. The metabolic activity was normalized to that of the untreated control. The depicted results are representative of three independent experiments. A summary of statistical data is presented in Supplementary Table 5.

3.4.4 Effect of cetuximab on the phosphorylation of EGFR

To assess the relationship between cetuximab effects on cell viability and the activation of EGFR, the phosphorylation status of the receptor was determined under cetuximab treatment by immunoblot analysis.

We examined the effects of cetuximab on the activation of EGFR in the panel of gastric cancer cell lines. Western blot analysis to detect the phosphorylation of EGFR on tyrosine residue Y1068 revealed that the activation of EGFR was significantly reduced in the cetuximab-responsive cell lines MKN1 and MKN28 in a concentration-dependent manner (Fig. 3.18A, B). Significant effects were detected at cetuximab concentrations of 100 µg/ml (MKN1: p=0.045) and 10 µg/ml (MKN28: p=0.049).
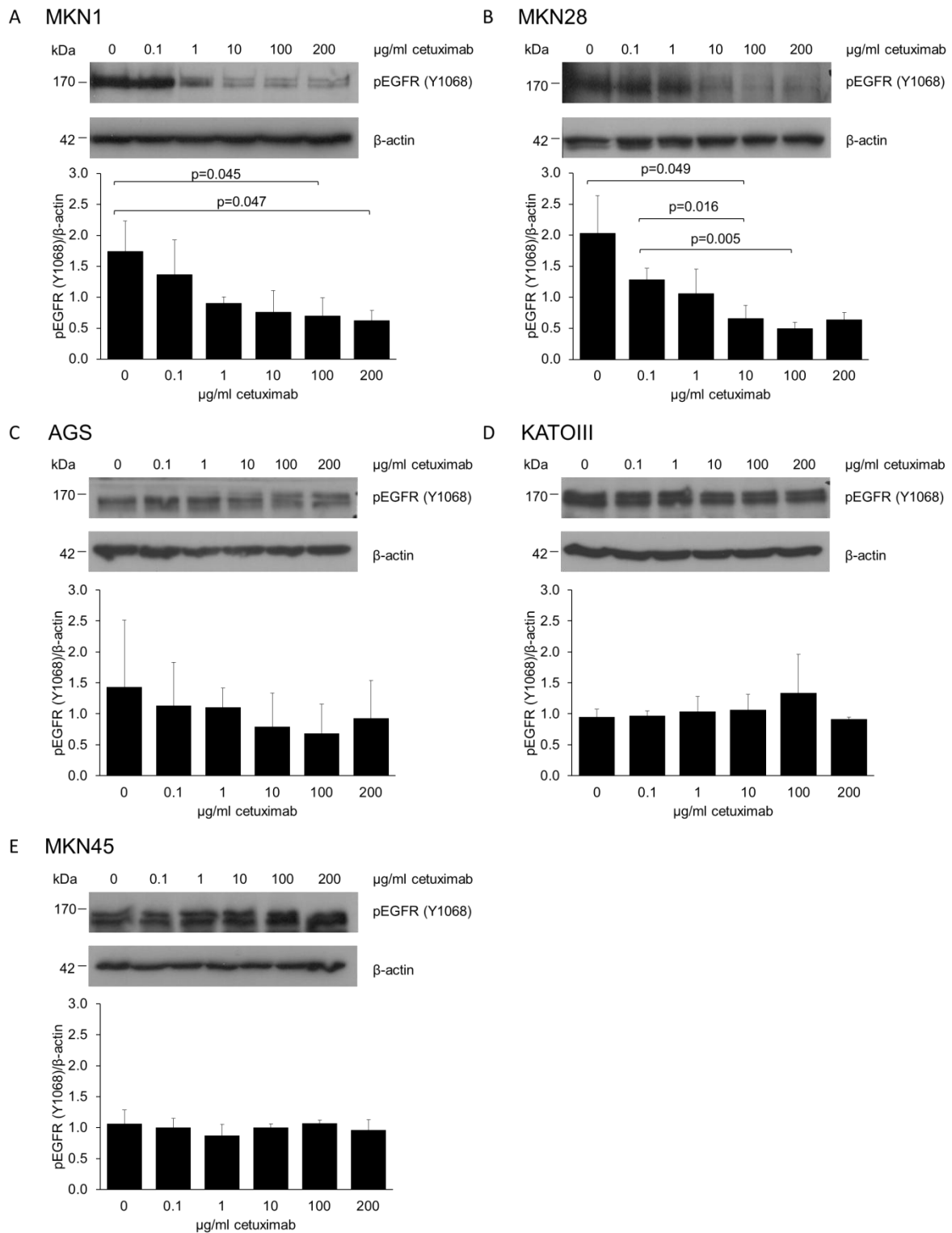
Figure 3.18 Effect of cetuximab on the phosphorylation of EGFR in responsive cell lines: The effects of cetuximab on the phosphorylation of EGFR were examined in the cell lines A: MKN1, B: MKN28, C: AGS, D: KATOIII and E: MKN45. Phosphorylation of EGFR was detected in the total lysates of cells by Western blot analysis using an antibody directed against tyrosine residue Y1068 of EGFR. Equal loading of the lanes was confirmed by the detection of b-actin. The depicted results are representative of three independent experiments. The average phosphorylation levels of EGFR were determined by densitometric analysis and were calculated in relation to the levels of b-actin. A summary of statistical data is presented in Supplementary Table 6.

Cetuximab failed completely to show any significant effect on the degree of EGFR phosphorylation in the cetuximab-non-responsive cell lines AGS, KATOIII and MKN45, even at a maximum concentration of 200 µg/ml (Fig. 3.18C, D, E).

These results indicate that the phosphorylation of EGFR was reduced by cetuximab in the responsive cell lines MKN1 and MKN28, which were also sensitive in the cell viability assay. In contrast, cetuximab was not active in the non-responsive cell lines with regard to EGFR activation or the metabolic activity of the cells.

3.4.5 Association of cetuximab responsiveness with E-cadherin expression and subcellular localization

Because E-cadherin is known to have a modulating impact on EGFR activation and localization [218, 224] as well as cellular responsiveness to cetuximab treatment in preclinical models [225], we determined the expression pattern and subcellular localization of E-cadherin in the panel of five gastric cancer cell lines by immunoblot, flow cytometry and immunofluorescence analysis. E-cadherin with a molecular weight of 120 kDa was detectable in lysates of the cell lines KATOIII, MKN28 and MKN45 by Western blot analysis (Fig. 3.19A). Additional smaller proteins were detected in the cell lines MKN28 (approximately 100 kDa) and MKN45 (approximately 80 kDa) that possibly corresponded to degradation products [133]. In contrast, no expression of E-cadherin was detected in AGS and MKN1 cells.

Flow cytometry analysis revealed surface localization of E-cadherin in the cell lines KATOIII, MKN28 and MKN45, and very faint signals of membranous E-cadherin were detectable in MKN1 cells (Fig. 3.19B).

Immunofluorescence analysis revealed strong E-cadherin staining at cell-cell contacts in the cell line MKN28 without staining of clone edges, which was similar to the pattern observed in the A431 control cells (Fig. 3.19C). Strong membranous E-cadherin staining was found in the cell lines KATOIII and MKN45, with similar signal intensities in regions with or without cell-cell contact, whereas the cell lines AGS and MKN1 were E-cadherin-negative.

Together, these results show that only three gastric cancer cell lines (KATOIII, MKN28 and MKN45) were E-cadherin-positive in all assays, of which one is a cetuximab-responsive cell line.
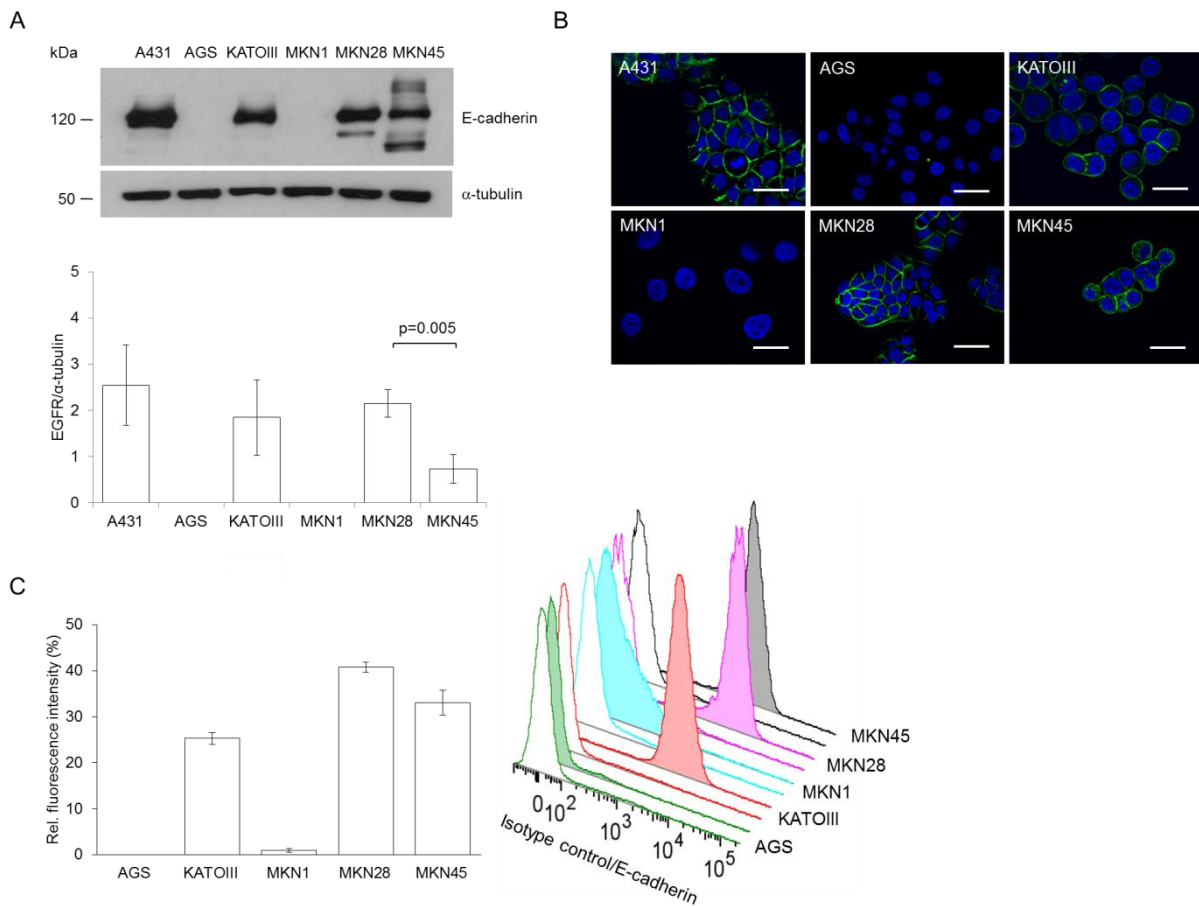
Figure 3.19 Expression and localization of E-cadherin: The expression and subcellular localization of E-cadherin were investigated in the gastric cancer cell lines. A: E-cadherin expression levels were determined in the total lysates of the cells by Western blot. Equal loading in each lane was demonstrated using the a-tubulin signal. The mean expression levels of E-cadherin were quantified in three independent experiments using densitometric analysis and were calculated in relation to the levels of a-tubulin (±SD). B: E-cadherin was visualized by immunofluorescence. Scale bar: 50 µm C: The surface localization of E-cadherin was detected by flow cytometry analysis. The mean relative fluorescence intensities of two independent experiments are shown (±SD). A summary of statistical data is presented in Supplementary Table 7.

3.4.6   Association of cetuximab responsiveness with genomic alterations

The experience with colorectal cancer shows that genetic alterations determine the resistance or sensitivity of targeted therapies; colorectal cancers lacking oncogenic activation of the EGFR downstream effectors, KRAS, BRAF, PI3K and PTEN, have the highest probability of a response to anti-EGFR therapies [226]. To test the possible role of genetic alterations in our cell culture system, we performed a database search for known mutations in our cell lines.

Several known mutations in cancer-relevant genes are present in the five gastric cancer cell lines (Table 2). The characteristics of the cetuximab-responsive cell line MKN1 include a polymorphism in *EGFR*, hypermethylation of the *CDH1* promoter region, a *PIK3CA* mutation (p.E545K) and a *KRAS* amplification, whereas in the second responder cell line, MKN28, no such mutations were described in *EGFR* and its downstream effectors or in *CDH1*. In contrast, the non-responder AGS cell line has a

59

classical *KRAS* mutation (p.G12D). Interestingly, in cell lines that were not reactive to cetuximab, mutations in the *CDH1* gene (AGS, KATOIII, MKN45) or amplification of the *MET* gene (KATOIII, MKN45) were described.

These results suggest that the cell lines used in this study harbor a variety of cancer-relevant mutations, of which some, such as *KRAS* mutations or *MET* amplification, have been linked to cetuximab resistance. In contrast, a relationship between *CDH1* mutations and cetuximab resistance has not been established to date.

Table 7 Summary of selected alterations on the genomic and protein level

Cell line	EGFR	E-cadherin	Others
AGS	n.d.	p.G579fs*9 (ins)	*KRAS*: p.G12D (sub) *CTNNB1*: p.G34E (sub) *PIK3CA*: p.E453K (sub)
KATOIII	p.R521K (pol)	p.E336E (sub)	*MET*: amp
MKN1	p.R521K (pol)	CpG hypermethylation	*PIK3CA*: p.E455K (sub) *FBXW7*: R465C
MKN28	n.d.	n.d.	-
MKN45	p.A1048V (sub)	p.G274_P277del (del)	*MET*: amp

Information about genomic alterations of the gastric cancer cell lines used in this study was taken from the COSMIC database (database of somatic mutation information in human cancer) of the Sanger Institute and cited references. Abbreviations: amp: amplification, del: deletion, ins: insertion, pol: polymorphism, sub: substitution, n. d.: not described.

3.4.7 Relationship between cetuximab responsiveness and MET activation

To investigate whether the described *MET* gene amplification in KATOIII and MKN45 cells results in MET activation that possibly influences the cetuximab responsiveness of the cell lines, the phosphorylation status of the receptor was examined by immunoblot analysis. Phosphorylation of MET was detected in total cell lysates by western blot analysis using an antibody directed against tyrosine residue Y1234/1235 of MET in KATOIII and stronger in MKN45 cells, whereas no such signals were observed in MKN1, MKN28 and AGS cells (Fig. 3.20).

This finding indicates that MET is activated in two of the three cetuximab-resistant cell lines. Interestingly, the same cell lines, KATOIII and MKN45, exhibit the highest levels of EGFR activation.
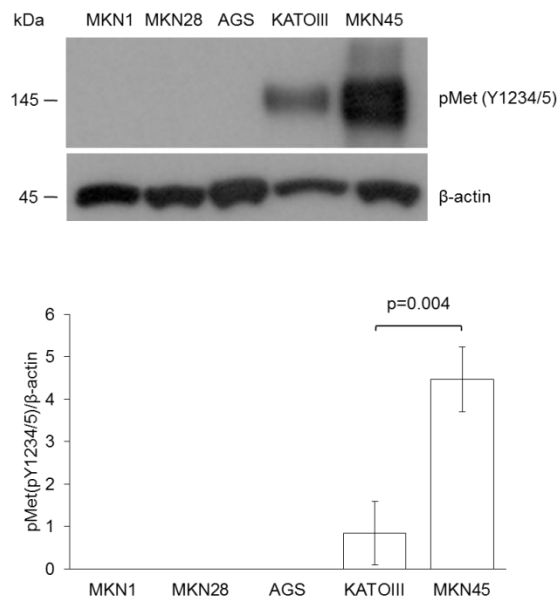
Figure 3.20 MET activation: The expression of phosphorylated MET was investigated in the gastric cancer cell lines. Phosphorylation of MET was detected in total lysates of cells by Western blot analysis using an antibody directed against tyrosine residue Y1234/1235 of MET. Equal loading of the lanes was confirmed by detection of b-actin. The average phosphorylation levels of MET were determined by densitometric analysis and calculated in relation to the levels of b-actin. The depicted results are representative of three independent experiments. A summary of statistical data is presented in Supplementary Table 8.

3.4.8 Summary and definition of response and resistance predictors

The results of the quantitative protein expression experiments for EGFR as well as activated EGFR and MET were transformed into relative signal intensities (Fig. 3.21). High expression of EGFR and low levels of receptor activation were associated with the response in the cell lines MKN1 and MKN28. In contrast, MET activation and mutation of *KRAS* were found to indicate resistance in the AGS, KATOIII and MKN45 cell lines.
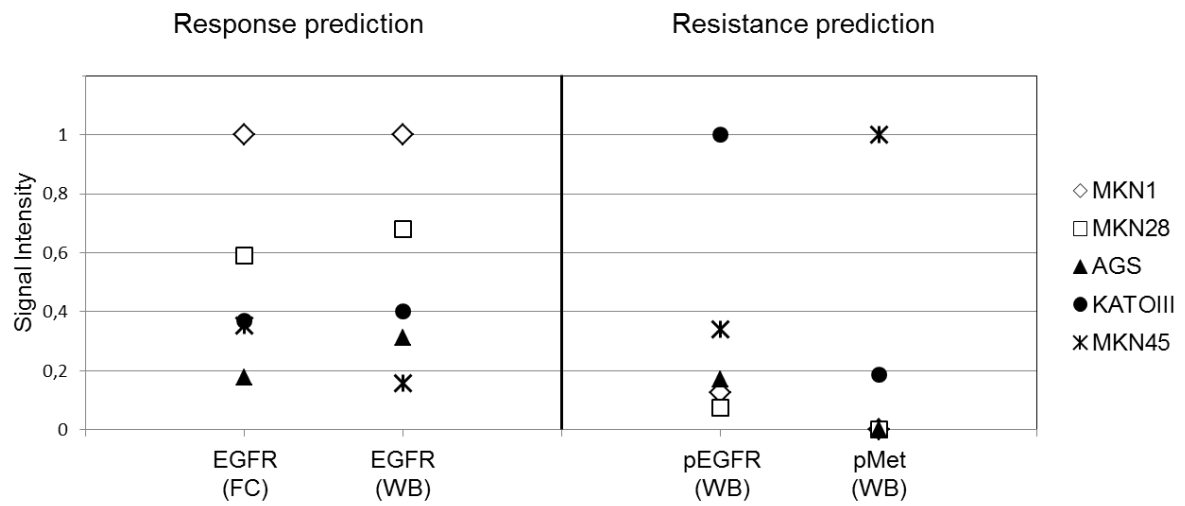
Figure 3.21 Summary of predictive factors for cetuximab response: The signal intensities derived from the flow cytometry (FC) and Western blot (WB) analysis of the cell lines were ranked according to the maximal signal for each parameter (EGFR, pEGFR and pMET). All illustrated parameters share some predictive power, as there is a clear separation of cetuximab-responsive cell lines (white symbols) and cetuximab-nonresponsive cell lines (black symbols)

4 DISCUSSION

4.1 Analysis of classical EGFR downstream signaling

4.1.1 RPPA validation

In cancer, genetic alterations lead to aberrant cellular signaling that is caused by changes in protein expression and activation levels. RPPAs represent a rapidly emerging technology facilitating molecular network analysis by measurement of protein expression and phosphorylation simultaneously across multiple samples and under identical experimental conditions [203, 227].

The RPPA represents a targeted approach, meaning that the proteins to be analyzed have to be known. The main requirement is the availability of highly specific antibodies against the proteins of interest. The micro Western dot-blot format does not resolve protein fractions by molecular weight as in gel-based methods [202]. Therefore, it is crucial to validate the antibody specificity by detection of specific bands in Western blot. In the present study, only two antibodies showed multiple bands in Western blot. In *del 8* cells, an additional E-cadherin band at about 80 kDa was detected, which has previously been described as putative degradation product [228]. In the case of Erk1/2, the chosen antibody simultaneously detects the two main isoforms Erk1 at 44 kDa and Erk2 at 42 kDa explaining the double bands in Western blot. In the present study, 11 antibodies were tested on the lysates (*pBat, wt, del 8*) to be used in RPPA and protocols have been optimized with respect to dilution, incubation time and the type of blocking. As illustrated in Fig. 3.2, all antibodies exhibited specific bands and were approved for use in RPPA.

In order to allow proper interpretation of the RPPA data, a combination of the two HKPs α-tubulin and β-actin was used as loading control. The reliability of normalization with the HKPs was assessed by bivariate comparison to normalization with FAST Green FCF, a total protein stain (Fig. 3.3A). A Spearman´s rank correlation coefficient of $r_s=0.890$ indicated equivalent results of both approaches. The reproducibility of the protocol was validated by intra-slide and inter-slide comparisons of multiple samples. Spearman´s rank correlation coefficients of $r_s=0.928$ for the intra-slide and $r_s=0.809$ for the inter-slide comparison (Fig. 3.3B and 3.3C, respectively) indicate a high reproducibility. Importantly, differently treated samples (after starvation, stimulated with EGF or cultivated in FCS containing medium) could equally well be analyzed.

Taken together, these data show that the established protocol is robust and produces reproducible results which can be properly evaluated and interpreted.

4.1.2 The expression profiles of E-cadherin and β-catenin reflect their close relationship

Multiple studies show that EGF stimulation and EGFR activation are able to disrupt the AJ-complex, of which E-cadherin and β-catenin are two major constituents. In order to analyze the impact of long-term EGF stimulation on the expression of both proteins RPPA was used.

EGF stimulation had no influence on the protein expression of E-cadherin and β-catenin, which remained unchanged over the entire observation period (Fig. 3.4A and B). In the investigated cell culture model, E-cadherin expression was not controlled by the native E-cadherin promoter, but was under the control of a β-actin promoter. As a consequence, transcription factors usually binding to the E-cadherin promoter to mediate E-cadherin repression, like e.g. Snail, fail to down regulate E-cadherin expression in the present cell culture model.

The significant differences of E-cadherin expression between all cell lines derive on the one hand from the complete lack of E-cadherin expression in *pBat* cells and on the other hand from the above mentioned simultaneous detection of a 80 kDa degradation product in *del 8* cells (Fig. 3.2) [228]. In the former case, the detected signal represents background noise and in the latter case the fragment is the result of the increased proteolytic activity of *del 8* cells.

A previous study of our group revealed abnormal perinuclear localization of β-catenin in *del 8* cells [229]. Translocation of β-catenin into the cytoplasm and the nucleus is associated with activation of the wnt/wingless signaling cascade [24-26, 122-130]. However, potential activation of this signaling pathway in *del 8* cells remains elusive.

Taken together, no influence of EGF stimulation on the expression levels of E-cadherin and β-catenin could be detected. The recruitment of β-catenin to adhesion complexes down regulating its transcriptional activity may represent a mechanism via which intact E-cadherin exerts a growth suppressive function [230-232].

4.1.3 Mutation of E-cadherin enhances EGFR activation

Emerging data suggest a functional crosstalk between E-cadherin and EGFR [218, 224, 233]. To characterize the impact of the E-cadherin status on the EGFR signaling pathway, the protein phosphorylation kinetics of EGFR were monitored by RPPA in high resolution time course experiments.

The RPPA approach revealed significantly enhanced activation of EGFR in *del 8* cells (Supplementary table 1; Fig. 3.5A and B) that was maintained for approximately 100 min. The detected activation was

independent of the protein expression levels, which remained essentially unchanged over the entire observation period.

Furthermore, the monitoring of EGFR activation under long-term stimulation (72 h) revealed that the peak activation is followed by a decline to base line activity without later recurrence of activation. Subsequent to activation, the receptor is internalized and can either be recycled to the surface or degraded [177, 178]. In the former case, a recurrence of at least low level activation would be expected. In the latter case, a decrease of protein expression should be detected, except protein synthesis rates equal the degradation rates.

Enhanced signaling of EGFR due to its overexpression is well-known in several carcinomas, including gastric carcinoma (22). Our group recently identified cancer related-mutation of E-cadherin in the extracellular domain as new mechanism for EGFR activation [218]. Reduced EGFR internalization and reduced complex formation between mutated E-cadherin and EGFR facilitating receptor activation represent possible explanations for the enhanced EGFR activation in *del 8* cells [114, 218, 224].

Taken together, the present results further characterize the impact of E-cadherin mutation on the dynamics of the ligand-dependent activation of EGFR under long-term EGF stimulation.

4.1.4 Loss of E-cadherin function by mutation activates Erk1/2 downstream of EGFR

The protein kinases Akt and Erk1/2 both are major downstream effectors of EGFR. To elucidate the consequences of receptor activation deregulated by mutation of E-cadherin on the downstream signaling, the temporal activation profiles of Akt and Erk1/2 were monitored by RPPA.

Activation of Akt as well as Erk1/2 was determined by detection of the phosphorylated key residues within their activation loops [219, 220]. In all cell lines, Akt was active for approximately 30 min with a maximum after 5 min of EGF stimulation. Erk1/2 activation with a peak at 10-15 min was maintained even longer for about 2 h. Both kinases showed non-recurring activation subsequently followed by a decline to base line activity. The delay of maximal activation of both proteins reflects their position within the signaling cascade.

The mutation of E-cadherin did not affect the activation of Akt. However, as no activation could be detected in *pBat* cells, the expression of E-cadherin seems to be essential for efficient Akt activation. In contrast, Erk1/2 activation in *del 8* cells was significantly enhanced compared to *pBat* and *wt* cells (Supplementary table 1), indicating that the deregulated EGFR signal is transduced through this pathway into the cell. The observed activation profiles cannot be explained by elevated protein expression levels, which for both proteins remained essentially unchanged over the entire observation

period. An activating mutation of BRAF (V600E) has been reported for the investigated cell lines [234], but as all of them derive from the same parental cell line and only differ in their E-cadherin expression, this does not explain the differential activation of Erk1/2.

Multiple studies revealed that the engagement of E-cadherin in cell-to-cell contacts suppresses Erk1/2 activity [235, 236]. In contrast, the disruption of E-cadherin function promotes the activation of the Erk1/2 pathway [237-239], inducing cellular motility and EMT [240-242]. Furthermore, upregulation of this pathway was associated with late-stage disease and poor survival in gastric adenocarcinoma [243].

In a previous study using the same cell culture, model Erk1/2 was found unaffected by mutation of E-cadherin, probably due to a different experimental approach. However, the present results suggest that mutation of E-cadherin represents a new mechanism of Erk1/2 activation downstream of EGFR and potentially explain the previously described phenotypes of enhanced proliferation [228], motility [156] and invasion [244] in *del 8* cells (Fig. 5).

4.1.5　Conclusion 1

The present study demonstrates the exceptional advantages of the RPPA technology for the extensive investigation of signal transduction networks. Important information about the sequence and the dynamics of EGFR signal transduction deregulated by mutation of E-cadherin could be determined.
The present data reveal that intact E-cadherin acts as inhibitor of EGFR and Erk1/2 activation. Loss of E-cadherin by mutation is followed by concomitant up-regulation of EGFR and Erk1/2 signaling that might contribute to the increased cell proliferation and motility observed in cell lines with E-cadherin mutation.

4.2 Analysis of EGFR signaling by forward phase protein microarrays

Forward phase protein microarrays provide numerous advantages compared to conventional proteomic techniques like Western blot. Due to their high grade of multiplexing capacity, they allow to analyze multiple proteins in parallel within a reasonable period of time. In the present study, two different commercially available forward phase protein microarrays were performed. By the simultaneous detection of site specific phosphorylation levels of 42 RTKs and 46 intracellular proteins, they facilitate evaluation of the effect enhanced EGFR activation in cells harboring mutation of E-cadherin.

4.2.1 RTK proteome profiler

The so-called "RTK Proteome Profiler" was applied to screen for EGFR-mediated RTK-transactivation in *del 8* cells. Thereby, key residues for the activation of the respective molecules were detected. In total, activity of six RTKs was detected, all of which have been reported to play key roles in cancer. These were EGFR, HER2, c-RET, EPHA4, EPHB2, and MSPR. The gene encoding the receptor c-RET is a proto-oncogene. The ephrin receptors, which share a common structural organization, but differ in their affinities the ligands ephrin-A and ephrin-B [245, 246] promote mammary tumor growth and tumor associated angiogenesis [247]. HER2 as well as MSPR, also known as Ron, contribute to breast cancer. Furthermore, these receptors interact in different ways with E-cadherin or other RTKs. MSPR, which belongs to the same family as MET, is known to associate with integrins, cadherins and other receptors and crosstalk between MSPR and its associated receptors has been demonstrated [248]. Upon ligand binding and auto phosphorylation EphA2 [249, 250] interacts with SH2 domain containing PI3kinase to activate MAPK pathways [251, 252]. Transcription of EphA2 is dependent on the expression of E-cadherin [253].

Only two receptors, EGFR and HER2, exhibited a clear increase of activation with EGF-stimulation. However, differential activation was found only for EGFR (Fig. 3.9). Hence, previous results could be confirmed also by this alternative approach. Importantly, the chosen stimulation time corresponds to the maximal activation of EGFR. Hence, it cannot be entirely excluded that by changing the stimulation period transactivation of other RTKs could be detected.

4.2.2 Phospho-kinase proteome profiler

In addition to the detailed analysis of classical EGFR downstream components by RPPA, the so-called "Phospho-kinase Proteome Profiler" protein microarray detecting relative activation levels of 46 different intracellular signaling proteins was performed.

In order to obtain a more comprehensive insight into the regulation of the investigated proteins FCS containing samples were included in the analysis. Serum provides optimal conditions for cell growth and its variable composition presumably resembles the in vivo situation more closely [254, 255]. In contrast, serum starvation reduces basal cellular activity and allows the detailed analysis of particular signaling pathways by stimulation with specific growth factors. For the phospho-kinase proteome profiler experiment EGF-stimulation times of 1 and 60 min were chosen, in order to capture immediate as well as late signaling events.

In order to provide new insights and to discover new not anticipated proteins with key roles in the function of both *wt* and mutant E-cadherin an unbiased selection by use of rigorous selection criteria was performed [256]. EGF-dependent differential regulation at both time points of EGF-stimulation and differential activation in the presence of serum were defined as selection criteria. This approach revealed 26 proteins displaying differential activation between *wt* and *del 8* cells either in an EGF-dependent manner or in the presence of FCS. To further refine and prioritize this list, only proteins with overlap between both criteria were considered, resulting in a subset of eight proteins, whose activation patterns indicate their putative involvement in deregulated EGFR signaling caused by mutation of E-cadherin.

Interestingly, two ubiquitously expressed members of Src family kinases (SFKs), Src and Yes were found in this group. As a prototypic member of this family and because of its known interaction with E-cadherin and EGFR [257] and its prominent role in cancer [258], Src was chosen as target for further analysis. Noteworthy, Erk1/2 and Akt, which have been analyzed by RPPA, were also evaluated by the protein microarray. As determined by RPPA their activation maxima in the investigated cell lines were detected at about 5 and 15 min. As in the present approach different EGF-stimulation times were defined, results could neither be confirmed nor disproved by the phospho-kinase protein microarray.

4.2.3 Investigation of the Src activation profile

Deregulation of the cytosolic tyrosine kinase Src represents a major oncogenic signature in cancer [259, 260]. Although some Src activating mutations were found in colon [261], mutations are very rare and oncogenic Src-function is rather due to deregulation [262]. Src was found overexpressed or hyperactivated in many different types of cancer like cancers of the colorectum, breast, prostate, pancreas, head and neck, lung cancer, glioma, melanoma and different types of sarcoms [258]. At the plasma membrane, Src takes part in two processes. On the one hand, it processes signaling from RTKs and on the other hand from adhesion receptors (integrins and E-cadherin), regulating mainly cytoskeleton functions [191, 192, 262]. A functional impact of E-cadherin mutations on Src activity has not yet been reported.

The Src activation profile determined in the protein microarray-based screening approach is characterized by an EGF-induced increase of activation in *wt* cells, whereas no induction was detected in *del 8* cells. Moreover, differential activation was also found in FCS-containing samples. These findings could be reproduced in independent Western blot experiments. In order to evaluate the contribution of EGFR to the differential regulation in the presence of FCS, the EGFR-inhibiting monoclonal antibody cetuximab was applied in a concentration approximately corresponding to half the achievable dose in cancer patients [215-217]. Importantly, differential activation in FCS containing culture medium was lost after cetuximab treatment suggesting that the differential activation observed in the presence of FCS is mainly mediated by EGFR.

Src activity is regulated by tyrosine phosphorylation at two sites with opposing effects. Phosphorylation at Y416 in the activation loop of the kinase domain upregulates enzyme activity whereas phosphorylation of Y529 in the carboxy-terminal tail renders the enzyme less active [263]. A similar phosphorylation pattern of the negative regulatory domain of Src (Y529) indicates that its increased phosphorylation is not the reason for the reduced activation found in *del 8* cells.

Taken together, the present data suggest that the EGF dependent induction of Src activation is abrogated in cells harboring a mutation of E-cadherin by an unknown mechanism. In agreement with these findings, studies investigating human desmoglein 3 as an upstream regulator of Src in E-cadherin adhesion show that loss and disruption of E-cadherin function decrease Src activation in basal keratinocytes [264]. In contrast, another study revealed that E-cadherin suppression coincides with elevated Src activity in a squamous cell carcinoma cell line [265], suggesting that the direction of regulation depends on the cellular context.

A previous study of our group using the identical cell culture model demonstrates that mutation of E-cadherin influences Rac1 and Rho activation in opposite directions and that both Rho GTPases are critically involved in the establishment of the migratory and invasive tumor cell phenotype [244]. Src is well known as upstream regulator of Rac1 as well as Rho via multiple pathways. Interestingly, the activation pattern of Src detected in the present study exactly matches with the activation of both Rho GTPases (Fig. 4.1). This suggests that mutation of E-cadherin via EGFR modulates the activation of Src, which in turn acts as an upstream effector of Rho and Rac1 to regulate cell migration and invasion.
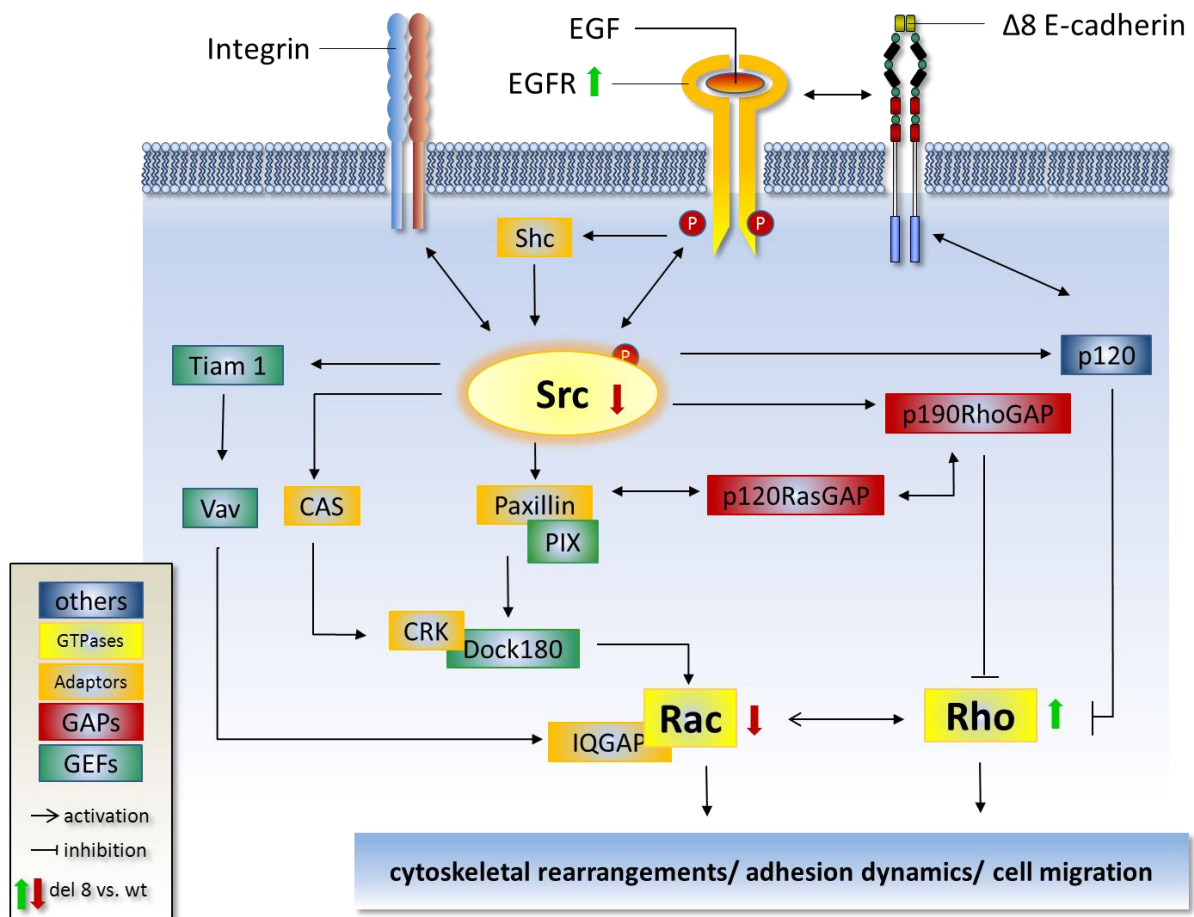
Figure 4.1 The interplay between EGFR, Src and Rho GTPases in cells harboring E-cadherin mutation: Mutation of E-cadherin via EGFR modulates the activation of Src, which in turn acts as an upstream effector of Rho and Rac1 to regulate cell migration and invasion.

4.2.4   Conclusion 2

In the present study the application of commercial protein microarrays revealed downregulation of Src activity in cells with an in frame deletion of exon 8 of E-cadherin. The differential regulation between *wt* and *del 8* cells was EGFR-dependent and could be reproduced by independent Western blot experiments. The detected activation profile of Src potentially explains the activation levels of the Rho GTPases Rac1 and Rho that were analyzed in a previous study of our group [244]. Due to their involvement in the establishment of the migratory and invasive phenotype, inhibition of the detected signaling axis may provide a strategy to prevent tumor cell spread. To substantiate this hypothesis and to clarify the importance of our findings for metastasis and for therapeutic intervention in gastric carcinoma patients, further functional investigations, using EGFR and Src inhibitors are necessary.

4.3 Analysis of cetuximab sensitivity of gastric cancer cell lines

The human gastric cancer cell lines AGS, KATOIII, MKN1, MKN28 and MKN45, with different EGFR and E-cadherin expression levels, were used in this study to investigate the effects of cetuximab on cell viability.

4.3.1 Growth-inhibitory and EGFR-inhibitory effects of cetuximab in gastric cancer cell lines

Two cell lines, MKN1 and MKN28, were identified whose metabolic activity was significantly reduced by cetuximab in a concentration-dependent manner. Consequently, these cell lines were classified as cetuximab-responsive cell lines. In contrast, cell lines MKN45, KATOIII and AGS were classified as cetuximab-nonresponsive cell lines. Consistently, only the two cetuximab-responsive cell lines exhibited significant reduction of EGFR activation after cetuximab treatment.

Considering that clinically relevant concentrations of cetuximab were used, the response to the antibody in the XTT assay was moderate, although the inhibition of EGFR activation was efficient. Importantly, all experiments were performed in the presence of fetal bovine serum to exclude adverse effects of starvation. Therefore, alternative pathways that mediate cell proliferation and survival other than the EGFR signaling pathway are likely to be active and possibly compensate the loss of EGFR activity under cetuximab treatment. Recently, cetuximab was found to have no significant effects on MKN28 and GLM-1 gastric cancer cell lines, whereas cetuximab significantly inhibited the subcutaneous and intraperitoneal tumor growth of MKN28 cells, but not GLM-1 cells, in a gastric cancer xenograft model [266]. A different study revealed that cetuximab alone did not show anti-proliferative or pro-apoptotic effects on the gastric cancer cell lines SGC-7901 and MKN45, but cetuximab enhanced the effect of the chemotherapeutic agent irinotecan on the cell lines by a mechanism that involved the down-regulation of the EGFR pathway that was up-regulated by irinotecan [267]. Together, the growth-inhibitory effects of anti- EGFR therapeutics alone or in combination with chemotherapeutic agents in gastric cancer cell lines have been examined in several studies, but most of the studies are based on a very small number of cell lines. Therefore, the conclusions that can be drawn from these studies are limited.

Anti-EGFR drugs inhibit cancer-cell proliferation, angiogenic growth factor production and tumor-induced angiogenesis, and they potentiate the anti-tumor activity of cytotoxic drugs and radiotherapy [268]. In several clinical phase II studies, cetuximab was assessed in combination with chemotherapeutic agents in the first-line treatment for advanced gastric and oesophageal gastric junction cancer, with high objective response rates between 41 to 65% [196-199]. Cetuximab plus capecitabine and cisplatin is currently being investigated in advanced gastric and oesophageal gastric

junction cancer in a randomized multinational phase III study. In patients, antibody-dependent cellular cytotoxicity and receptor internalization are likely to contribute to the anti-tumor activity of cetuximab in addition to the direct effect on EGFR activation.

4.3.2   Effects of EGFR expression and activation on cetuximab response

Whereas both responder cell lines, MKN1 and MKN28, showed high EGFR expression levels, only moderate or weak EGFR signals were detectable in the non-responder cell lines AGS, KATOIII and MKN45. In our panel of cell lines, no correlation was found between the expression level and the endogenous phosphorylation status of EGFR. As reported earlier, EGFR staining was distributed evenly on the entire cell in the MKN1 cell line. This cell line harbors a mutation in the gene encoding the ubiquitin ligase FBXW7 that changes arginine to cysteine in codon 465 (R465C, cosmic database). Arginine 465 is important for substrate binding. Because it has been shown that FBXW7 controls the degradation of EGFR [269] and the described mutation could lead to reduced substrate binding and subsequent cytoplasmic accumulation of EGFR, we conclude that the FBXW7 mutation might be responsible for the distribution of EGFR in MKN1 cells.

Interestingly, strong activation of EGFR was observed in the non-responsive cell lines KATOIII and MKN45, whereas the phosphorylation of EGFR was hardly detectable in the three other lines. We therefore found that high EGFR expression and low EGFR activation were associated with the cetuximab response in this panel of cell lines. In agreement with our findings, cell lines with acquired resistance to EGFR inhibitors derived from the human head and neck squamous cell carcinoma tumor cell line SCC-1 were recently reported to display elevated levels of pEGFR, pAkt and STAT3 that were associated with reduced apoptotic capacity [270]. Clinical data on the predictive value of activated EGFR in gastric cancer patients treated with cetuximab plus chemotherapy indicate that this biomarker may help to identify subgroups of patients who are likely to benefit from EGFR-targeted therapy in combination with chemotherapy [271].

The growth-inhibiting effect of lapatinib, which is a dual inhibitor of EGFR and HER2/Neu, has been shown in gastric cancer cell lines [272]. The expression of total and phosphorylated EGFR was not associated with the lapitinib response of the tumor cell lines. Furthermore, cetuximab preclinical anti-tumor activity was not predicted by relative total or activated EGFR tumor expression levels [273].

There is still a controversial discussion on the predictive value of the presence of EGFR on tumor cell membranes in the treatment of cancer patients with cetuximab plus chemotherapy. The expression of EGFR in tumor cells was not predictive of the therapeutic response in gastric and oesophageal-gastric junction cancer in various phase II trials of cetuximab in combination with chemotherapeutic agents [196, 198, 274], whereas in other studies, a tumor response was more commonly found in patients whose tumors expressed EGFR [199, 274]. In colorectal cancer, it has been suggested that the immunohistochemical measurement of EGFR expression may not be useful to predict the response to

cetuximab therapy [226, 275]. EGFR expression in gastric carcinomas is frequently characterized by strong intratumoral heterogeneity, with a range of completely negative to weakly or highly positive cancer cells within an individual tumor sample [276]. This peculiarity of pronounced EGFR heterogeneity may be of importance for the therapeutic response and for the evaluation of the EGFR expression level as a biomarker of response prediction.

4.3.3   Effects of genetic alterations on cetuximab response

Genetic alterations determine the resistance or sensitivity of EGFR-targeted therapies [226]. In our study, the non-responder cell lines harbor mutations in *KRAS* (AGS) or *CDH1* (AGS, KATOIII, MKN45) or an amplification of the *MET* gene (KATOIII, MKN45). In addition, one responder and one non-responder cell line, MKN1 and AGS, respectively, share mutations in *PIK3CA*, which indicates no relationship to cetuximab sensitivity. This finding is in line the literature showing that the separation of cell lines according to the *PIK3CA* mutation status alone did not distinguish cetuximab-sensitive from cetuximab-resistant colon cancer cell lines [277]. Whereas *KRAS* mutations and *MET* amplification have been linked to cetuximab resistance before, a relationship between *CDH1* mutations and cetuximab-resistance has not yet been suggested.

Several studies address the amplification of the *MET* gene or the activation of MET. In KATOIII cells, the low-level increased *MET* gene copy number is associated with five individual copies of chromosome 7 (aneuploidy), whereas AGS and MKN28 cells contain no such amplification [278]. Bertotti et al. have identified MKN45 and Hs746T as "MET-addicted" gastric cancer cell lines, whereas AGS and KATOIII cells are considered "MET-independent" cell lines [279].

4.3.4   Effect of MET activation on cetuximab response

Amplification of the *MET* gene was found in both non-responder cell lines MKN45 and KATOIII. In non-small cell lung cancer patients treated with the EGFR tyrosine kinase inhibitors gefitinib and erlotinib, the anti-EGFR therapy is effective in patients whose tumors harbor somatic mutations in EGFR. All patients, however, ultimately develop resistance to these agents, and several studies have identified two different EGFR tyrosine kinase inhibitor resistance mechanisms: a secondary mutation in EGFR, EGFR T790M, and amplification of the *MET* oncogene [280, 281].

Although *MET* amplification plays only a marginal role in the primary resistance to cetuximab in colorectal cancer patients [282], activation of MET was associated with resistance to cetuximab in other studies [283, 284]. For gastric cancer, the role of *MET* gene amplification and receptor activation has yet to be established.

However, it was shown that an intimate relationship exists between MET and EGFR, including physical interaction and ligand-dependent or ligand-independent transactivation, and that co-activation

of multiple RTKs in cancer cells conferred resistance to single-agent therapy [285, 286]. Hence, co-activated MET would explain the ineffectiveness of anti-EGFR therapy in the two non-responder cell lines, KATOIII and MKN45. "Oncogene addiction" should allow cells with *MET* amplification to respond well to MET inhibition [287, 288], which leads to the hypothesis that MET inhibition could potentially circumvent cetuximab resistance in our cell lines.

4.3.5 Effects of E-cadherin expression and mutation on the cetuximab response

Several cell culture studies suggest that the expression of E-cadherin is important for the response of neoplastic cells to anti-EGFR treatment. In non-small cell lung cancer cell lines, low E-cadherin and high urokinase-type plasminogen activator receptor (u-PAR), but not EGFR, are associated with the resistance to cetuximab [289]. The epithelial to mesenchymal transition was determined in a panel of 12 human hepatoma cell lines, and the epithelial cell lines (as classified based on their expression of E-cadherin and vimentin) were found to be significantly more susceptible to erlotinib, gefitinib and cetuximab than the mesenchymal cell lines [290]. Sensitivity to cetuximab in urothelial carcinoma cells requires E-cadherin expression [225]. Restoration of E-cadherin expression increases the sensitivity to gefitinib in lung cancer cell lines [291].

Based on these results, lung cell lines with low ErbB3 and E-cadherin expression were treated with a combination of HDAC and EGFR-tyrosine kinase inhibitors, and these cells underwent apoptosis [291].

In our study, it is not possible to draw conclusions on the role of E-cadherin expression for the prediction of the sensitivity to cetuximab in gastric cancer cell lines, because only one of the two responder cell lines is E-cadherin-positive.

However, E-cadherin gene mutations were found in all non-responder cell lines (AGS, KATOIII, and MKN45). The mutations in KATOIII and MKN45 are close to the exon/intron boundary and therefore affect regular splice sites [292]. As a result, aberrant mRNAs are produced. In MKN45 cells, this results to a 4-amino-acid deletion that affects the key Ca^{2+}-binding domain. In KATOIII cells, a G>A base substitution leads to the truncation of the protein. In AGS cells, a frame-shift mutation is likely to affect protein expression, which explains the failed detection in our experiments. These genetic alterations might therefore result in non-functional proteins or the complete inhibition of protein expression. We present evidence that the *CDH1* mutations are associated with enhanced EGFR activation in MKN45 and KATOIII cells, which is in agreement with previous observations of our group [218, 224]. The enhanced EGFR activation in the presence of these mutations provides an alternative mechanism to explain the cetuximab resistance.

4.3.6 Effects of the combination of cetuximab and chemotherapy

The present results show that the combination of cetuximab, 5-FU and cisplatin in clinically relevant concentrations did not improve the treatment outcome compared with cetuximab monotherapy. Only when five-fold-higher concentrations of the chemotherapeutic drugs were used, was the combination of cetuximab, 5-FU and cisplatin more efficacious than the cetuximab monotherapy in the MKN1 and the KATOIII cell lines. Under these conditions, the non-responder cell line KATOIII was sensitized by cetuximab for chemotherapeutic treatment.

4.3.7 Conclusion 3

In conclusion, in the present study five gastric cancer cell lines (AGS, KATOIII, MKN1, MKN28 and MKN45) were classified based on their response to cetuximab monotherapy. The initial classification remained valid when cetuximab was combined with chemotherapy. Molecular characterization allowed identification of potential predictive markers for the response to cetuximab. High expression of EGFR and low levels of receptor activation were associated with the response, whereas mutations in *KRAS* and MET activation were found to indicate resistance. We confirmed previous data showing that mutations in *CDH1* lead to enhanced EGFR activation [218], and we identified mutations in *CDH1* to predict resistance to cetuximab therapy.

5 SUMMARY

Although the mortality of gastric cancer is steadily decreasing it is still the second leading cause of cancer-related deaths worldwide. The onset of the disease is triggered by multiple genetic and epigenetic alterations. These events lead to the activation of oncogenes or the silencing of tumor suppressor genes, and thus to the transformation of normal gastric epithelial cells into malignant neoplasms.

Mutations of the tumor suppressive cell adhesion molecule E-cadherin and overexpression of the receptor tyrosine kinase EGFR are among the most frequent genetic alterations associated with diffuse type gastric cancer. Enhanced activation of EGFR was found in cells harboring E-cadherin mutation and suggests a novel mechanism for EGFR activation.

In the present study, the impact of one of the most frequent gastric cancer-related mutations of E-cadherin, a deletion of exon 8, on classical EGFR downstream components under long-term EGF stimulation was analyzed by reverse phase protein micro array. In addition to fine-resolved protein activation kinetics, this approach revealed enhanced activation of ERK1/2, a promoter of cell proliferation and migration, in cells harboring the E-cadherin mutation. Furthermore, down regulation of Src kinase activity was detected in the same cells using forward phase protein microarray. Interestingly, these data are in consistency with the activation levels of the Src downstream effectors Rac1 and Rho, which regulate cytoskeletal rearrangements and cell migration.

Taken together, the detected changes of EGFR, ERK1/2 and Src activation could explain the increased cell proliferation and motility observed in cells harboring E-cadherin mutations. Further functional investigations are necessary to evaluate the inhibition of the identified signaling molecules as a future strategy to prevent tumor cell spread in patients suffering from diffuse type gastric cancer.

These results further substantiate the important role of E-cadherin in EGFR signaling. In order to evaluate E-cadherin as potential biomarker for the response to treatment with the EGFR-inhibitory monoclonal antibody cetuximab, a panel of gastric cancer cell lines with different E-cadherin status was used. As determined previously, mutations of E-cadherin were found to enhance EGFR activation and were identified to predict resistance to cetuximab therapy. Comprehensive molecular characterization allowed identification of additional potential markers for response prediction. High expression of EGFR and low levels of receptor activation were associated with response, whereas mutations in *KRAS* and MET activation were found to indicate resistance.

In summary, the present study provides further insights of how mutation of E-cadherin affects EGFR mediated signaling and demonstrates the importance of the E-cadherin status as predictive marker for therapeutic intervention in gastric cancer.

6 SUPPLEMENT

Supplementary Table 1 Statistical data of the RPPA experiments

Protein	Groups (X vs.Y)		Diff.	p-value
	X	Y		
pEGFR	*pBat*	*wt*	-0.006	<0.001
		del 8	0.01	0.03
	del 8	*wt*	0.004	0.142
pErk1/2	*pBat*	*wt*	0	0.961
		del 8	0.003	0.025
	del 8	*wt*	-0.003	0.022
pAkt	*pBat*	*wt*	0.003	0.054
		del 8	0.004	0.014
	del 8	*wt*	-0.001	0.609
E-cadherin	*pBat*	*wt*	0.009	<0.001
		del 8	0.014	<0.001
	del 8	*wt*	0.005	<0.001
β-catenin	*pBat*	*wt*	0.001	0.096
		del 8	0.004	<0.001
	del 8	*wt*	-0.003	0.002
EGFR	*pBat*	*wt*	-0.002	<0.001
		del 8	0.001	0.030
	del 8	*wt*	-0.001	0.142
Erk1/2	*pBat*	*wt*	0.000	<0.001
		del 8	0.000	<0.001
	del 8	*wt*	0.000	1.000
Akt	*pBat*	*wt*	-0.001	0.069
		del 8	0.000	0.999
	del 8	*wt*	-0.001	0.070

Supplementary Table 2 Statistical data for EGFR expression

Groups (X vs. Y) X	Y	Mean ± SD (X)	Mean ± SD (Y)	p-value
A431	AGS	3.310 ± 0.821	0.353 ± 0.095	0.024
	KATOIII		0.457 ± 0.159	0.023
	MKN-1		1.137 ± 0.177	0.039
	MKN-28		0.777 ± 0.384	0.019
	MKN-45		0.180 ± 0.062	0.022
AGS	KATOIII	0.353 ± 0.095	0.457 ± 0.159	0.399
	MKN-1		1.137 ± 0.177	0.006
	MKN-28		0.777 ± 0.384	0.191
	MKN-45		0.180 ± 0.062	0.066
KATOIII	MKN-1	0.457 ± 0.159	1.137 ± 0.177	0.008
	MKN-28		0.777 ± 0.384	0.285
	MKN-45		0.180 ± 0.062	0.079
MKN-1	MKN-28	1.137 ± 0.177	0.777 ± 0.384	0.242
	MKN-45		0.180 ± 0.062	0.006
MKN-28	MKN-45	0.777 ± 0.384	0.180 ± 0.062	0.111

Supplementary Table 3 Statistical data for EGFR activation

Groups (X vs. Y) X	Y	Mean ± SD (X)	Mean ± SD (Y)	p-value
KATOIII	AGS	2.160 ± 0.499	0.368 ± 0.196	0.015
MKN1	KATOIII	0.275 ± 0.240	2.160 ± 0.499	0.011
	AGS		0.368 ± 0.196	0.634
MKN28	MKN1	0.160 ± 0.175	0.275 ± 0.240	0.540
	KATOIII		2.160 ± 0.499	0.013
	AGS		0.368 ± 0.196	0.243
MKN45	MKN28	0.736 ± 0.474	0.160 ± 0.175	0.159
	MKN1		0.275 ± 0.240	0.231
	KATOIII		2.160 ± 0.499	0.023
	AGS		0.368 ± 0.196	0.312

Supplementary Table 4 Statistical data for cetuximab sensitivity of gastric cancer cell lines

Cell line	Groups (X vs. Y) X	Y	Mean ± SD (X)	Mean ± SD (Y)	p-value
AGS					
	0	0.1	99.557 ± 0.812	98.063 ± 1.541	0.233
		1		93.040 ± 6.729	0.234
		10		94.023 ± 5.573	0.226
		100		92.987 ± 9.608	0.358
		200		86.573 ± 2.649	0.009
		GC		100.970 ± 11.424	0.850
		ISO		99.830 ± 11.433	0.971
	0.1	1	98.063 ± 1.541	93.040 ± 6.729	0.324
		10		94.023 ± 5.573	0.336
		100		92.987 ± 9.608	0.458
		200		86.573 ± 2.649	0.006

		GC		100.970 ± 11.424	0.704
		ISO		99.830 ± 11.433	0.815
	1	10	93.040 ± 6.729	94.023 ± 5.573	0.855
		100		92.987 ± 9.608	0.994
		200		86.573 ± 2.649	0.232
		GC		100.970 ± 11.424	0.371
		ISO		99.830 ± 11.433	0.436
	10	100	94.023 ± 5.573	92.987 ± 9.608	0.881
		200		86.573 ± 2.649	0.132
		GC		100.970 ± 11.424	0.416
		ISO		99.830 ± 11.433	0.489
	100	200	92.987 ± 9.608	86.573 ± 2.649	0.368
		GC		100.970 ± 11.424	0.408
		ISO		99.830 ± 11.433	0.473
	200	GC	86.573 ± 2.649	100.970 ± 11.424	0.155
		ISO		99.830 ± 11.433	0.177
	GC	ISO	100.970 ± 11.424	99.830 ± 11.433	0.909
KATOIII					
	0	0.1	98.777 ± 0.973	101.457 ± 7.214	0.587
		1		101.463 ± 3.259	0.287
		10		103.423 ± 8.805	0.458
		100		98.733 ± 4.316	0.988
		200		93.303 ± 3.778	0.121
		GC		102.867 ± 2.991	0.131
		ISO		100.077 ± 2.742	0.506
	0.1	1	101.457 ± 7.214	101.463 ± 3.259	0.999
		10		103.423 ± 8.805	0.780
		100		98.733 ± 4.316	0.611
		200		93.303 ± 3.778	0.181
		GC		102.867 ± 2.991	0.777
		ISO		100.077 ± 2.742	0.780
	1	10	101.463 ± 3.259	103.423 ± 8.805	0.746
		100		98.733 ± 4.316	0.435
		200		93.303 ± 3.778	0.048
		GC		102.867 ± 2.991	0.612
		ISO		100.077 ± 2.742	0.604
	10	100	103.423 ± 8.805	98.733 ± 4.316	0.470
		200		93.303 ± 3.778	0.174
		GC		102.867 ± 2.991	0.925
		ISO		100.077 ± 2.742	0.585
	100	200	98.733 ± 4.316	93.303 ± 3.778	0.178
		GC	98.733 ± 4.316	102.867 ± 2.991	0.253
		ISO		100.077 ± 2.742	0.677
	200	GC	93.303 ± 3.778	102.867 ± 2.991	0.029
		ISO		100.077 ± 2.742	0.072
	GC	ISO	102.867 ± 2.991	100.077 ± 2.742	0.30
MKN1					
	0	0.1	101.493 ± 3.533	99.640 ± 11.014	0.803
		1		93.007 ± 1.438	0.038
		10		87.380 ± 4.378	0.013
		100		71.767 ± 2.948	<0.001
		200		59.500 ± 3.486	<0.001
		GC		98.430 ± 3.490	0.346
		ISO		100.087 ± 5.988	0.748
	0.1	1	99.640 ± 11.014	93.007 ± 1.438	0.407
		10		87.380 ± 4.378	0.184
		100		71.767 ± 2.948	0.041
		200		59.500 ± 3.486	0.017

		GC		98.430 ± 3.490	0.870
		ISO		100.087 ± 5.988	0.955
	1	10	93.007 ± 1.438	87.380 ± 4.378	0.146
		100		71.767 ± 2.948	0.002
		200		59.500 ± 3.486	0.001
		GC		98.430 ± 3.490	0.099
		ISO		100.087 ± 5.988	0.171
	10	100	87.380 ± 4.378	71.767 ± 2.948	0.010
		200		59.500 ± 3.486	0.001
		GC		98.430 ± 3.490	0.029
		ISO		100.087 ± 5.988	0.046
	100	200	71.767 ± 2.948	59.500 ± 3.486	0.010
		GC		98.430 ± 3.490	0.001
		ISO		100.087 ± 5.988	0.006
	200	GC	59.500 ± 3.486	98.430 ± 3.490	<0.001
		ISO		100.087 ± 5.988	0.002
	GC	ISO	98.430 ± 3.490	100.087 ± 5.988	0.705
MKN28					
	0	0.1	99.243 ± 1.220	98.290 ± 3.613	0.700
		1		90.787 ± 2.229	0.009
		10		89.017 ± 7.899	0.151
		100		83.423 ± 6.388	0.046
		200		80.367 ± 4.094	0.010
		GC		105.930 ± 7.383	0.255
		ISO		105.353 ± 4.326	0.125
	0.1	1	98.290 ± 3.613	90.787 ± 2.229	0.048
		10		89.017 ± 7.899	0.168
		100		83.423 ± 6.388	0.036
		200		80.367 ± 4.094	0.005
		GC		105.930 ± 7.383	0.209
		ISO		105.353 ± 4.326	0.098
	1	10	90.787 ± 2.229	89.017 ± 7.899	0.740
		100		83.423 ± 6.388	0.175
		200		80.367 ± 4.094	0.029
		GC		105.930 ± 7.383	0.061
		ISO		105.353 ± 4.326	0.014
	10	100	89.017 ± 7.899	83.423 ± 6.388	0.396
		200		80.367 ± 4.094	0.191
		GC		105.930 ± 7.383	0.054
		ISO		105.353 ± 4.326	0.049
	100	200	83.423 ± 6.388	80.367 ± 4.094	0.530
		GC		105.930 ± 7.383	0.017
		ISO		105.353 ± 4.326	0.011
	200	GC	80.367 ± 4.094	105.930 ± 7.383	0.012
		ISO		105.353 ± 4.326	0.002
	GC	ISO	105.930 ± 7.383	105.353 ± 4.326	0.914
MKN45					
	0	0.1	97.240 ± 3.283	107.533 ± 3.654	0.023
		1		107.170 ± 9.123	0.192
		10		102.130 ± 8.709	0.440
		100		89.867 ± 10.365	0.344
		200		88.257 ± 5.512	0.087
		GC		108.047 ± 10.250	0.203
		ISO		110.300 ± 8.389	0.100
	0.1	1	107.533 ± 3.654	107.170 ± 9.123	0.953
		10		102.130 ± 8.709	0.402
		100		89.867 ± 10.365	0.085
		200		88.257 ± 5.512	0.010

X	Y	Mean ± SD (X)	Mean ± SD (Y)	p-value
	GC		108.047 ± 10.250	0.941
	ISO		110.300 ± 8.389	0.640
1	10	107.170 ± 9.123	102.130 ± 8.709	0.527
	100		89.867 ± 10.365	0.097
	200		88.257 ± 5.512	0.048
	GC		108.047 ± 10.250	0.917
	ISO		110.300 ± 8.389	0.685
10	100	102.130 ± 8.709	89.867 ± 10.365	0.194
	200		88.257 ± 5.512	0.092
	GC		108.047 ± 10.250	0.490
	ISO		110.300 ± 8.389	0.307
100	200	89.867 ± 10.365	88.257 ± 5.512	0.827
	GC		108.047 ± 10.250	0.097
	ISO		110.300 ± 8.389	0.059
200	GC	88.257 ± 5.512	108.047 ± 10.250	0.059
	ISO		110.300 ± 8.389	0.025
GC	ISO	108.047 ± 10.250	110.300 ± 8.389	0.783

Supplementary Table 5 Statistical data for the effect of a combination of cetuximab plus chemotherapy

Cell line	Groups (X vs. Y) X	Y	Mean ± SD (X)	Mean ± SD (Y)	p-value
KATOIII					
	chemotherapy 2	combination 2	111.235 ± 58.077	45.792 ± 57.208	0.237
	chemotherapy 2	cetuximab		116.208 ± 34.686	0.906
	chemotherapy 2	chemotherapy 1		133.227 ± 38.173	0.617
	chemotherapy 2	combination 1		101.678 ± 47.507	0.837
	chemotherapy 2	untreated		102.324 ± 3.781	0.816
	combination 2	cetuximab	45.792 ± 57.208	116.208 ± 34.686	0.158
	combination 2	chemotherapy 1		133.227 ± 38.173	0.102
	combination 2	combination 1		101.678 ± 47.507	0.265
	combination 2	untreated		102.324 ± 3.781	0.229
	cetuximab	chemotherapy 1	116.208 ± 34.686	133.227 ± 38.173	0.598
	cetuximab	combination 1		101.678 ± 47.507	0.693
	cetuximab	untreated		102.324 ± 3.781	0.560
	chemotherapy 1	combination 1	133.227 ± 38.173	101.678 ± 47.507	0.423
	chemotherapy 1	untreated		102.324 ± 3.781	0.295
	combination 1	untreated	101.678 ± 47.507	102.324 ± 3.781	0.983
MKN1					
	chemotherapy 2	combination 2	24.516 ± 32.313	-10.133 ± 34.599	0.274
	chemotherapy 2	cetuximab		60.569 ± 6.491	0.189
	chemotherapy 2	chemotherapy 1		97.138 ± 13.703	0.044
	chemotherapy 2	combination 1		50.502 ± 8.243	0.296
	chemotherapy 2	untreated		100.161 ± 0.787	0.056
	combination 2	cetuximab	-10.133 ± 34.599	60.569 ± 6.491	0.067
	combination 2	chemotherapy 1		97.138 ± 13.703	0.021
	combination 2	combination 1		50.502 ± 8.243	0.086
	combination 2	untreated		100.161 ± 0.787	0.031
	cetuximab	chemotherapy 1	60.569 ± 6.491	97.138 ± 13.703	0.028
	cetuximab	combination 1		50.502 ± 8.243	0.176
	cetuximab	untreated		100.161 ± 0.787	0.008
	chemotherapy 1	combination 1	97.138 ± 13.703	50.502 ± 8.243	0.012
	chemotherapy 1	untreated		100.161 ± 0.787	0.739
	combination 1	untreated	50.502 ± 8.243	100.161 ± 0.787	0.009

chemotherapy 1 = 5-FU [0.05 μg/m]/cisplatin [0.5 μg/ml]

combination 1 = 5-FU [0.05 μg/m]/cisplatin [0.5 μg/ml]/cetuximab [100 μg/ml]
chemotherapy 2 = 5-FU [0.25 μg/m]/cisplatin [2.5 μg/ml]
combination 2 = 5-FU [0.25 μg/m]/cisplatin [2.5 μg/ml]/cetuximab [100 μg/ml]

Supplementary Table 6 Statistical data for the effect of cetuximab on the phosphorylation level of EGFR

Cell line	Groups (X vs. Y) X	Y	Mean ± SD (X)	Mean ± SD (Y)	p-value
AGS					
	0	0.1	1.433 ± 1.080	1.137 ± 0.698	0.713
		1		1.103 ± 0.316	0.655
		10		0.787 ± 0.545	0.424
		100		0.683 ± 0.471	0.358
		200		0.927 ± 0.611	0.528
	0.1	1	1.137 ± 0.698	1.103 ± 0.316	0.945
		10		0.787 ± 0.545	0.533
		100		0.683 ± 0.471	0.411
		200		0.927 ± 0.611	0.715
	1	10	1.103 ± 0.316	0.787 ± 0.545	0.444
		100		0.683 ± 0.471	0.278
		200		0.927 ± 0.611	0.687
	10	100	0.787 ± 0.545	0.683 ± 0.471	0.816
		200		0.927 ± 0.611	0.782
	100	200	0.683 ± 0.471	0.927 ± 0.611	0.615
KATOIII					
	0	0.1	0.950 ± 0.123	0.970 ± 0.080	0.827
		1		1.040 ± 0.242	0.607
		10		1.067 ± 0.248	0.519
		100		1.333 ± 0.621	0.398
		200		0.910 ± 0.035	0.635
	0.1	1	0.970 ± 0.080	1.040 ± 0.242	0.674
		10		1.067 ± 0.248	0.576
		100		1.333 ± 0.621	0.418
		200		0.910 ± 0.035	0.327
	1	10	1.040 ± 0.242	1.067 ± 0.248	0.900
		100		1.333 ± 0.621	0.509
		200		0.910 ± 0.035	0.452
	10	100	1.067 ± 0.248	1.333 ± 0.621	0.546
		200		0.910 ± 0.035	0.388
	100	200	1.333 ± 0.621	0.910 ± 0.035	0.359
MKN1					
	0	0.1	1.743 ± 0.490	1.363 ± 0.560	0.427
		1		0.900 ± 0.106	0.09
		10		0.760 ± 0.347	0.053
		100		0.700 ± 0.295	0.045
		200		0.623 ± 0.163	0.047
	0.1	1	1.363 ± 0.560	0.900 ± 0.106	0.287
		10		0.760 ± 0.347	0.202
		100		0.700 ± 0.295	0.166
		200		0.623 ± 0.163	0.141
	1	10	0.900 ± 0.106	0.760 ± 0.347	0.563
		100		0.700 ± 0.295	0.364
		200		0.623 ± 0.163	0.079
	10	100	0.760 ± 0.347	0.700 ± 0.295	0.831
		200		0.623 ± 0.163	0.583

	100	200	0.700 ± 0.295	0.623 ± 0.163	0.719
MKN28					
	0	0.1	2.027 ± 0.608	1.290 ± 0.176	0.163
		1		1.060 ± 0.397	0.093
		10		0.663 ± 0.201	0.049
		100		0.497 ± 0.100	0.046
		200		0.640 ± 0.115	0.054
	0.1	1	1.290 ± 0.176	1.060 ± 0.397	0.432
		10		0.663 ± 0.201	0.016
		100		0.497 ± 0.100	0.005
		200		0.640 ± 0.115	0.009
	1	10	1.060 ± 0.397	0.663 ± 0.201	0.222
		100		0.497 ± 0.100	0.126
		200		0.640 ± 0.115	0.202
	10	100	0.663 ± 0.201	0.497 ± 0.100	0.291
		200		0.640 ± 0.115	0.872
	100	200	0.497 ± 0.1	0.640 ± 0.115	0.181
MKN45					
	0	0.1	1.067 ± 0.218	1.000 ± 0.151	0.689
		1		0.877 ± 0.178	0.310
		10		1.007 ± 0.061	0.686
		100		1.073 ± 0.047	0.963
		200		0.963 ± 0.172	0.557
	0.1	1	1.000 ± 0.151	0.877 ± 0.178	0.413
		10		1.007 ± 0.061	0.949
		100		1.073 ± 0.047	0.494
		200		0.963 ± 0.172	0.796
	1	10	0.877 ± 0.178	1.007 ± 0.061	0.334
		100		1.073 ± 0.047	0.190
		200		0.963 ± 0.172	0.577
	10	100	1.007 ±0.061	1.073 ± 0.047	0.214
		200		0.963 ± 0.172	0.714
	100	200	1.073 ± 0.047	0.963 ± 0.172	0.386

Supplementary Table 7 Statistical data for E-cadherin expression

Groups (X vs. Y)		Mean ± SD (X)	Mean ± SD (Y)	p-value
X	Y			
A431	KATOIII	2.543 ± 0.873	1.850 ± 0.814	0.372
	MKN-28		2.157 ± 0.292	0.530
	MKN-45		0.733 ± 0.315	0.056
KATOIII	MKN-28	1.850 ± 0.814	2.157 ± 0.292	0.590
	MKN-45		0.733 ± 0.315	0.128
MKN-28	MKN-45	2.157 ± 0.292	0.733 ± 0.315	0.005

Supplementary Table 8 Statistical data for the phosphorylation of MET

Groups (X vs. Y)		Mean ± SD (X)	Mean ± SD (Y)	p-value
X	Y			
KATOIII	MKN45	0.840 ± 0.745	4.467 ± 0.766	0.004

7 ABBREVIATIONS

AA	amino acid
mAb/pAb	monoclonal/polyclonal antibody
ABC	antibody binding capacity
AR	amphiregulin
AJ	adherens junction
APC	adenomatous polyposis coli
APS	ammonium persulfate
ATCC	American Type Culture Collection
ATP	adenosine triphosphate
BTC	betacellulin
BSA	bovine serum albumin
°C	degree Celsius
CCC	cytoplasmic cell-adhesion complex
del 8/del 9	deletion of exon 8 or 9
DMEM	Dulbecco's Modified Eagle's Medium
DMSO	dimethyl sulfoxide
DNA	deoxyribonucleic acid
dNTP	deoxynucleotide triphosphate
E-cadherin	epithelial (E)-cadherin
EC-/CAD domain	extracellular E-cadherin domain
ECL	enhanced chemiluminescence
ECM	extracellular matrix
EGFR	epidermal growth factor receptor
EMT	epithelial-to-mesenchyme transition
EPR	epiregulin
ErbB	avian erythroblastosis oncogene B
FACS	fluorescence-activated cell sorter
FCS	fetal calf serum
FITC	fluorescein isothiocyanate
FPPA	forward phase protein array
FRAP	fluorescence recovery after photobleaching
FRET	fluorescence resonance energy transfer
g	gram
g	earth's gravity
GDP	guanosine diphosphate

GRB2	growth factor receptor binding protein 2
GTP	guanosine triphosphate
h	hour
HB-EGF	heparin-binding growth factor
HDGC	hereditary diffuse gastric carcinoma
HGF	hepatocyte growth factor
HNPCC	hereditary nonpolyposis colorectal cancer
HRP	horseradish peroxidase
IHC	immunohistochemistry
IP	immunoprecipitation
kD	kiloDalton
l	litre
L-CAM	liver cell adhesion molecule
LOH	loss of heterozygosity
NSCLC	non-smal cell lung cancer
M	molar
MAPK	mitogen-activated protein kinase
min	minute
Met-/HGF	receptor hepatocyte growth factor receptor
MSI	microsatellite instability
μ	micro
NRG	neuregulin
PAGE	polyacrylamide gel electrophoresis
PBS	phosphate buffered saline
PCR	polymerase chain reaction
PI3K	phosphatidylinositol 3-kinase
PKC	protein kinase C
PLCγ	phospholipase C-γ
PMSF	phenylmethylsulphonyl fluoride
PTB	domain phosphotyrosine binding domain
PVDF	polyvinylidene fluoride
Rpm	rotations per minute
RPPA	reverse phase protein microarray
RT	room temperature
RTK	receptor tyrosine kinase
SCID	severe combined immunodeficiency
SDS	sodium dodecyl sulfate
s	second

SH2 domain	Src homology 2 domain
SHC	Src homologues and collagen protein
SNP	single nucleotide polymorphism
SOS	son-of-sevenless protein
STAT	signal transducer and activator of transcription
TBS	tris buffered saline
TEMED	tetramethylethylenediamine
TGF-α	transforming growth factor-α
TKI	small-molecule tyrosine-kinase inhibitor
Tris	tris(hydroxymethyl)aminomethane
U	enzyme activity unit
V	volt
% v/v	volume-volume percentage
wt	wild-type
% w/v	mass-volume percentage

8 PUBLICATIONS

8.1 Research articles

2012   Kneissl J., Keller S., Lorber T., **Heindl S.**, Keller G., Rauser S., Drexler I.,Hapfelmeier A., Höfler H., Luber B.
Association of amphiregulin with the cetuximab sensitivity of gastric cancer cell lines
Int J Oncol. 2012 Aug;41(2):733-44; PMID:22614881

2012   **Heindl S**., Eggenstein E., Keller S., Kneissl J., Keller G., Mutze K., Rauser S., Gasteiger G., Drexler I, Hapfelmeier A., Höfler H., Luber B.
Relevance of MET activation and genetic alterations of KRAS and E-cadherin for cetuximab sensitivity of gastric cancer cell lines
J Cancer Res Clin Oncol. 2012 Jan 31. PMID:22290393

2010   Rasper M., Schäfer A., Piontek G., Teufel J., Brockhoff G., Ringel F., **Heindl S.**, Zimmer C., Schlegel J.
Aldehyde dehydrogenase 1 positive glioblastoma cells show brain tumor stem cell capacity.
Neuro Oncol. 2010 Oct;12(10):1024-33. Epub 2010 Jul 13. PMID:20627895

2009   Mateus AR., Simões-Correia J., Figueiredo J., **Heindl S.**, Alves CC., Suriano G., Luber B., Seruca R.
E-cadherin mutations and cell motility: a genotype-phenotype correlation.
Exp Cell Res. 2009 May 1;315(8):1393-402. Epub 2009 Mar 4. PMID:19268661

2008   Glatt S., Halbauer D., **Heindl S.**, Wernitznig A., Kozina D., Su K.C., Puri C., Garin-Chesa P., Sommergruber W.
hGPR87 contributes to viability of human tumor cells.
Int J Cancer. 2008 May 1;122(9):2008-16. PMID:18183596

8.2 Posters

2011   53rd Symposium of the Society for Histochemistry, München

       Heindl S., Lang C., Wolff C., Malinowsky K., Becker KF., Luber B.
E-cadherin mutations contribute to gastric carcinogenesis by modulating multiple EGFR-dependent downstream signalling pathways.

2010   AACR 101st Annual Meeting, Washington, DC, USA

       Heindl S., Lang C., Wolff C., Malinowsky K., Becker KF., Luber B.
E-cadherin mutations contribute to gastric carcinogenesis by modulating multiple EGFR-dependent downstream signalling pathways.

8.3 Talk

2012   96. Jahrestagung der Deutschen Gesellschaft für Pathologie e.V.

Heindl S., Eggenstein E., Keller S., Kneissl J., Keller G., Mutze K., Rauser S., Gasteiger G., Drexler I, Hapfelmeier A., Höfler H., Luber B.
Relevance of MET activation and genetic alterations of KRAS and E-cadherin for cetuximab sensitivity of gastric cancer cell lines (presented by S. Keller)

9 REFERENCES

1. Ferlay, J., et al., *Estimates of worldwide burden of cancer in 2008: GLOBOCAN 2008.* Int J Cancer, 2010. **127**(12): p. 2893-917.
2. Ricci, V., M. Romano, and P. Boquet, *Molecular cross-talk between Helicobacter pylori and human gastric mucosa.* World J Gastroenterol, 2011. **17**(11): p. 1383-99.
3. Herszenyi, L. and Z. Tulassay, *Epidemiology of gastrointestinal and liver tumors.* Eur Rev Med Pharmacol Sci, 2010. **14**(4): p. 249-58.
4. Jemal, A., et al., *Cancer statistics, 2008.* CA Cancer J Clin, 2008. **58**(2): p. 71-96.
5. Kamangar, F., G.M. Dores, and W.F. Anderson, *Patterns of cancer incidence, mortality, and prevalence across five continents: defining priorities to reduce cancer disparities in different geographic regions of the world.* J Clin Oncol, 2006. **24**(14): p. 2137-50.
6. Gonzalez, C.A. and A. Agudo, *Carcinogenesis, prevention and early detection of gastric cancer: Where we are and where we should go.* Int J Cancer, 2011.
7. Satoh, S., et al., *Retrospective evaluation of sequential outpatient chemotherapy for advanced gastric cancer.* Chemotherapy, 2007. **53**(3): p. 226-32.
8. Lauren, P., *The Two Histological Main Types of Gastric Carcinoma: Diffuse and So-Called Intestinal-Type Carcinoma. An Attempt at a Histo-Clinical Classification.* Acta Pathol Microbiol Scand, 1965. **64**: p. 31-49.
9. Stemmermann, G.N., *Intestinal metaplasia of the stomach. A status report.* Cancer, 1994. **74**(2): p. 556-64.
10. Catalano, V., et al., *Gastric cancer.* Crit Rev Oncol Hematol, 2009. **71**(2): p. 127-64.
11. Hamilton, S. and L. Aaltonen, *WHO classification of tumors. Pathology and Genetics of tumours of the Digestive System.* IARC Press, 2000.
12. Lauren, P.A. and T.J. Nevalainen, *Epidemiology of intestinal and diffuse types of gastric carcinoma. A time-trend study in Finland with comparison between studies from high- and low-risk areas.* Cancer, 1993. **71**(10): p. 2926-33.
13. Munoz, N. and R. Connelly, *Time trends of intestinal and diffuse types of gastric cancer in the United States.* Int J Cancer, 1971. **8**(1): p. 158-64.
14. Roukos, D., M. Lorenz, and C. Hottenrott, *[Prognostic significance of the Lauren classification of patients with stomach carcinoma. A statistical analysis of long-term results following gastrectomy].* Schweiz Med Wochenschr, 1989. **119**(21): p. 755-9.
15. Crew, K.D. and A.I. Neugut, *Epidemiology of gastric cancer.* World J Gastroenterol, 2006. **12**(3): p. 354-62.
16. Forman, D. and V.J. Burley, *Gastric cancer: global pattern of the disease and an overview of environmental risk factors.* Best Pract Res Clin Gastroenterol, 2006. **20**(4): p. 633-49.
17. Kelley, J.R. and J.M. Duggan, *Gastric cancer epidemiology and risk factors.* J Clin Epidemiol, 2003. **56**(1): p. 1-9.
18. Gonzalez, C.A., et al., *Helicobacter pylori infection assessed by ELISA and by immunoblot and noncardia gastric cancer risk in a prospective study: the Eurgast-EPIC project.* Ann Oncol, 2011.
19. Wang, T.C. and J.G. Fox, *Helicobacter pylori and gastric cancer: Koch's postulates fulfilled?* Gastroenterology, 1998. **115**(3): p. 780-3.

20. Wang, R., *[The epidemiological study of subtype risk factors of gastric cancer].* Zhonghua Liu Xing Bing Xue Za Zhi, 1993. **14**(5): p. 295-9.

21. Herrera, V. and J. Parsonnet, *Helicobacter pylori and gastric adenocarcinoma.* Clin Microbiol Infect, 2009. **15**(11): p. 971-6.

22. Hocker, M., et al., *Oxidative stress activates the human histidine decarboxylase promoter in AGS gastric cancer cells.* J Biol Chem, 1998. **273**(36): p. 23046-54.

23. Peek, R.M., Jr. and M.J. Blaser, *Helicobacter pylori and gastrointestinal tract adenocarcinomas.* Nat Rev Cancer, 2002. **2**(1): p. 28-37.

24. Singh, K. and U.C. Ghoshal, *Causal role of Helicobacter pylori infection in gastric cancer: an Asian enigma.* World J Gastroenterol, 2006. **12**(9): p. 1346-51.

25. Go, M.F., *Helicobacter pylori: its role in ulcer disease and gastric cancer and how to detect the infection.* Acta Gastroenterol Latinoam, 1996. **26**(1): p. 45-9.

26. Brenner, H., et al., *Is Helicobacter pylori infection a necessary condition for noncardia gastric cancer?* Am J Epidemiol, 2004. **159**(3): p. 252-8.

27. Miwa, H., et al., *Improvement of reflux symptoms 3 years after cure of Helicobacter pylori infection: a case-controlled study in the Japanese population.* Helicobacter, 2002. **7**(4): p. 219-24.

28. Gonzalez, C.A., et al., *Smoking and the risk of gastric cancer in the European Prospective Investigation Into Cancer and Nutrition (EPIC).* Int J Cancer, 2003. **107**(4): p. 629-34.

29. Palli, D., *Epidemiology of gastric cancer: an evaluation of available evidence.* J Gastroenterol, 2000. **35 Suppl 12**: p. 84-9.

30. Wang, X.Q., P.D. Terry, and H. Yan, *Review of salt consumption and stomach cancer risk: epidemiological and biological evidence.* World J Gastroenterol, 2009. **15**(18): p. 2204-13.

31. Ushijima, T. and M. Sasako, *Focus on gastric cancer.* Cancer Cell, 2004. **5**(2): p. 121-5.

32. Potter, J.D., *Diet and cancer: possible explanations for the higher risk of cancer in the poor.* IARC Sci Publ, 1997(138): p. 265-83.

33. La Vecchia, C., et al., *Family history and the risk of stomach and colorectal cancer.* Cancer, 1992. **70**(1): p. 50-5.

34. Vogiatzi, P., et al., *Deciphering the underlying genetic and epigenetic events leading to gastric carcinogenesis.* J Cell Physiol, 2007. **211**(2): p. 287-95.

35. Keller, G., H. Hofler, and K.F. Becker, *Molecular medicine of gastric adenocarcinomas.* Expert Rev Mol Med, 2005. **7**(17): p. 1-13.

36. Fitzgerald, R.C., et al., *Hereditary diffuse gastric cancer: updated consensus guidelines for clinical management and directions for future research.* J Med Genet, 2010. **47**(7): p. 436-44.

37. Jemal, A., et al., *Global patterns of cancer incidence and mortality rates and trends.* Cancer Epidemiol Biomarkers Prev, 2010. **19**(8): p. 1893-907.

38. Becker, K. and G. Keller, *Gastric Cancer.* In: Encyclopedia of Life Science, 2010: p. Doi:10.1002/9780470015902.a0006056.pub2.

39. Fishel, R., et al., *The human mutator gene homolog MSH2 and its association with hereditary nonpolyposis colon cancer.* Cell, 1993. **75**(5): p. 1027-38.

40. Papadopoulos, N., et al., *Mutation of a mutL homolog in hereditary colon cancer.* Science, 1994. **263**(5153): p. 1625-9.

41. Oberhuber, G. and M. Stolte, *Gastric polyps: an update of their pathology and biological significance.* Virchows Arch, 2000. **437**(6): p. 581-90.

42. Becker, K.F., et al., *E-cadherin gene mutations provide clues to diffuse type gastric carcinomas.* Cancer Res, 1994. **54**(14): p. 3845-52.

43. Hattori, Y., et al., *K-sam, an amplified gene in stomach cancer, is a member of the heparin-binding growth factor receptor genes.* Proc Natl Acad Sci U S A, 1990. **87**(15): p. 5983-7.

44. Yonemura, Y., et al., *Expression of c-erbB-2 oncoprotein in gastric carcinoma. Immunoreactivity for c-erbB-2 protein is an independent indicator of poor short-term prognosis in patients with gastric carcinoma.* Cancer, 1991. **67**(11): p. 2914-8.

45. Kim, M.A., et al., *Evaluation of HER-2 gene status in gastric carcinoma using immunohistochemistry, fluorescence in situ hybridization, and real-time quantitative polymerase chain reaction.* Hum Pathol, 2007. **38**(9): p. 1386-93.

46. Park, W.S., et al., *Frequent somatic mutations of the beta-catenin gene in intestinal-type gastric cancer.* Cancer Res, 1999. **59**(17): p. 4257-60.

47. Kuniyasu, H., et al., *Aberrant expression of c-met mRNA in human gastric carcinomas.* Int J Cancer, 1993. **55**(1): p. 72-5.

48. Arkenau, H.T., *Gastric cancer in the era of molecularly targeted agents: current drug development strategies.* J Cancer Res Clin Oncol, 2009. **135**(7): p. 855-66.

49. Keller, G., et al., *Microsatellite instability in adenocarcinomas of the upper gastrointestinal tract. Relation to clinicopathological data and family history.* Am J Pathol, 1995. **147**(3): p. 593-600.

50. dos Santos, N.R., et al., *Microsatellite instability at multiple loci in gastric carcinoma: clinicopathologic implications and prognosis.* Gastroenterology, 1996. **110**(1): p. 38-44.

51. Buonsanti, G., et al., *Microsatellite instability in intestinal- and diffuse-type gastric carcinoma.* J Pathol, 1997. **182**(2): p. 167-73.

52. Panani, A.D., *Cytogenetic and molecular aspects of gastric cancer: clinical implications.* Cancer Lett, 2008. **266**(2): p. 99-115.

53. Wu, W.K., et al., *Dysregulation of cellular signaling in gastric cancer.* Cancer Lett, 2010. **295**(2): p. 144-53.

54. Strachan, T. and A.P. Read, 1999.

55. Siewert, J.R., et al., *Relevant prognostic factors in gastric cancer: ten-year results of the German Gastric Cancer Study.* Ann Surg, 1998. **228**(4): p. 449-61.

56. Ott, K., et al., *Neoadjuvant chemotherapy with cisplatin, 5-FU, and leucovorin (PLF) in locally advanced gastric cancer: a prospective phase II study.* Gastric Cancer, 2003. **6**(3): p. 159-67.

57. Ajani, J.A., et al., *Resectable gastric carcinoma. An evaluation of preoperative and postoperative chemotherapy.* Cancer, 1991. **68**(7): p. 1501-6.

58. Kelsen, D.P., *Adjuvant and neoadjuvant therapy for gastric cancer.* Semin Oncol, 1996. **23**(3): p. 379-89.

59. Lordick, F. and J.R. Siewert, *Recent advances in multimodal treatment for gastric cancer: a review.* Gastric Cancer, 2005. **8**(2): p. 78-85.

60. Wagner, A.D., et al., *Chemotherapy in advanced gastric cancer: a systematic review and meta-analysis based on aggregate data.* J Clin Oncol, 2006. **24**(18): p. 2903-9.

61. Kim, J.G., H.Y. Chung, and W. Yu, *Recent advances in chemotherapy for advanced gastric cancer.* World J Gastrointest Oncol, 2010. **2**(7): p. 287-94.

62. Bang, Y.J., et al., *Trastuzumab in combination with chemotherapy versus chemotherapy alone for treatment of HER2-positive advanced gastric or gastro-oesophageal junction cancer (ToGA): a phase 3, open-label, randomised controlled trial.* Lancet, 2010. **376**(9742): p. 687-97.

63. Brooke, M.A., D. Nitoiu, and D.P. Kelsell, *Cell-cell connectivity: desmosomes and disease.* J Pathol, 2012. **226**(2): p. 158-71.

64.   Ye, H., J. Liu, and J.Y. Wu, *Cell adhesion molecules and their involvement in autism spectrum disorder.* Neurosignals, 2010. **18**(2): p. 62-71.

65.   Gonzalez-Amaro, R. and F. Sanchez-Madrid, *Cell adhesion molecules: selectins and integrins.* Crit Rev Immunol, 1999. **19**(5-6): p. 389-429.

66.   Rojas, A.I. and A.R. Ahmed, *Adhesion receptors in health and disease.* Crit Rev Oral Biol Med, 1999. **10**(3): p. 337-58.

67.   Hynes, R.O., *Cell adhesion: old and new questions.* Trends Cell Biol, 1999. **9**(12): p. M33-7.

68.   Joseph-Silverstein, J. and R.L. Silverstein, *Cell adhesion molecules: an overview.* Cancer Invest, 1998. **16**(3): p. 176-82.

69.   Christofori, G. and H. Semb, *The role of the cell-adhesion molecule E-cadherin as a tumour-suppressor gene.* Trends Biochem Sci, 1999. **24**(2): p. 73-6.

70.   Bryant, D.M. and K.E. Mostov, *From cells to organs: building polarized tissue.* Nat Rev Mol Cell Biol, 2008. **9**(11): p. 887-901.

71.   Tepass, U., et al., *shotgun encodes Drosophila E-cadherin and is preferentially required during cell rearrangement in the neurectoderm and other morphogenetically active epithelia.* Genes Dev, 1996. **10**(6): p. 672-85.

72.   Angst, B.D., C. Marcozzi, and A.I. Magee, *The cadherin superfamily: diversity in form and function.* J Cell Sci, 2001. **114**(Pt 4): p. 629-41.

73.   Cailliez, F. and R. Lavery, *Cadherin mechanics and complexation: the importance of calcium binding.* Biophys J, 2005. **89**(6): p. 3895-903.

74.   Ivanov, D.B., M.P. Philippova, and V.A. Tkachuk, *Structure and functions of classical cadherins.* Biochemistry (Mosc), 2001. **66**(10): p. 1174-86.

75.   Ozawa, M., M. Ringwald, and R. Kemler, *Uvomorulin-catenin complex formation is regulated by a specific domain in the cytoplasmic region of the cell adhesion molecule.* Proc Natl Acad Sci U S A, 1990. **87**(11): p. 4246-50.

76.   Yagi, T. and M. Takeichi, *Cadherin superfamily genes: functions, genomic organization, and neurologic diversity.* Genes Dev, 2000. **14**(10): p. 1169-80.

77.   Overduin, M., et al., *Solution structure of the epithelial cadherin domain responsible for selective cell adhesion.* Science, 1995. **267**(5196): p. 386-9.

78.   Takeichi, M., *The cadherins: cell-cell adhesion molecules controlling animal morphogenesis.* Development, 1988. **102**(4): p. 639-55.

79.   Grunwald, G.B., et al., *Enzymatic dissection of embryonic cell adhesive mechanisms. II. Developmental regulation of an endogenous adhesive system in the chick neural retina.* Dev Biol, 1981. **86**(2): p. 327-38.

80.   Hyafil, F., et al., *A cell surface glycoprotein involved in the compaction of embryonal carcinoma cells and cleavage stage embryos.* Cell, 1980. **21**(3): p. 927-34.

81.   Takeichi, M., *Cadherin cell adhesion receptors as a morphogenetic regulator.* Science, 1991. **251**(5000): p. 1451-5.

82.   Kemler, R., *Classical cadherins.* Semin Cell Biol, 1992. **3**(3): p. 149-55.

83.   Larue, L., et al., *E-cadherin null mutant embryos fail to form a trophectoderm epithelium.* Proc Natl Acad Sci U S A, 1994. **91**(17): p. 8263-7.

84.   Takeichi, M., *Morphogenetic roles of classic cadherins.* Curr Opin Cell Biol, 1995. **7**(5): p. 619-27.

85.   Hatta, K., et al., *Cloning and expression of cDNA encoding a neural calcium-dependent cell adhesion molecule: its identity in the cadherin gene family.* J Cell Biol, 1988. **106**(3): p. 873-81.

86.   Blaschuk, O.W., et al., *Identification of a cadherin cell adhesion recognition sequence.* Dev Biol, 1990. **139**(1): p. 227-9.

87. Troyanovsky, S., *Cadherin dimers in cell-cell adhesion.* Eur J Cell Biol, 2005. **84**(2-3): p. 225-33.

88. Chitaev, N.A. and S.M. Troyanovsky, *Direct Ca2+-dependent heterophilic interaction between desmosomal cadherins, desmoglein and desmocollin, contributes to cell-cell adhesion.* J Cell Biol, 1997. **138**(1): p. 193-201.

89. Marcozzi, C., et al., *Coexpression of both types of desmosomal cadherin and plakoglobin confers strong intercellular adhesion.* J Cell Sci, 1998. **111 (Pt 4)**: p. 495-509.

90. Volk, T., O. Cohen, and B. Geiger, *Formation of heterotypic adherens-type junctions between L-CAM-containing liver cells and A-CAM-containing lens cells.* Cell, 1987. **50**(6): p. 987-94.

91. Miyatani, S., et al., *Neural cadherin: role in selective cell-cell adhesion.* Science, 1989. **245**(4918): p. 631-5.

92. Tepass, U., et al., *Cadherins in embryonic and neural morphogenesis.* Nat Rev Mol Cell Biol, 2000. **1**(2): p. 91-100.

93. Nollet, F., P. Kools, and F. van Roy, *Phylogenetic analysis of the cadherin superfamily allows identification of six major subfamilies besides several solitary members.* J Mol Biol, 2000. **299**(3): p. 551-72.

94. Gumbiner, B.M., *Cell adhesion: the molecular basis of tissue architecture and morphogenesis.* Cell, 1996. **84**(3): p. 345-57.

95. Meng, W. and M. Takeichi, *Adherens junction: molecular architecture and regulation.* Cold Spring Harb Perspect Biol, 2009. **1**(6): p. a002899.

96. Peyrieras, N., et al., *Uvomorulin: a nonintegral membrane protein of early mouse embryo.* Proc Natl Acad Sci U S A, 1983. **80**(20): p. 6274-7.

97. Hyafil, F., C. Babinet, and F. Jacob, *Cell-cell interactions in early embryogenesis: a molecular approach to the role of calcium.* Cell, 1981. **26**(3 Pt 1): p. 447-54.

98. Gallin, W.J., G.M. Edelman, and B.A. Cunningham, *Characterization of L-CAM, a major cell adhesion molecule from embryonic liver cells.* Proc Natl Acad Sci U S A, 1983. **80**(4): p. 1038-42.

99. Schuh, R., et al., *Molecular cloning of the mouse cell adhesion molecule uvomorulin: cDNA contains a B1-related sequence.* Proc Natl Acad Sci U S A, 1986. **83**(5): p. 1364-8.

100. Kemler, R., *From cadherins to catenins: cytoplasmic protein interactions and regulation of cell adhesion.* Trends Genet, 1993. **9**(9): p. 317-21.

101. Lilien, J., et al., *Turn-off, drop-out: functional state switching of cadherins.* Dev Dyn, 2002. **224**(1): p. 18-29.

102. Anastasiadis, P.Z., et al., *Inhibition of RhoA by p120 catenin.* Nat Cell Biol, 2000. **2**(9): p. 637-44.

103. Anastasiadis, P.Z. and A.B. Reynolds, *The p120 catenin family: complex roles in adhesion, signaling and cancer.* J Cell Sci, 2000. **113 (Pt 8)**: p. 1319-34.

104. Daniel, J.M. and A.B. Reynolds, *The tyrosine kinase substrate p120cas binds directly to E-cadherin but not to the adenomatous polyposis coli protein or alpha-catenin.* Mol Cell Biol, 1995. **15**(9): p. 4819-24.

105. Ireton, R.C., et al., *A novel role for p120 catenin in E-cadherin function.* J Cell Biol, 2002. **159**(3): p. 465-76.

106. Reynolds, A.B., *p120-catenin: Past and present.* Biochim Biophys Acta, 2007. **1773**(1): p. 2-7.

107. Thoreson, M.A., et al., *Selective uncoupling of p120(ctn) from E-cadherin disrupts strong adhesion.* J Cell Biol, 2000. **148**(1): p. 189-202.

108. Delva, E. and A.P. Kowalczyk, *Regulation of cadherin trafficking.* Traffic, 2009. **10**(3): p. 259-67.
109. Cavallaro, U. and G. Christofori, *Cell adhesion and signalling by cadherins and Ig-CAMs in cancer.* Nat Rev Cancer, 2004. **4**(2): p. 118-32.
110. Cavallaro, U. and E. Dejana, *Adhesion molecule signalling: not always a sticky business.* Nat Rev Mol Cell Biol, 2011. **12**(3): p. 189-97.
111. Crepaldi, T., et al., *Targeting of the SF/HGF receptor to the basolateral domain of polarized epithelial cells.* J Cell Biol, 1994. **125**(2): p. 313-20.
112. Hoschuetzky, H., H. Aberle, and R. Kemler, *Beta-catenin mediates the interaction of the cadherin-catenin complex with epidermal growth factor receptor.* J Cell Biol, 1994. **127**(5): p. 1375-80.
113. Pece, S. and J.S. Gutkind, *Signaling from E-cadherins to the MAPK pathway by the recruitment and activation of epidermal growth factor receptors upon cell-cell contact formation.* J Biol Chem, 2000. **275**(52): p. 41227-33.
114. Qian, X., et al., *E-cadherin-mediated adhesion inhibits ligand-dependent activation of diverse receptor tyrosine kinases.* EMBO J, 2004. **23**(8): p. 1739-48.
115. Andl, C.D. and A.K. Rustgi, *No one-way street: cross-talk between e-cadherin and receptor tyrosine kinase (RTK) signaling: a mechanism to regulate RTK activity.* Cancer Biol Ther, 2005. **4**(1): p. 28-31.
116. Fedor-Chaiken, M., et al., *E-cadherin binding modulates EGF receptor activation.* Cell Commun Adhes, 2003. **10**(2): p. 105-18.
117. Kim, S.H., Z. Li, and D.B. Sacks, *E-cadherin-mediated cell-cell attachment activates Cdc42.* J Biol Chem, 2000. **275**(47): p. 36999-7005.
118. Kraemer, A., et al., *Rac is a dominant regulator of cadherin-directed actin assembly that is activated by adhesive ligation independently of Tiam1.* Am J Physiol Cell Physiol, 2007. **292**(3): p. C1061-9.
119. Nakagawa, M., et al., *Recruitment and activation of Rac1 by the formation of E-cadherin-mediated cell-cell adhesion sites.* J Cell Sci, 2001. **114**(Pt 10): p. 1829-38.
120. Arthur, W.T., N.K. Noren, and K. Burridge, *Regulation of Rho family GTPases by cell-cell and cell-matrix adhesion.* Biol Res, 2002. **35**(2): p. 239-46.
121. Noren, N.K., et al., *Cadherin engagement regulates Rho family GTPases.* J Biol Chem, 2001. **276**(36): p. 33305-8.
122. Mimeault, M. and S.K. Batra, *Interplay of distinct growth factors during epithelial mesenchymal transition of cancer progenitor cells and molecular targeting as novel cancer therapies.* Ann Oncol, 2007. **18**(10): p. 1605-19.
123. Brembeck, F.H., M. Rosario, and W. Birchmeier, *Balancing cell adhesion and Wnt signaling, the key role of beta-catenin.* Curr Opin Genet Dev, 2006. **16**(1): p. 51-9.
124. Lu, Z., et al., *Downregulation of caveolin-1 function by EGF leads to the loss of E-cadherin, increased transcriptional activity of beta-catenin, and enhanced tumor cell invasion.* Cancer Cell, 2003. **4**(6): p. 499-515.
125. Nelson, W.J. and R. Nusse, *Convergence of Wnt, beta-catenin, and cadherin pathways.* Science, 2004. **303**(5663): p. 1483-7.
126. Lee, C.H., et al., *Epidermal growth factor receptor regulates beta-catenin location, stability, and transcriptional activity in oral cancer.* Mol Cancer, 2010. **9**: p. 64.
127. Huelsken, J., et al., *Requirement for beta-catenin in anterior-posterior axis formation in mice.* J Cell Biol, 2000. **148**(3): p. 567-78.
128. Wodarz, A. and R. Nusse, *Mechanisms of Wnt signaling in development.* Annu Rev Cell Dev Biol, 1998. **14**: p. 59-88.

129. Cattan, N., et al., *Establishment of two new human bladder carcinoma cell lines, CAL 29 and CAL 185. Comparative study of cell scattering and epithelial to mesenchyme transition induced by growth factors.* Br J Cancer, 2001. **85**(9): p. 1412-7.

130. Beavon, I.R., *The E-cadherin-catenin complex in tumour metastasis: structure, function and regulation.* Eur J Cancer, 2000. **36**(13 Spec No): p. 1607-20.

131. Birchmeier, W., *Molecular aspects of the loss of cell adhesion and gain of invasiveness in carcinomas.* Princess Takamatsu Symp, 1994. **24**: p. 214-32.

132. Birchmeier, W. and J. Behrens, *Cadherin expression in carcinomas: role in the formation of cell junctions and the prevention of invasiveness.* Biochim Biophys Acta, 1994. **1198**(1): p. 11-26.

133. Frixen, U.H., et al., *E-cadherin-mediated cell-cell adhesion prevents invasiveness of human carcinoma cells.* J Cell Biol, 1991. **113**(1): p. 173-85.

134. Bracke, M.E., F.M. Van Roy, and M.M. Mareel, *The E-cadherin/catenin complex in invasion and metastasis.* Curr Top Microbiol Immunol, 1996. **213 (Pt 1)**: p. 123-61.

135. Mareel, M., M. Bracke, and F. Van Roy, *Invasion promoter versus invasion suppressor molecules: the paradigm of E-cadherin.* Mol Biol Rep, 1994. **19**(1): p. 45-67.

136. Shino, Y., et al., *Clinicopathologic evaluation of immunohistochemical E-cadherin expression in human gastric carcinomas.* Cancer, 1995. **76**(11): p. 2193-201.

137. Tamura, G., et al., *Inactivation of the E-cadherin gene in primary gastric carcinomas and gastric carcinoma cell lines.* Jpn J Cancer Res, 1996. **87**(11): p. 1153-9.

138. Hirohashi, S., *Inactivation of the E-cadherin-mediated cell adhesion system in human cancers.* Am J Pathol, 1998. **153**(2): p. 333-9.

139. Schipper, J.H., et al., *E-cadherin expression in squamous cell carcinomas of head and neck: inverse correlation with tumor dedifferentiation and lymph node metastasis.* Cancer Res, 1991. **51**(23 Pt 1): p. 6328-37.

140. Takeichi, M., *Cadherins in cancer: implications for invasion and metastasis.* Curr Opin Cell Biol, 1993. **5**(5): p. 806-11.

141. Vleminckx, K., et al., *Genetic manipulation of E-cadherin expression by epithelial tumor cells reveals an invasion suppressor role.* Cell, 1991. **66**(1): p. 107-19.

142. Perl, A.K., et al., *A causal role for E-cadherin in the transition from adenoma to carcinoma.* Nature, 1998. **392**(6672): p. 190-3.

143. Nagafuchi, A., et al., *Transformation of cell adhesion properties by exogenously introduced E-cadherin cDNA.* Nature, 1987. **329**(6137): p. 341-3.

144. Behrens, J., et al., *Dissecting tumor cell invasion: epithelial cells acquire invasive properties after the loss of uvomorulin-mediated cell-cell adhesion.* J Cell Biol, 1989. **108**(6): p. 2435-47.

145. Guilford, P., et al., *E-cadherin germline mutations in familial gastric cancer.* Nature, 1998. **392**(6674): p. 402-5.

146. Berx, G., et al., *E-cadherin is a tumour/invasion suppressor gene mutated in human lobular breast cancers.* EMBO J, 1995. **14**(24): p. 6107-15.

147. Berx, G., et al., *Mutations of the human E-cadherin (CDH1) gene.* Hum Mutat, 1998. **12**(4): p. 226-37.

148. Brooks-Wilson, A.R., et al., *Germline E-cadherin mutations in hereditary diffuse gastric cancer: assessment of 42 new families and review of genetic screening criteria.* J Med Genet, 2004. **41**(7): p. 508-17.

149. Grady, W.M., et al., *Methylation of the CDH1 promoter as the second genetic hit in hereditary diffuse gastric cancer.* Nat Genet, 2000. **26**(1): p. 16-7.

150.   Guilford, P.J., et al., *E-cadherin germline mutations define an inherited cancer syndrome dominated by diffuse gastric cancer.* Hum Mutat, 1999. **14**(3): p. 249-55.

151.   Humar, B. and P. Guilford, *Hereditary diffuse gastric cancer: a manifestation of lost cell polarity.* Cancer Sci, 2009. **100**(7): p. 1151-7.

152.   Van Aken, E., et al., *Defective E-cadherin/catenin complexes in human cancer.* Virchows Arch, 2001. **439**(6): p. 725-51.

153.   Risinger, J.I., et al., *Mutations of the E-cadherin gene in human gynecologic cancers.* Nat Genet, 1994. **7**(1): p. 98-102.

154.   Kanai, Y., et al., *Point mutation of the E-cadherin gene in invasive lobular carcinoma of the breast.* Jpn J Cancer Res, 1994. **85**(10): p. 1035-9.

155.   Handschuh, G., et al., *Tumour-associated E-cadherin mutations alter cellular morphology, decrease cellular adhesion and increase cellular motility.* Oncogene, 1999. **18**(30): p. 4301-12.

156.   Fuchs, M., et al., *Motility enhancement by tumor-derived mutant E-cadherin is sensitive to treatment with epidermal growth factor receptor and phosphatidylinositol 3-kinase inhibitors.* Exp Cell Res, 2002. **276**(2): p. 129-41.

157.   Fuchs, M., et al., *Dynamics of cell adhesion and motility in living cells is altered by a single amino acid change in E-cadherin fused to enhanced green fluorescent protein.* Cell Motil Cytoskeleton, 2004. **59**(1): p. 50-61.

158.   Fuchs, M., et al., *Effect of tumor-associated mutant E-cadherin variants with defects in exons 8 or 9 on matrix metalloproteinase 3.* J Cell Physiol, 2005. **202**(3): p. 805-13.

159.   Handschuh, G., et al., *Single amino acid substitutions in conserved extracellular domains of E-cadherin differ in their functional consequences.* J Mol Biol, 2001. **314**(3): p. 445-54.

160.   Kremer, M., et al., *Influence of tumor-associated E-cadherin mutations on tumorigenicity and metastasis.* Carcinogenesis, 2003. **24**(12): p. 1879-86.

161.   Gamboa-Dominguez, A., et al., *E-cadherin expression in sporadic gastric cancer from Mexico: exon 8 and 9 deletions are infrequent events associated with poor survival.* Hum Pathol, 2005. **36**(1): p. 29-35.

162.   Schlessinger, J., *Ligand-induced, receptor-mediated dimerization and activation of EGF receptor.* Cell, 2002. **110**(6): p. 669-72.

163.   Citri, A. and Y. Yarden, *EGF-ERBB signalling: towards the systems level.* Nat Rev Mol Cell Biol, 2006. **7**(7): p. 505-16.

164.   Yarden, Y. and M.X. Sliwkowski, *Untangling the ErbB signalling network.* Nat Rev Mol Cell Biol, 2001. **2**(2): p. 127-37.

165.   Bublil, E.M. and Y. Yarden, *The EGF receptor family: spearheading a merger of signaling and therapeutics.* Curr Opin Cell Biol, 2007. **19**(2): p. 124-34.

166.   Citri, A., K.B. Skaria, and Y. Yarden, *The deaf and the dumb: the biology of ErbB-2 and ErbB-3.* Exp Cell Res, 2003. **284**(1): p. 54-65.

167.   Guy, P.M., et al., *Insect cell-expressed p180erbB3 possesses an impaired tyrosine kinase activity.* Proc Natl Acad Sci U S A, 1994. **91**(17): p. 8132-6.

168.   Casalini, P., et al., *Role of HER receptors family in development and differentiation.* J Cell Physiol, 2004. **200**(3): p. 343-50.

169.   Yarden, Y., *The EGFR family and its ligands in human cancer. signalling mechanisms and therapeutic opportunities.* Eur J Cancer, 2001. **37 Suppl 4**: p. S3-8.

170.   Zhang, D., et al., *Neuregulin-3 (NRG3): a novel neural tissue-enriched protein that binds and activates ErbB4.* Proc Natl Acad Sci U S A, 1997. **94**(18): p. 9562-7.

171. Harari, D., et al., *Neuregulin-4: a novel growth factor that acts through the ErbB-4 receptor tyrosine kinase.* Oncogene, 1999. **18**(17): p. 2681-9.

172. Hynes, N.E. and H.A. Lane, *ERBB receptors and cancer: the complexity of targeted inhibitors.* Nat Rev Cancer, 2005. **5**(5): p. 341-54.

173. Garrett, T.P., et al., *Crystal structure of a truncated epidermal growth factor receptor extracellular domain bound to transforming growth factor alpha.* Cell, 2002. **110**(6): p. 763-73.

174. Ogiso, H., et al., *Crystal structure of the complex of human epidermal growth factor and receptor extracellular domains.* Cell, 2002. **110**(6): p. 775-87.

175. Ferguson, K.M., et al., *EGF activates its receptor by removing interactions that autoinhibit ectodomain dimerization.* Mol Cell, 2003. **11**(2): p. 507-17.

176. Garrett, T.P., et al., *The crystal structure of a truncated ErbB2 ectodomain reveals an active conformation, poised to interact with other ErbB receptors.* Mol Cell, 2003. **11**(2): p. 495-505.

177. Husnjak, K. and I. Dikic, *EGFR trafficking: parkin' in a jam.* Nat Cell Biol, 2006. **8**(8): p. 787-8.

178. Waterman, H. and Y. Yarden, *Molecular mechanisms underlying endocytosis and sorting of ErbB receptor tyrosine kinases.* FEBS Lett, 2001. **490**(3): p. 142-52.

179. Waterman, H., et al., *Alternative intracellular routing of ErbB receptors may determine signaling potency.* J Biol Chem, 1998. **273**(22): p. 13819-27.

180. Shilo, B.Z., *Regulating the dynamics of EGF receptor signaling in space and time.* Development, 2005. **132**(18): p. 4017-27.

181. Zandi, R., et al., *Mechanisms for oncogenic activation of the epidermal growth factor receptor.* Cell Signal, 2007. **19**(10): p. 2013-23.

182. Quesnelle, K.M., A.L. Boehm, and J.R. Grandis, *STAT-mediated EGFR signaling in cancer.* J Cell Biochem, 2007. **102**(2): p. 311-9.

183. Schlessinger, J. and D. Bar-Sagi, *Activation of Ras and other signaling pathways by receptor tyrosine kinases.* Cold Spring Harb Symp Quant Biol, 1994. **59**: p. 173-9.

184. Marais, R., et al., *Ras recruits Raf-1 to the plasma membrane for activation by tyrosine phosphorylation.* EMBO J, 1995. **14**(13): p. 3136-45.

185. Dillon, R.L., D.E. White, and W.J. Muller, *The phosphatidyl inositol 3-kinase signaling network: implications for human breast cancer.* Oncogene, 2007. **26**(9): p. 1338-45.

186. Hennessy, B.T., et al., *Exploiting the PI3K/AKT pathway for cancer drug discovery.* Nat Rev Drug Discov, 2005. **4**(12): p. 988-1004.

187. Martin, G.S., *The hunting of the Src.* Nat Rev Mol Cell Biol, 2001. **2**(6): p. 467-75.

188. Puls, L.N., M. Eadens, and W. Messersmith, *Current status of SRC inhibitors in solid tumor malignancies.* Oncologist, 2011. **16**(5): p. 566-78.

189. Thomas, S.M. and J.S. Brugge, *Cellular functions regulated by Src family kinases.* Annu Rev Cell Dev Biol, 1997. **13**: p. 513-609.

190. Luttrell, D.K., L.M. Luttrell, and S.J. Parsons, *Augmented mitogenic responsiveness to epidermal growth factor in murine fibroblasts that overexpress pp60c-src.* Mol Cell Biol, 1988. **8**(1): p. 497-501.

191. Bromann, P.A., H. Korkaya, and S.A. Courtneidge, *The interplay between Src family kinases and receptor tyrosine kinases.* Oncogene, 2004. **23**(48): p. 7957-68.

192. Bjorge, J.D., A. Jakymiw, and D.J. Fujita, *Selected glimpses into the activation and function of Src kinase.* Oncogene, 2000. **19**(49): p. 5620-35.

193. Bowman, T., et al., *STATs in oncogenesis.* Oncogene, 2000. **19**(21): p. 2474-88.

194. Adams, G.P. and L.M. Weiner, *Monoclonal antibody therapy of cancer.* Nat Biotechnol, 2005. **23**(9): p. 1147-57.

195. Harari, P.M., *Epidermal growth factor receptor inhibition strategies in oncology.* Endocr Relat Cancer, 2004. **11**(4): p. 689-708.
196. Pinto, C., et al., *Phase II study of cetuximab in combination with FOLFIRI in patients with untreated advanced gastric or gastroesophageal junction adenocarcinoma (FOLCETUX study).* Ann Oncol, 2007. **18**(3): p. 510-7.
197. Pinto, C., et al., *Phase II study of cetuximab in combination with cisplatin and docetaxel in patients with untreated advanced gastric or gastro-oesophageal junction adenocarcinoma (DOCETUX study).* Br J Cancer, 2009. **101**(8): p. 1261-8.
198. Lordick, F., et al., *Cetuximab plus oxaliplatin/leucovorin/5-fluorouracil in first-line metastatic gastric cancer: a phase II study of the Arbeitsgemeinschaft Internistische Onkologie (AIO).* Br J Cancer, 2010. **102**(3): p. 500-5.
199. Moehler, M., et al., *Cetuximab with irinotecan, folinic acid and 5-fluorouracil as first-line treatment in advanced gastroesophageal cancer: a prospective multi-center biomarker-oriented phase II study.* Ann Oncol, 2011. **22**(6): p. 1358-66.
200. Espina, V., et al., *Protein microarrays: molecular profiling technologies for clinical specimens.* Proteomics, 2003. **3**(11): p. 2091-100.
201. Sheehan, K.M., et al., *Use of reverse phase protein microarrays and reference standard development for molecular network analysis of metastatic ovarian carcinoma.* Mol Cell Proteomics, 2005. **4**(4): p. 346-55.
202. Spurrier, B., et al., *Antibody screening database for protein kinetic modeling.* Proteomics, 2007. **7**(18): p. 3259-63.
203. Sanchez-Carbayo, M., *Antibody array-based technologies for cancer protein profiling and functional proteomic analyses using serum and tissue specimens.* Tumour Biol, 2010. **31**(2): p. 103-12.
204. Liotta, L.A., et al., *Protein microarrays: meeting analytical challenges for clinical applications.* Cancer Cell, 2003. **3**(4): p. 317-25.
205. Voshol, H., et al., *Antibody-based proteomics: analysis of signaling networks using reverse protein arrays.* FEBS J, 2009. **276**(23): p. 6871-9.
206. Cailleau, R., M. Olive, and Q.V. Cruciger, *Long-term human breast carcinoma cell lines of metastatic origin: preliminary characterization.* In Vitro, 1978. **14**(11): p. 911-5.
207. Ross, D.T., et al., *Systematic variation in gene expression patterns in human cancer cell lines.* Nat Genet, 2000. **24**(3): p. 227-35.
208. Garraway, L.A., et al., *Integrative genomic analyses identify MITF as a lineage survival oncogene amplified in malignant melanoma.* Nature, 2005. **436**(7047): p. 117-22.
209. Barranco, S.C., et al., *Establishment and characterization of an in vitro model system for human adenocarcinoma of the stomach.* Cancer Res, 1983. **43**(4): p. 1703-9.
210. Sekiguchi, M., K. Sakakibara, and G. Fujii, *Establishment of cultured cell lines derived from a human gastric carcinoma.* Jpn J Exp Med, 1978. **48**(1): p. 61-8.
211. Motoyama, T., H. Hojo, and H. Watanabe, *Comparison of seven cell lines derived from human gastric carcinomas.* Acta Pathol Jpn, 1986. **36**(1): p. 65-83.
212. Giard, D.J., et al., *In vitro cultivation of human tumors: establishment of cell lines derived from a series of solid tumors.* J Natl Cancer Inst, 1973. **51**(5): p. 1417-23.
213. Paull, K.D., et al., *Display and analysis of patterns of differential activity of drugs against human tumor cell lines: development of mean graph and COMPARE algorithm.* J Natl Cancer Inst, 1989. **81**(14): p. 1088-92.
214. Dietel, M., et al., *In vitro prediction of cytostatic drug resistance in primary cell cultures of solid malignant tumours.* Eur J Cancer, 1993. **29A**(3): p. 416-20.

215. Luo, F.R., et al., *Correlation of pharmacokinetics with the antitumor activity of Cetuximab in nude mice bearing the GEO human colon carcinoma xenograft.* Cancer Chemother Pharmacol, 2005. **56**(5): p. 455-64.

216. Robert, F., et al., *Phase I study of anti--epidermal growth factor receptor antibody cetuximab in combination with radiation therapy in patients with advanced head and neck cancer.* J Clin Oncol, 2001. **19**(13): p. 3234-43.

217. Baselga, J., et al., *Phase I studies of anti-epidermal growth factor receptor chimeric antibody C225 alone and in combination with cisplatin.* J Clin Oncol, 2000. **18**(4): p. 904-14.

218. Bremm, A., et al., *Enhanced activation of epidermal growth factor receptor caused by tumor-derived E-cadherin mutations.* Cancer Res, 2008. **68**(3): p. 707-14.

219. Sarbassov, D.D., et al., *Phosphorylation and regulation of Akt/PKB by the rictor-mTOR complex.* Science, 2005. **307**(5712): p. 1098-101.

220. Ramos, J.W., *The regulation of extracellular signal-regulated kinase (ERK) in mammalian cells.* Int J Biochem Cell Biol, 2008. **40**(12): p. 2707-19.

221. Yeatman, T.J., *A renaissance for SRC.* Nat Rev Cancer, 2004. **4**(6): p. 470-80.

222. Roussel, R.R., et al., *Selective binding of activated pp60c-src by an immobilized synthetic phosphopeptide modeled on the carboxyl terminus of pp60c-src.* Proc Natl Acad Sci U S A, 1991. **88**(23): p. 10696-700.

223. Xu, W., et al., *Crystal structures of c-Src reveal features of its autoinhibitory mechanism.* Mol Cell, 1999. **3**(5): p. 629-38.

224. Mateus, A.R., et al., *EGFR regulates RhoA-GTP dependent cell motility in E-cadherin mutant cells.* Hum Mol Genet, 2007. **16**(13): p. 1639-47.

225. Black, P.C., et al., *Sensitivity to epidermal growth factor receptor inhibitor requires E-cadherin expression in urothelial carcinoma cells.* Clin Cancer Res, 2008. **14**(5): p. 1478-86.

226. Bardelli, A. and S. Siena, *Molecular mechanisms of resistance to cetuximab and panitumumab in colorectal cancer.* J Clin Oncol, 2010. **28**(7): p. 1254-61.

227. Spurrier, B., S. Ramalingam, and S. Nishizuka, *Reverse-phase protein lysate microarrays for cell signaling analysis.* Nat Protoc, 2008. **3**(11): p. 1796-808.

228. Fricke, E., et al., *Effect of wild-type and mutant E-cadherin on cell proliferation and responsiveness to the chemotherapeutic agents cisplatin, etoposide, and 5-fluorouracil.* Oncology, 2004. **66**(2): p. 150-9.

229. Luber, B., et al., *Tumor-derived mutated E-cadherin influences beta-catenin localization and increases susceptibility to actin cytoskeletal changes induced by pervanadate.* Cell Adhes Commun, 2000. **7**(5): p. 391-408.

230. Mariadason, J.M., et al., *Down-regulation of beta-catenin TCF signaling is linked to colonic epithelial cell differentiation.* Cancer Res, 2001. **61**(8): p. 3465-71.

231. Stockinger, A., et al., *E-cadherin regulates cell growth by modulating proliferation-dependent beta-catenin transcriptional activity.* J Cell Biol, 2001. **154**(6): p. 1185-96.

232. Kolligs, F.T., G. Bommer, and B. Goke, *Wnt/beta-catenin/tcf signaling: a critical pathway in gastrointestinal tumorigenesis.* Digestion, 2002. **66**(3): p. 131-44.

233. Yasmeen, A., T.A. Bismar, and A.E. Al Moustafa, *ErbB receptors and epithelial-cadherin-catenin complex in human carcinomas.* Future Oncol, 2006. **2**(6): p. 765-81.

234. ([www.sanger.ac.uk)](www.sanger.ac.uk), S.I.C.C.L.P.

235. Iwashita, J., et al., *Inhibition of E-cadherin dependent cell-cell contact promotes MUC5AC mucin production through the activation of epidermal growth factor receptors.* Biosci Biotechnol Biochem, 2011. **75**(4): p. 688-93.

236. Aliaga, J.C., et al., *Requirement of the MAP kinase cascade for cell cycle progression and differentiation of human intestinal cells.* Am J Physiol, 1999. **277**(3 Pt 1): p. G631-41.

237. Laprise, P., et al., *Down-regulation of MEK/ERK signaling by E-cadherin-dependent PI3K/Akt pathway in differentiating intestinal epithelial cells.* J Cell Physiol, 2004. **199**(1): p. 32-9.

238. Bryant, D.M., et al., *EGF induces macropinocytosis and SNX1-modulated recycling of E-cadherin.* J Cell Sci, 2007. **120**(Pt 10): p. 1818-28.

239. Kleiner, S., A. Faisal, and Y. Nagamine, *Induction of uPA gene expression by the blockage of E-cadherin via Src- and Shc-dependent Erk signaling.* FEBS J, 2007. **274**(1): p. 227-40.

240. Ahmed, N., et al., *Molecular pathways regulating EGF-induced epithelio-mesenchymal transition in human ovarian surface epithelium.* Am J Physiol Cell Physiol, 2006. **290**(6): p. C1532-42.

241. Davies, M., et al., *Induction of an epithelial to mesenchymal transition in human immortal and malignant keratinocytes by TGF-beta1 involves MAPK, Smad and AP-1 signalling pathways.* J Cell Biochem, 2005. **95**(5): p. 918-31.

242. Shin, S.Y., et al., *Functional roles of multiple feedback loops in extracellular signal-regulated kinase and Wnt signaling pathways that regulate epithelial-mesenchymal transition.* Cancer Res, 2010. **70**(17): p. 6715-24.

243. Keld, R., et al., *PEA3/ETV4-related transcription factors coupled with active ERK signalling are associated with poor prognosis in gastric adenocarcinoma.* Br J Cancer, 2011. **105**(1): p. 124-30.

244. Deplazes, J., et al., *Rac1 and Rho contribute to the migratory and invasive phenotype associated with somatic E-cadherin mutation.* Hum Mol Genet, 2009. **18**(19): p. 3632-44.

245. Poliakov, A., M. Cotrina, and D.G. Wilkinson, *Diverse roles of eph receptors and ephrins in the regulation of cell migration and tissue assembly.* Dev Cell, 2004. **7**(4): p. 465-80.

246. Davy, A. and P. Soriano, *Ephrin signaling in vivo: look both ways.* Dev Dyn, 2005. **232**(1): p. 1-10.

247. Noren, N.K., et al., *Interplay between EphB4 on tumor cells and vascular ephrin-B2 regulates tumor growth.* Proc Natl Acad Sci U S A, 2004. **101**(15): p. 5583-8.

248. Danilkovitch-Miagkova, A., et al., *Integrin-mediated RON growth factor receptor phosphorylation requires tyrosine kinase activity of both the receptor and c-Src.* J Biol Chem, 2000. **275**(20): p. 14783-6.

249. Pandey, A., et al., *Role of B61, the ligand for the Eck receptor tyrosine kinase, in TNF-alpha-induced angiogenesis.* Science, 1995. **268**(5210): p. 567-9.

250. Bartley, T.D., et al., *B61 is a ligand for the ECK receptor protein-tyrosine kinase.* Nature, 1994. **368**(6471): p. 558-60.

251. Pandey, A., et al., *Activation of the Eck receptor protein tyrosine kinase stimulates phosphatidylinositol 3-kinase activity.* J Biol Chem, 1994. **269**(48): p. 30154-7.

252. Miao, H., et al., *Activation of EphA receptor tyrosine kinase inhibits the Ras/MAPK pathway.* Nat Cell Biol, 2001. **3**(5): p. 527-30.

253. Orsulic, S. and R. Kemler, *Expression of Eph receptors and ephrins is differentially regulated by E-cadherin.* J Cell Sci, 2000. **113 (Pt 10)**: p. 1793-802.

254. van der Valk, J., et al., *Optimization of chemically defined cell culture media--replacing fetal bovine serum in mammalian in vitro methods.* Toxicol In Vitro, 2010. **24**(4): p. 1053-63.

255. Zheng, X., et al., *Proteomic analysis for the assessment of different lots of fetal bovine serum as a raw material for cell culture. Part IV. Application of proteomics to the manufacture of biological drugs.* Biotechnol Prog, 2006. **22**(5): p. 1294-300.

256. Knowles, J. and G. Gromo, *A guide to drug discovery: Target selection in drug discovery.* Nat Rev Drug Discov, 2003. **2**(1): p. 63-9.

257. Serrels, A., et al., *Src/FAK-mediated regulation of E-cadherin as a mechanism for controlling collective cell movement: insights from in vivo imaging.* Cell Adh Migr, 2011. **5**(4): p. 360-5.

258. Frame, M.C., *Src in cancer: deregulation and consequences for cell behaviour.* Biochim Biophys Acta, 2002. **1602**(2): p. 114-30.

259. Bild, A.H., et al., *Oncogenic pathway signatures in human cancers as a guide to targeted therapies.* Nature, 2006. **439**(7074): p. 353-7.

260. Irby, R.B. and T.J. Yeatman, *Role of Src expression and activation in human cancer.* Oncogene, 2000. **19**(49): p. 5636-42.

261. Irby, R.B., et al., *Activating SRC mutation in a subset of advanced human colon cancers.* Nat Genet, 1999. **21**(2): p. 187-90.

262. Summy, J.M. and G.E. Gallick, *Src family kinases in tumor progression and metastasis.* Cancer Metastasis Rev, 2003. **22**(4): p. 337-58.

263. Hunter, T., *A tail of two src's: mutatis mutandis.* Cell, 1987. **49**(1): p. 1-4.

264. Tsang, S.M., et al., *Non-junctional human desmoglein 3 acts as an upstream regulator of Src in E-cadherin adhesion, a pathway possibly involved in the pathogenesis of pemphigus vulgaris.* J Pathol, 2012. **227**(1): p. 81-93.

265. Alt-Holland, A., et al., *E-cadherin suppression directs cytoskeletal rearrangement and intraepithelial tumor cell migration in 3D human skin equivalents.* J Invest Dermatol, 2008. **128**(10): p. 2498-507.

266. Hara, M., et al., *Interleukin-2 potentiation of cetuximab antitumor activity for epidermal growth factor receptor-overexpressing gastric cancer xenografts through antibody-dependent cellular cytotoxicity.* Cancer Sci, 2008. **99**(7): p. 1471-8.

267. Liu, X., et al., *Cetuximab enhances the activities of irinotecan on gastric cancer cell lines through downregulating the EGFR pathway upregulated by irinotecan.* Cancer Chemother Pharmacol, 2011. **68**(4): p. 871-8.

268. Ciardiello, F. and G. Tortora, *EGFR antagonists in cancer treatment.* N Engl J Med, 2008. **358**(11): p. 1160-74.

269. Rocher-Ros, V., et al., *Presenilin modulates EGFR signaling and cell transformation by regulating the ubiquitin ligase Fbw7.* Oncogene, 2010. **29**(20): p. 2950-61.

270. Benavente, S., et al., *Establishment and characterization of a model of acquired resistance to epidermal growth factor receptor targeting agents in human cancer cells.* Clin Cancer Res, 2009. **15**(5): p. 1585-92.

271. Luber, B., et al., *Biomarker analysis of cetuximab plus oxaliplatin/leucovorin/5-fluorouracil in first-line metastatic gastric and oesophago-gastric junction cancer: results from a phase II trial of the Arbeitsgemeinschaft Internistische Onkologie (AIO).* BMC Cancer, 2011. **11**: p. 509.

272. Kim, J.W., et al., *The growth inhibitory effect of lapatinib, a dual inhibitor of EGFR and HER2 tyrosine kinase, in gastric cancer cell lines.* Cancer Lett, 2008. **272**(2): p. 296-306.

273. Wild, R., et al., *Cetuximab preclinical antitumor activity (monotherapy and combination based) is not predicted by relative total or activated epidermal growth factor receptor tumor expression levels.* Mol Cancer Ther, 2006. **5**(1): p. 104-13.

274. Han, S.W., et al., *Phase II study and biomarker analysis of cetuximab combined with modified FOLFOX6 in advanced gastric cancer.* Br J Cancer, 2009. **100**(2): p. 298-304.

275. Chung, K.Y., et al., *Cetuximab shows activity in colorectal cancer patients with tumors that do not express the epidermal growth factor receptor by immunohistochemistry.* J Clin Oncol, 2005. **23**(9): p. 1803-10.

276. Gamboa-Dominguez, A., et al., *Epidermal growth factor receptor expression correlates with poor survival in gastric adenocarcinoma from Mexican patients: a multivariate analysis using a standardized immunohistochemical detection system.* Mod Pathol, 2004. **17**(5): p. 579-87.

277. Jhawer, M., et al., *PIK3CA mutation/PTEN expression status predicts response of colon cancer cells to the epidermal growth factor receptor inhibitor cetuximab.* Cancer Res, 2008. **68**(6): p. 1953-61.

278. Smolen, G.A., et al., *Frequent met oncogene amplification in a Brca1/Trp53 mouse model of mammary tumorigenesis.* Cancer Res, 2006. **66**(7): p. 3452-5.

279. Bertotti, A., et al., *Inhibition of Src impairs the growth of met-addicted gastric tumors.* Clin Cancer Res, 2010. **16**(15): p. 3933-43.

280. Engelman, J.A. and P.A. Janne, *Mechanisms of acquired resistance to epidermal growth factor receptor tyrosine kinase inhibitors in non-small cell lung cancer.* Clin Cancer Res, 2008. **14**(10): p. 2895-9.

281. Engelman, J.A. and J. Settleman, *Acquired resistance to tyrosine kinase inhibitors during cancer therapy.* Curr Opin Genet Dev, 2008. **18**(1): p. 73-9.

282. Cappuzzo, F., et al., *Primary resistance to cetuximab therapy in EGFR FISH-positive colorectal cancer patients.* Br J Cancer, 2008. **99**(1): p. 83-9.

283. Krumbach, R., et al., *Primary resistance to cetuximab in a panel of patient-derived tumour xenograft models: activation of MET as one mechanism for drug resistance.* Eur J Cancer, 2011. **47**(8): p. 1231-43.

284. Liska, D., et al., *HGF rescues colorectal cancer cells from EGFR inhibition via MET activation.* Clin Cancer Res, 2011. **17**(3): p. 472-82.

285. Stommel, J.M., et al., *Coactivation of receptor tyrosine kinases affects the response of tumor cells to targeted therapies.* Science, 2007. **318**(5848): p. 287-90.

286. Agarwal, S., et al., *Association of constitutively activated hepatocyte growth factor receptor (Met) with resistance to a dual EGFR/Her2 inhibitor in non-small-cell lung cancer cells.* Br J Cancer, 2009. **100**(6): p. 941-9.

287. Engelman, J.A., et al., *MET amplification leads to gefitinib resistance in lung cancer by activating ERBB3 signaling.* Science, 2007. **316**(5827): p. 1039-43.

288. Bachleitner-Hofmann, T., et al., *HER kinase activation confers resistance to MET tyrosine kinase inhibition in MET oncogene-addicted gastric cancer cells.* Mol Cancer Ther, 2008. **7**(11): p. 3499-508.

289. Nikolova, D.A., et al., *Cetuximab attenuates metastasis and u-PAR expression in non-small cell lung cancer: u-PAR and E-cadherin are novel biomarkers of cetuximab sensitivity.* Cancer Res, 2009. **69**(6): p. 2461-70.

290. Fuchs, B.C., et al., *Epithelial-to-mesenchymal transition and integrin-linked kinase mediate sensitivity to epidermal growth factor receptor inhibition in human hepatoma cells.* Cancer Res, 2008. **68**(7): p. 2391-9.

291. Witta, S.E., et al., *ErbB-3 expression is associated with E-cadherin and their coexpression restores response to gefitinib in non-small-cell lung cancer (NSCLC).* Ann Oncol, 2009. **20**(4): p. 689-95.

292. Oda, T., et al., *E-cadherin gene mutations in human gastric carcinoma cell lines.* Proc Natl Acad Sci U S A, 1994. **91**(5): p. 1858-62.